Pontifícia Universidade Católica
do Rio de Janeiro

Arthur de Castro Brigatto

Ensuring Reserve Deployment in Hydrothermal Power Systems Planning

DISSERTAÇÃO DE MESTRADO

Dissertation presented to the Programa de Pós-Graduação em Engenharia Elétrica of the Departamento de Engenharia Elétrica, PUC–Rio as partial fulfillment of the requirements for the degree of Mestre em Engenharia Elétrica.

Advisor : Prof. Alexandre Street de Aguiar
Co–Advisor: Prof. Davi Michel Valladão

Rio de Janeiro
March 2016

Pontifícia Universidade Católica
do Rio de Janeiro

Arthur de Castro Brigatto

Ensuring Reserve Deployment in Hydrothermal Power Systems Planning

Dissertation presented to the Programa de Pós-Graduação em Engenharia Elétrica of the Departamento de Engenharia Elétrica do Centro Técnico Científico da PUC–Rio, as partial fulfillment of the requirements for the degree of Mestre.

Prof. Alexandre Street de Aguiar
Advisor
Departamento de Engenharia Elétrica — PUC–Rio

Prof. Davi Michel Valladão
Co–Advisor
Departamento de Engenharia Industrial — PUC–Rio

Prof. Mario Veiga Ferraz Pereira
PSR Soluções e Consultoria em Engenharia Ltda

Prof. André Luiz Diniz Souto Lima
Centro de Pesquisas de Energia Elétrica - CEPEL

Prof. Joari Paulo da Costa
Operador Nacional do Sistema Elétrico - ONS

Prof. Márcio Da Silveira Carvalho
Coordinator of the Centro Técnico Científico — PUC–Rio

Rio de Janeiro, March 21st, 2016

Arthur de Castro Brigatto

Arthur de Castro Brigatto graduated in 2013 in Electrical Engineering from Federal University of Juiz de Fora, Juiz de Fora - Brazil. In 2014, he started the master course at Pontifical Catholic University of Rio de Janeiro, Rio de Janeiro - Brazil. During this period, he joined the research group in power system economics at the Laboratory of Applied Mathematical Programming and Statistics (LAMPS) where he worked as a researcher in the area of hydrothermal power systems operation planning.

Bibliographic data

Brigatto, Arthur de Castro

Ensuring Reserve Deployment in Hydrothermal Power Systems Planning / Arthur de Castro Brigatto ; advisor: Alexandre Street de Aguiar; co–advisor: Davi Michel Valladão — 2016.
109 f. : il. ; 30 cm

Dissertação (Mestrado em Engenharia Elétrica)-Pontifícia Universidade Católica do Rio de Janeiro, Departamento de Engenharia Elétrica, Rio de Janeiro, 2016.
Inclui bibliografia

1. Engenharia Elétrica – Teses. 2. Otimização Estocástica. 3. Otimização Robusta. 4. Programação Dual Dinâmica Estocástica. 5. Algoritmo de Geração de Coluna e Restrição. 6. Planejamento da Operação de Sistemas de Potência Hidrotérmicos. 7. Inconsistência Temporal. I. Street, Alexandre de Aguiar. II. Valladão, Davi Michel. III. Pontifícia Universidade Católica do Rio de Janeiro. Departamento de Engenharia Elétrica. IV. Título.

CDD: 621.3

Acknowledgments

First of all, I would like to express my deepest gratitude to my advisors and friends Alexandre Street de Aguiar and Davi Michel Valladão for the remarkable shared knowledge, support, guidance and patience provided during the realization of this work. Thank you both for helping me contribute to science.

I would like to thank my parents Maria Teresa Nunes de Castro and Marcos Emilio Brigatto for helping me becoming the person I am today and supporting my decision to continue my studies.

I would like to thank my uncles Carlos Heleno Netto Barbosa and Maria Inês Nunes de Castro Barbosa for providing me a place to stay during the first few months in Rio de Janeiro. This acknowledgement is extended to my cousins Renata Maria de Castro Barbosa and Maria Letícia de Castro Barbosa.

I would like to thank all my family members for the affection and encouragement not only during the realization of this work, but in all my life.

I would like to thank all my friends from Juiz de Fora, to whom I managed to stay close even in distance, for continuously providing me great times.

I would like to thank my great friend Bruno Fânzeres to whom I had the privilege of learning from and getting phenomenal help during the countless work hours spent in the laboratory.

I would like to thank all members of LAMPS: Ana Luiza, Alexandre Moreira, Mario Souto, Joaquim Garcia, Marcelo Ruas, Henrique Helfer and Lucas Freire for making the laboratory a fun place to work.

I would like to thank all the friends I have made outside of the university since moving to Rio de Janeiro for helping me remembering that there is life outside of academia.

I would like to warmly thank Joana Siqueira for standing by my side during the realization of this work and understanding the times I could not be around. I am immensely grateful for you making it all easier for me.

Lastly, I would like to thank CAPES, CNPq and UTE Parnaíba Geração de Energia S\A for the financial support provided. Without it, this work would not be possible.

Abstract

Brigatto, Arthur de Castro; Street, Alexandre de Aguiar (Advisor); Valladão, Davi Michel. **Ensuring Reserve Deployment in Hydrothermal Power Systems Planning**. Rio de Janeiro, 2016. 109p. MSc. Dissertation — Departamento de Engenharia Elétrica, Pontifícia Universidade Católica do Rio de Janeiro.

The current state of the art method used for medium/long-term planning studies of hydrothermal power system operation is the Stochastic Dual Dynamic Programming (SDDP) algorithm. The computational savings provided by this method notwithstanding, it still relies on major system simplifications to achieve acceptable performances in practical applications. Simplifications in the planning stage in contrast to the actual implementation might induce time inconsistent policies and, consequently, a sub-optimality gap. Time inconsistency in hydrothermal planning might be induced by, for instance, assuming a constant coefficient production for hydro plants, reservoir aggregation, neglecting Kirchhoff's voltage law, and neglecting security criteria in planning models, which are then incorporated in implementating models. Unaccounted for reservoir depletion and inadequate spinning reserve deliverability situations that were observed in the Brazilian power system might be induced by time inconsistency. And this can lead to higher operational costs. Both these consequences are utterly negative since they pose the system to a great systemic risk of energy rationing or ultimately, system blackouts. In addition, the sub-optimility gap may also lead to energy markets distortions. Hence, it seems reasonable that further investigations on consequences of time inconsistency in hydrothermal planning should be undertaken. Along these lines, this work proposes an extension to previous work on the subject of time inconsistency to measure the effects of modeling simplifications in the SDDP framework for hydrothermal operation planning. The approach consists of using a simplified model for planning the system, which is done by means of the assessment of the recourse (cost-to-go) function, and a detailed model for its operation (implementation of the policy). Case studies involving simplifications in transmission lines modeling and in security criteria are carried out. Nevertheless, the focus of this work is on the later source as it is more difficult to address due to the complexity involved in the characterization of this effect. However, incorporating security criteria in planning models poses a major challenge to system operators. This is because the size of the model tends to grow exponentially as tighter security criteria are adopted. Motivated by this, the main objective of this work is to propose a new framework that allows security criteria to be incorporated in planning models and consequently ensure reserve deliverability in planning policies. The problem formulation is a multiperiod stochastic extension of Adjustable Robust Optimization (ARO) based models already proposed in literature to successfully address the dimensionality issue regarding the incorporation of security criteria $n - K$ and its variants. The solution methodology involves a hybrid Robust-SDDP algorithm that by means of sharing active contingency states amongst periods and possible inflow scenarios in the SDDP algorithm is capable of achieving computational tractability. Then, with the proposed approach it is possible to (i) address the optimal scheduling of energy and reserve in hydrothermal power systems ensuring reserve deliverability under an $n - K$ security criterion and (ii) assess the cost and side effects of disregarding security criteria in the planning stage.

Keywords

Stochastic Optimization; Robust Optimization; Stochastic Dual Dynamic Programming; Column-and-Constraint-Generation Algorithm; Hydrothermal Power Systems Operation Planning; Time Inconsistency

Resumo

Brigatto, Arthur de Castro; Street, Alexandre de Aguiar (Orientador); Valladão, Davi Michel. **Garantindo a Entregabilidade de Reservas no Planejamento de Sistemas de Potência Hidrotérmicos**. Rio de Janeiro, 2016. 109p. Dissertação de Mestrado — Departamento de Engenharia Elétrica, Pontifícia Universidade Católica do Rio de Janeiro.

Atualmente a metodologia correspondente ao estado da arte utilizada para o planejamento de médio-/longo-prazo da operação de sistemas elétricos de potência é a Programação Dual Dinâmica Estocástica (PDDE). No entanto, a tratabilidade computacional proporcionada por este método ainda requer simplificações consideráveis de detalhes de sistemas reais de maneira a atingir performaces aceitáveis em aplicações práticas. Simplificações feitas no estágio de planejamento em contraste com a implementação das decisões podem induzir políticas temporalmente inconsistentes e, consequentemente, um gap de sub-otimalidade. Inconsisência temporal em planejamento hidrotérmico pode ser induzida, por exemplo, ao assumir um coeficiente de produtividade constante para as hidrelétricas, ao agregar os reservatórios, ao negligenciar a segunda lei de Kirchhoff e neglienciando-se critérios de segurança em modelos de planejamento. As mesmas restrições são posteriormente consideradas na etapa de implementação do sistema. Esse fato pode estar envolvido com esvaziamento não planejado de reservatórios e entregabilidade inadequada de reservas girantes. Ambos podem levar a altos custos operacionais. Além disso, o sistema pode ficar exposto a um risco sistêmico de racionamento e em última instância, *blackouts*. O gap de sub-otimalidade pode também levar a distorções em mercados de energia. Assim, é razoável que as consequências da inconstência temporal em sistemas hidrotérmicos sejam estudadas. Nesse sentido, este trabalho propõe uma extensão de trabalhos já realizados relacionados à inconsistência temporal para medir os efeitos de simplificações de modelagem em modelos de planejamento resolvidos pela PDDE. A abordagem proposta consiste em usar um modelo simplificado para o planejamento do sistema, que é feito pela avaliação da função de recurso, e um modelo detalhado para a sua operação. Estudos de caso envolvendo simplificações em modelagem de linhas de transmissão e critérios de segurança são realizados. No entanto, o foco deste trabalho se dará na segunda fonte, já que a mesma apresenta maior complexidade na caracterização do efeito. No entanto, a incorporação de critérios de segurança é um grande desafio para operadores de sistemas elétricos, pois o tamanho do modelo tende a crescer exponencialmente quando critérios de segurança reforçados são aplicados. Motivado por isso, o principal objetivo deste trabalho é propor uma nova abordagem ao problema que permite que critérios de segurança possam ser incorporados em modelos de planejamento e consequentemente garantir a entregabilidade de reservas em políticas de planejamento. A formulação do problema é uma extensão multiperiodo e estocástica the modelos de Otimização Robusta Ajustável que já foram propostos na literatura para resolver o problema relacionado à dimensionalidade para um período. A metodologia de solução involve um algoritmo híbrido Robusto-PDDE que por meio do compartilhamento de estados de contingência ativos entre os períodos e cenários de afluência é capaz de atingir tratabilidade computacional. Com a nova abordagem proposta, é possível (i) resolver o problema de agendamento ótimo das reservas em sistemas hidrotérmicos garantindo a entregabilidade das reservas em um critério $n - K$ e (ii) calcular o custo e os efeitos negativos de se negligenciar critérios de segurança no planejamento.

Palavras–chave

Otimização Estocástica; Otimização Robusta; Programação Dual Dinâmica Estocástica; Algoritmo de Geração de Coluna e Restrição; Planejamento da Operação de Sistemas de Potência Hidrotérmicos; Inconsistência Temporal.

Contents

List of Figures

List of Tables

1
Introduction

Medium- and long-term hydrothermal power systems operation planning is a challenging problem faced by electricity systems with high penetration levels of hydro reserves. To begin with, more than a single hydro power plant may be built in the same river giving rise to a complex cascade disposition. As one consequence, the energy produced by a given hydro power plant depends on the water discharge of another one placed upstream, which makes their coordination highly difficult. And there also must be coordination of water used for energy production and of water used for irrigation and recreation. Finally, there must exist a minimum water level so that the river remains navigable at all times and a maximum water level to prevent flood [6].

In addition, operation of hydro power plants depends on, of course, the amount of water inflow upstream, which may be due to rain or snow melting, for example. Either way, water inflow remains uncertain. This raises the question of how much water stored in reservoirs should be discharged today and how much of it should remain stored for future use. If, on the one hand, a large amount of water is discharged at some point, followed by a low water inflow realization, thermal plants which are known to be more expensive than hydro plants may need to be dispatched in order to meet energy demand. On the other hand, if a small amount of water is used at some point followed by a high water inflow realization, it may be necessary to spill some of the water. This situation can also be economically negative since it is essentially a waste of cheap resources and it might also ultimately lead to flooding issues.

In this sense, in systems with centralized operation such as the Brazilian one, an Independent System Operator (ISO) usually carries out medium-/long-term planning studies of the system that takes into account uncertainty in water inflow. The main purpose of the future planning is to qualify the value of water to ensure supply adequacy. This gives rise to a set of recourse functions that can be coupled in short-term operation planning models [7]. Ultimately, it can also be used to, for instance, give a sign for the need of transmission and generation capacity expansion (see [7, 8]), to help energy market agents planning their future portfolio [9] and to obtain an energy deficit risk probability distribution [10]. Since the planning problem is highly subjected to uncertainty regarding inflows, its nature is essentially stochastic. Also, power systems usually have a large number of power plants and the problem might comprise a large number of planning periods. Hence, the planning problem can be characterized as a large-scale multistage stochastic program with recourse [11].

When considering a large number of periods and scenarios, the size of the problem grows exponentially and can easily become computationally intractable to be solved with usual linear programming techniques. The Stochastic Dual Dynamic Programming (SDDP) algorithm [12] and its variants [13–15] are known to successfully tackle such particularities. In Brazil, the Government research center CEPEL [16] is responsible for developing a chain of optimization models to support operation and coordination of the Brazilian hydrothermal power system [10]. The software NEWAVE has the SDDP algorithm built in and is used by both the Brazilian ISO and other electricity sector agents for medium-/long-term planning studies [10]. The planning range in NEWAVE goes up to 5 years in official studies and decisions are discretized in monthly steps. Then, outcomes from the NEWAVE software are coupled with the DECOMP software, also developed by CEPEL. The DECOMP software is responsible for short-term planning of the Brazilian hydrothermal power system. The planning range in the DECOMP model goes up to 12 months, although official studies only consider up to 2 months.

Ever since it was first published, many discussions regarding the SDDP algorithm have taken place. For instance, the convergence criterion originally proposed in [12] can be too optimistic, as discussed in [17], and even though other convergence criteria have been proposed, none of them is presented as a definitive solution. Thus, it remains an open topic in literature [17–19].

In the NEWAVE software, the problem of planning the Brazilian hydrothermal power system is solved considering a periodic autoregressive (PAR) model for inflow scenarios [7, 20–22]. However, even though the PAR model approximates the model to the real-world, as pointed out in [19] it can significantly augment the solution variability. One major consequence of this is that weak signals for system expansion can be obtained, followed by a possible energy crisis [8, 23]. This is because energy market agents might rely on such informations to plan new generation ventures. The authors in [19] present a manner for mitigating the solution variability by reducing the state space of the problem.

As originally proposed, the planning model in Brazil aims at minimizing the total expected operation cost. However, in order to avoid energy deficits in low inflow scenarios, a number of risk averse approaches to the SDDP method were introduced in literature. In [24] the authors introduce the ideas of polyhedral risk measures in multistage stochastic programs. These ideas were further extended in order to incorporate the SDDP method in [25]. In [17] the author introduced a risk measure given by the combination of expectation and Conditional Value-at-Risk (CVaR). The CVaR risk measure was proposed in [26] and insights into combining expectation and CVaR are explored in [27]. CVaR has been applied many times to different electricity sector problems [9, 28–33] and has also been incorporated to the SDDP method applied to operation planning of hydrothermal power systems [34–36]. In such works, the authors state that the incorporation of CVaR in the SDDP method applied to hydrothermal power systems planning significantly reduce high quantile costs of individual periods with practically no extra computational time. The incorporation of CVaR to the NEWAVE model is detailed in [37].

In contrast to planned policies, such as the ones evaluated by the NEWAVE software, models for short-term unit dispatch implementation might take into account system details such as transmission line modeling, nonlinear-technological constraints of hydro power plants [38], security criteria ($n-1$ and/or $n-2$ depending of the system) [39,40], intermittent generation from renewable sources, demand uncertainty [41], among others. Nevertheless, computational tractability issues prevent ISOs from introducing this level of detail in the medium/long-term operative plan drawn by the SDDP policy. In this scenario, short-term decisions, which make use of the information obtained from long-term studies by means of the cost-to-go (or recourse) function, are made under inaccurate (inconsistent) information about the future system operation. Therefore, implemented decisions are generally likely to deviate from those obtained in the planning step, which is the definition of time inconsistency (see [42–44]). According to [42], time inconsistent policies potentially creates sub-optimality gaps that measure the overall impact (aggregated) of day by day inconsistently implemented policies.

Time consistency of optimal policies is conceptually defined by [42]: "*a policy is time consistent if and only if the future planned decisions are actually going to be implemented*". The most common referred and analyzed source of time inconsistency is that induced by nonlinearities in the probability measure (see [42–45] and references therein for recent publications in operations research and [46] for a more conceptual discussion on the economic and behavioral side). The relevance of this source of inconsistency notwithstanding, modeling simplifications may also induce time inconsistent policies, as they generate sub-optimal recourse functions under the perspective of the most realistic, or complete, model of the system. Moreover, the consequence of this type of inconsistency is, generally, an optimistic view of the system, or incomplete view of systems resources, which often makes system controllers (ISOs) blind to potentially dangerous states of the systems.

Generally, the cumulative side effect due to the inconsistency produced by modeling simplification is difficult to be tracked. This is because the state of the system is updated after each period and errors within each single interval of time are controlled and, therefore, acceptable. However, the optimistic view of the future due to some modeling simplifications can gradually deteriorate the system's security, exposing it to non-frequent adversities. Notwithstanding, in real life, every computed policy tends to be time inconsistent since it is generally intractable/impossible to perfectly represent reality. Nevertheless, some sources of inconsistency may be classified as more dangerous than others. For the best of the authors knowledge, there is no work proposing a methodology to analyze the effects of time inconsistent policies induced by modeling simplifications in hydrothermal scheduling.

A motivation for further analyzing time inconsistency in hydrothermal planning comes from the year of 2012 in which the Brazilian power system experienced a sharp depletion of its main reservoirs in the Southeastern area (which concentrates more than 70% of the total-storage capacity). Energy storage levels started that year at a high-record and ended in the same year at a low-record if compared to the last decade, without observing a severe dry period [47] (this situation is discussed in more depth in Chapter 2). The many possible explanations for this situation notwithstanding, one interesting fact can be pointed out: differently from the usual, in 2012, the Brazilian ISO was implementing the system operation taking into account security criterion $n - 2$ and, in the presence of storms, the system reliability was raised to $n - 3$ [48]. In this context, it is natural to question whether these two facts are related.

This work is not intended to answer such question, but rather to introduce a methodology to investigate the effects of time inconsistency in hydrothermal power systems operation. The proposed approach is introduced in Chapter 4. It consists of using a simplified model for planning the system, which is done by means of the assessment of the recourse function, and a detailed model for its operation (implementation of the policy). Then, time consistency due to neglecting Kirchhoffs

Voltage Law in planning models is analyzed. Results show that, under inconsistent policies, not only the reservoir-depletion effect is present but also energy spot prices are likely to spike in the presence of dry conditions.

Then, motivated by the fact that recent blackouts that happened in February the Third, 2014 and in January the Nineteenth, 2015 in the Brazilian system (see [49] and [50]) were attributed precisely to the lack of reserves in the hours that preceded the events[1], Chapter 5 introduces a new model to co-optimize energy and ancillary services in the medium-/long-term planning of hydrothermal power systems under general deterministic security criteria.

Deterministic security criteria, such as the $n-K$, have been widely explored in recent literature (see [6, 39, 53–59]). Due to their relevance for current industry practices, recent works in robust optimization applied to power systems have been addressing this subject in short-term operational problems (see [39, 40, 59, 60]). For instance, in order to address a standard $n-2$ security criterion, contingency-constrained models must ensure power balancer under each post-contingency state comprising the loss of up to two elements. However, the number of possible contingencies in a $n-K$ security criterion is equal to $\sum_{i=1}^{K}\binom{n}{i}$ and this results in the main drawback of contingency-dependent models: the size of the problem exponentially grows with K. Recently, robust optimization with polyhedral uncertainty sets, introduced in [61], was firstly proposed in [40] to address the $n-K$ security criterion without the need of explicitly accounting for all post-contingency states of generation outages. In [60], a two-stage robust unit commitment model was proposed to account for the $n-K$ security criterion under the presence of network constraints, while in [39] a two-stage robust model was proposed to extend the energy and reserve scheduling model proposed in [40] to a general generation and transmission (GT) security criterion. The main technique used to solve two-stage robust optimization problems, [62], is currently the column-and-constraint generation (CCG) [63].

To address power system reliability standards, operators allocate up and down reserves through generators to implement ancillary services, [6], through many different sequential market mechanisms that receive the energy-market schedule as an input. Notwithstanding, in [54, 55], the benefit of the co-optimization of energy and reserves in a joint market clearing process was introduced through a contingency-constrained scheduling model. In [39], such work was extended through the afore-

[1] This was widely covered by the local media at the time [51, 52].

mentioned two-stage robust optimization approach to address a general $n-K$ security criterion within reasonable computational burden. In this setting, a least-cost reserve allocation through generators is defined (co-optimized) so that reserves are deliverable across the network in all comprised post-contingency states defined by parameter K. Thus, the total level and siting of reserves in the system is endogenously defined and is an output of the model.

The incorporation of security criteria and ancillary services in the SDDP framework applied to hydrothermal planning should mitigate the effects of time inconsistency and provide more reliable signals from the future planning. However, if techniques based on robust optimization, such as the one devised in [39], were to be applied to the SDDP framework, the CCG method would be run to all nodes in inflows the scenario tree and periods in the planning horizon. This could still lead the model to take unreasonable computational time to converge. However, the umbrella set of contingencies can be shared among all periods and scenarios involved in the problem, which can significantly reduce computational burden. This approach is justifiable since the umbrella set of contingencies presents low sensitivity to changes in the problem parameters [64]. Chapter 5 presents a new algorithm that combines the SDDP and the CCG methods. The resulting hybrid algorithm is capable of solving the planning problem whilst taking security criteria into account and achieving reasonable computational time.

Hence, the objectives of this work are to introduce the discussion of time inconsistency in hydrothermal power systems operation planning and provide an extension to the inconsistent gap in [42] to the SDDP framework. Also, to devise a new methodology, based on the two-stage robust modeling approach presented in [39], for incorporating a general security criterion $n-K$, and its variants ($n-K_G-K_L$, see [39]), in long-term hydrothermal operative planning models

Finally, the contributions of this work are summarized as follows:

1. To include the modeling simplification under the umbrella of possible sources of time inconsistencies [42].

2. To extend the time-inconsistency sub-optimality gap, proposed in [42] for a complete scenario tree, to the SDDP framework.

3. To illustrate how the theoretical sub-optimality gap could be used to provide an indicative measure of impact for a given inconsistency source in hydrothermal power system operation.

4. To introduce a multistage contingency-constrained robust model that co-optimizes the generation dispatch and individual up and down reserve allocations through generators based on [39]. In this framework, the model considers DC-linearized network constraints for both pre- and post-contingency states, generation and transmission line outages, and inflow scenarios.

5. To propose a hybrid SDDP and CCG solution methodology to solve the least-cost dispatch of energy and reserves problem with storage capacity under a general security criterion. The methodology takes advantage from the robustness of the umbrella set contingencies to improve the algorithm convergence by sharing critical post-contingency states found for different subproblems of the SDDP procedure.

6. To show that the methodology proposed in 5 is suitable to mitigate the effects of time inconsistency in hydrothermal power systems operation, providing more accurate information about future outcomes in a reasonable computational time.

1.1 Organization of the rest of this work

This work is organized as follows: Chapter 2 discusses the actual situation of the Brazilian system and introduces part of the notation and nomenclature to be used in later chapters. Chapter 3 discusses aspects and implementation details of the SDDP algorithm. Chapter 4 introduces the concepts of time inconsistency in hydrothermal power systems operation. It also presents the models to be used to study the effects and the methodology to model the time inconsistency gap. Chapter 5 presents a novel methodology to incorporate security constraints in the medium-/long-term planning of hydrothermal power systems by means of a hybrid robust-SDDP algorithm. Finally, in Chapter 6 the conclusions from this work are drawn.

2
Brazilian Power System

The Brazilian Power System had by the end of July of 2015 an installed capacity of 146,380.4MW[1] making it the biggest in Latin America [65]. A total of 98.3% of the system is interconnected leaving just few regions located mainly in the Amazon region disconnected from the main grid [4]. Energy demand reached a total of 463.2 GWh in the year of 2014 and it is expected to grow up to 535.2 GWh by the year of 2019 and most of it will be consumed by the industrial sector.

The main sources of electrical energy in Brazil are hydro, thermal, wind and solar power as indicated in Table 2.1.

Tab. 2.1: Power Sources in Brazilian Interconnected Power System in 2015. [5]

Power Source	Number of plants	Installed capacity (MW)	% of Installed capacity
Hydro	1,211	94,736.5	64.89%
Thermal	2,879	43,194.3	29.21%
Wind	345	8,422.7	5.88%
Solar	37	26.9	0.02%
Total	4,472	146,380.4	

Thermal generation in Brazil utilizes several types of fuel such as liquefied natural gas (LNG), biomass, petroleum oil, coal, nuclear, among others. Hydro plants are divided as run-of-the-river and reservoir plants. All these different power sources are distributed throughout the country and are interconnected with demand centers by a 126,650 km energy transmission system with tension class varying from 230kV up to 750kV. The Brazilian transmission system also has international connections with Argentina, Uruguay and Paraguay.

It is evident from Table 2.1 that hydro plants are Brazil's main source of electrical energy. Indeed, the hydro system has a multi-year regularization capacity and many hydro plants are located at the same river in a cascade configuration, making the system's topology highly complex as shown in Fig. 2.1. Thus, when making medium-/long-term planning studies it was originally proposed, based on the ideas in [66] and [67], a reduction in the problem dimension by aggregating hydro plants into 4 main reservoirs. A more advanced approach on reservoir aggregation that

[1] Throughout this work decimals will be separated by . and thousands will be separated by ,.

allows subsystems to be hydraulic coupled is presented in [68]. This resulted in four main areas in the system that were named subsystems. The four subsystems are South (S), South-East (SE), North (N) and North-East (NE) as shown in figure 2.2. Node ”Imperatriz” is an actual transshipment node.

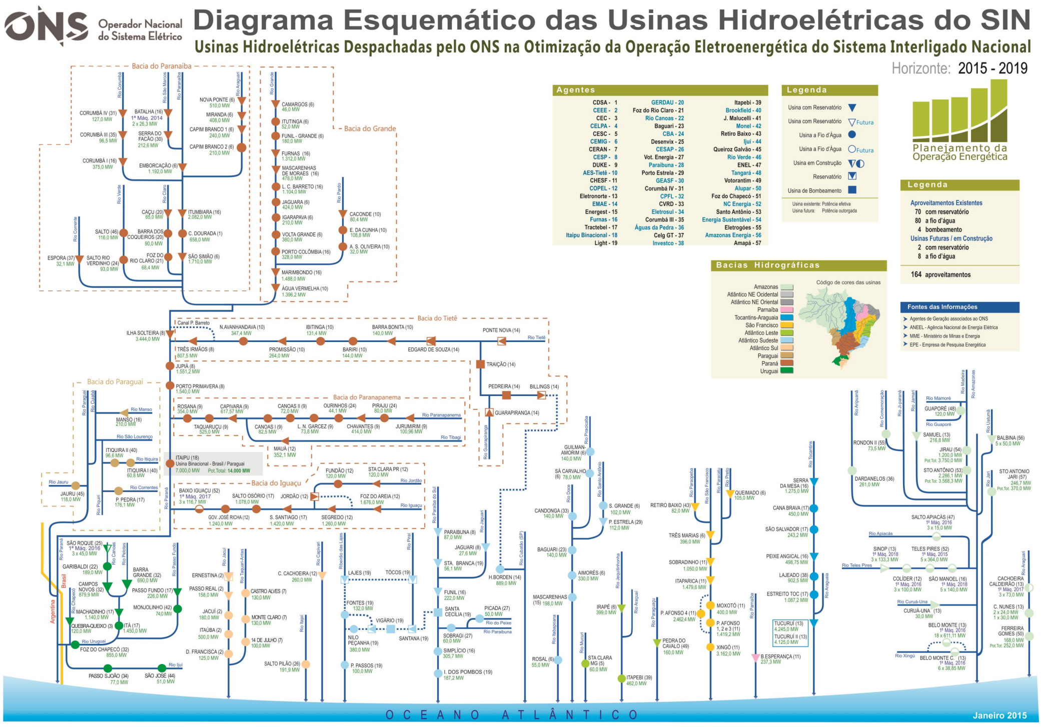

Fig. 2.1: *Brazilian Hydro Plants Connections Schematics [1].*

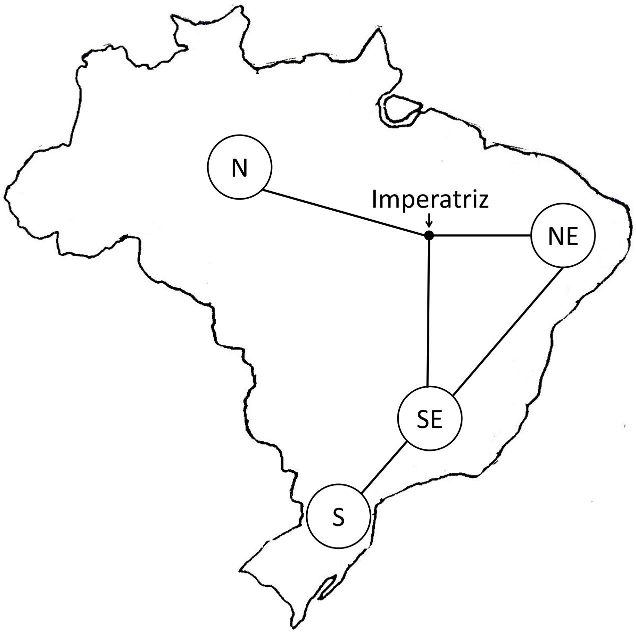

Fig. 2.2: Brazilian Energy Subsystems Schematics.

Typically, Brazil experiences a rain season between the months of November and March and a dry season in the remaining months. Consequently hydro units are most likely to be dispatched between December and March when resources are most likely to be available. The exception to this is the S subsystem as it has a behavior that is the opposite of the other subsystems. Thermal units act mostly as backup sources and tend to be more frequently dispatched in the dry season. Fig. 2.3 shows the average inflow energy at each subsystem between the years of 1931 and 2013 for each month.

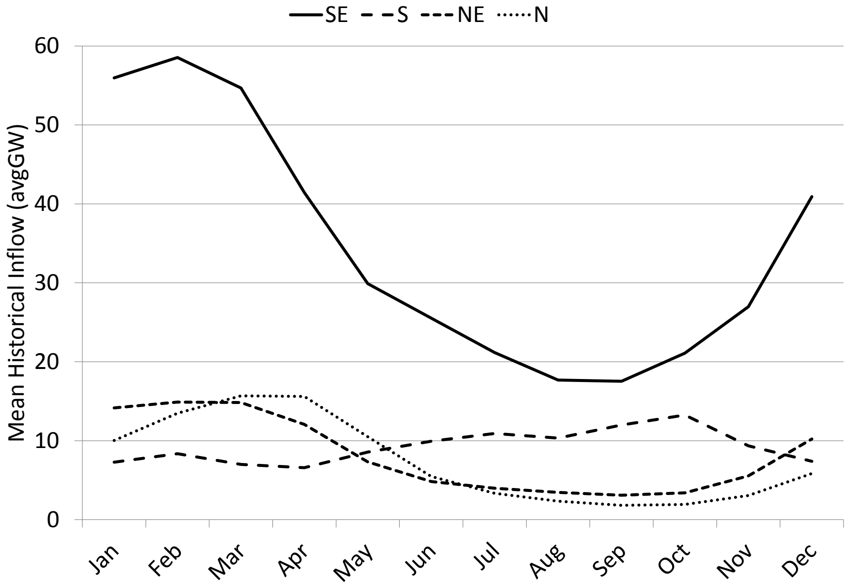

Fig. 2.3: Mean Historical Inflow (1931-2013).

2.1 Renewable Energy in Brazil

In the past years there has been a major attention directed to renewable energy sources worldwide. This is mainly because they present themselves as an alternative to power plants that emit high amounts of greenhouse gas such as thermal power plants. Power sources such as wind, biomass, small hydros and photovoltaic have its share in energy matrices of various countries constantly increased. To exemplify, Fig. 2.4 shows the evolution of wind power in the world over the last years.

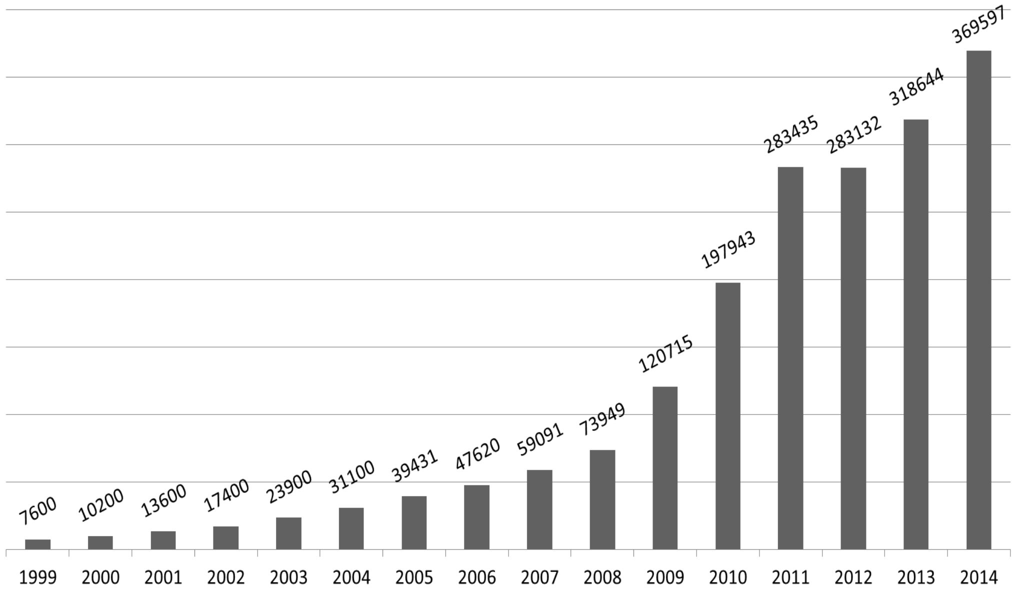

Fig. 2.4: Wind Power Growth Worldwide (MW) [2].

It is evident that wind power penetration is growing exponentially since 1997 in the world. In the end of 2014, China was leading wind power production with about 31% share of the total world production. In second place came the United States of America with a quota of 17.8%.

Brazil currently follows this global tendency and had by the end of 2014 a share of 1.6% of the total wind energy production in the world. As a matter of fact, one of the major guidelines in Brazil energy generation expansion is to focus on renewable energy capacity expansion. It is expected a total growth of 34.685 MW in installed capacity of wind, solar, biomass, and small hydros power with special attention to wind power until 2024. Fig. 2.5 shows the planned amount of renewable energy capacity expansion to be installed in Brazil between the years of 2015 and 2024 by subsystem.

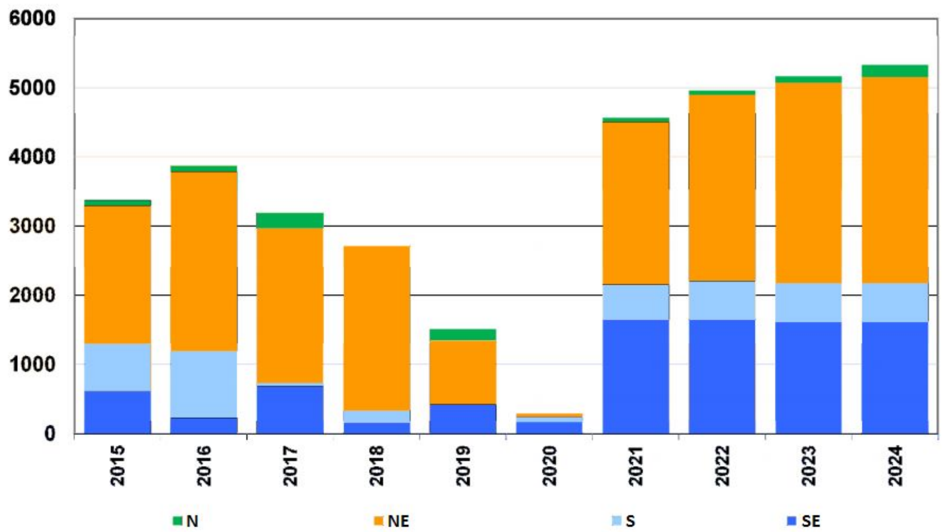

Fig. 2.5: Renewable Energy Expansion in Brazil (MW) [3].

However, even though renewable power sources represent a solid way to achieve a sustainable energy matrix, they are well known to be highly intermittent [69]. Fig. 2.6 shows a pattern of a typical small run-of-river hydro plant in Brazil and Fig. 2.7 shows a pattern for a wind power plant in Brazil. It is clear that there is considerable uncertainty in generation in both sources.

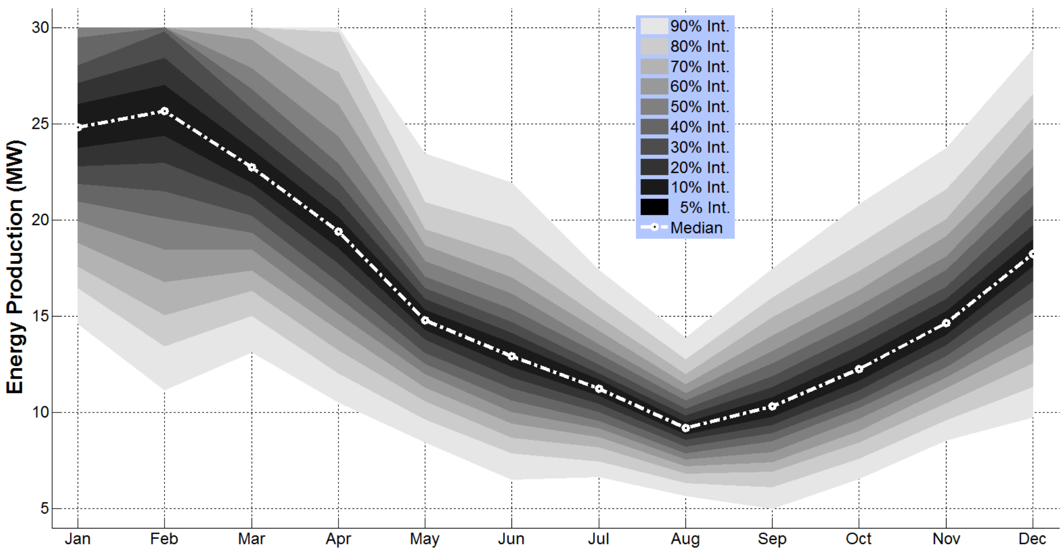

Fig. 2.6: Distribution of energy production of a typical small hydro plant in the Southeastern area of Brazil.

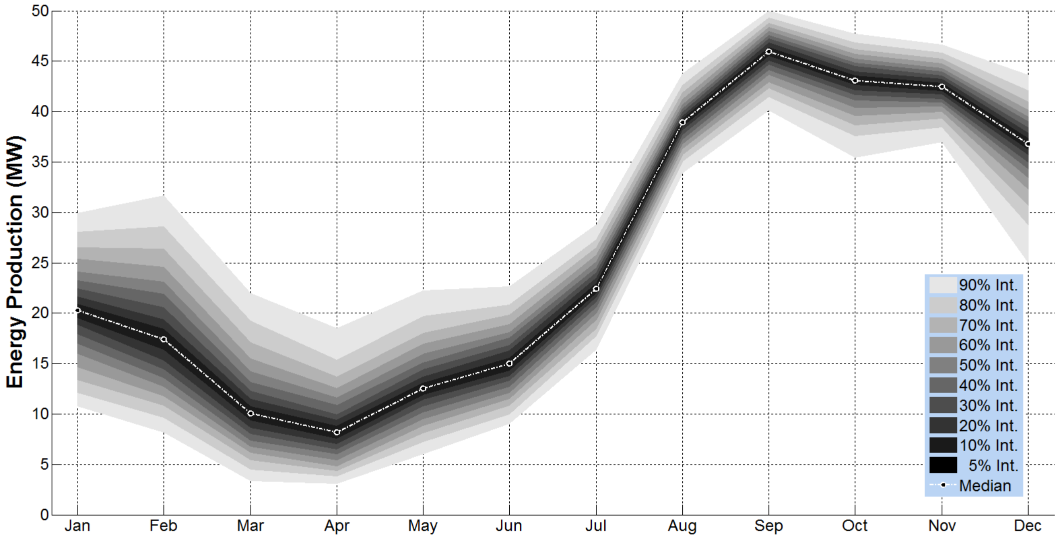

Fig. 2.7: Distribution of energy production of a typical wind farm in the Northeastern area of Brazil

Nevertheless, despite the uncertainty, renewable sources are a major interest of agents in the Brazilian Free Energy Market (see [8,9]). This is because the government has encouraged free energy market participants to trade renewable energy in exchange of a discount of 50% or even 100% in the transmission fees. However, intermittence of these sources poses a major challenge to these agents as they have to plan their portfolio under high levels of uncertainty [9]. This leads agents to be exposed to risks of heavy wealth losses.

Moreover, high penetration of renewable energy injection in the system poses a challenge to ISOs as well [70]. When planning the system for years ahead, the ISO has only a probability distribution of possible renewable injection scenarios. And it is highly difficult to incorporate them in the planning models as the need for many renewable generation scenarios could lead to computational tractability issues. Nowadays in Brazil, no scenario simulation regarding renewable energy output is taken into account in the future planning. The ISO is only informed about the available energy of such sources by agents (see [37]) which, as will be discussed in later sections, may be posing a risk to the system operation.

2.2 Hydrothermal Power Systems Operation in Brazil

The centralized operation of a power system is done in two main steps: (i) planning and (ii) actually implementing it. In either of them the ISO relies on optimization models whose level of detail varies highly depending on the time horizon of the step. For instance, in the actual implementation the level of detail is increased in order to obtain a model that is as close to reality as possible. On the other hand, in the medium-/long-term planning step various system details are neglected so that the problem remains computationally tractable as the problem can grow up to be large scale as it has to take a considerably large number of periods into account. The usual claim is that this will not affect the actual operation of the system and any deviations that occur in the planning step can be taken care of in the day by day decisions.

The planning step is divided into medium-/long-term and short-term. For the former, in the Brazilian electricity sector the NEWAVE software is used. The planning model built in NEWAVE will be hereinafter called NEWAVE model. The long-term planning is done in monthly discretizations encompassing a planning horizon that goes up to 120 months. However, only the first 60 months are actually considered in subsequent studies to avoid end-effects.

The planning problem is highly subjected to uncertainty as the ISO can only access a probability distribution of future inflows. If the operator decides on using water from reservoirs, for example, this results on a low immediate cost due to low usage of thermal units. Nevertheless, this also results in less stored water for subsequent periods which may lead to thermal units being dispatched and consequently in higher operation costs. On the other hand, if the ISO decides on not using water from reservoirs, the immediate cost increases but the chances of future energy deficits decreases even in low inflow scenarios. However, if a high inflow realization takes place, there is water spillage and consequently cheap resources waste. This situation is usually called the ISO's dilemma and is illustrated in Fig. 2.8.

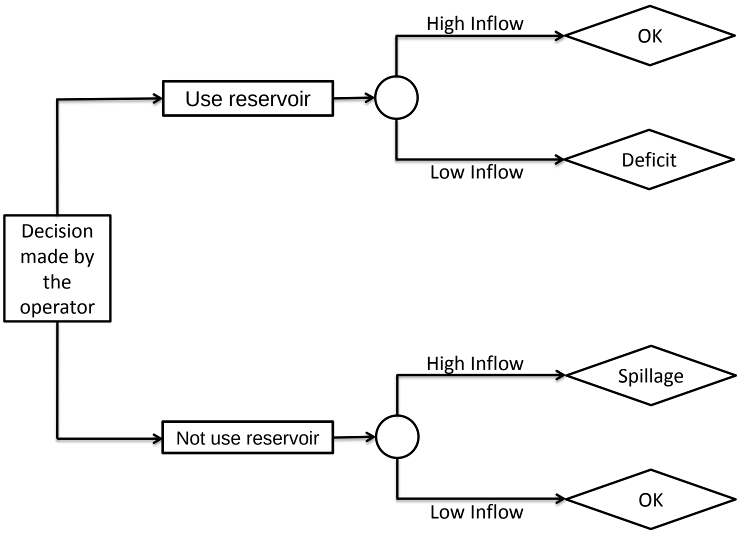

Fig. 2.8: ISO's Dilemma.

As depicted in Fig. 2.2, in the NEWAVE model (see [7]) the system is subdivided in 4 subsystems[2]. By running the NEWAVE model the ISO obtains an expected value and the CVaR of the operation cost for 120 months ahead and a set of the recourse function for each period.

As the problem of planning a hydrothermal power system is stochastic and can easily become large-scale, it is suitable to be solved by the class of Sampling Based Benders Decomposition algorithms. This work will retain its attention to the SDDP method which is used in NEWAVE. Its applicability to power systems planning will be discussed in Chapter 3.

After the medium-/long-term planning step is over, the set of recourse functions obtained will be coupled with the DECOMP software which is responsible for the short-term operation planning. The planning model built in DECOMP will be hereinafter called DECOMP model. The DECOMP model evaluates a planning policy for the system for up to twelve months[3] with the first month being discretized in weekly stages and the remaining planning horizon discretized monthly. A Multistage Benders Decomposition technique (see [71]), which visits all problems in the scenario tree, is used as a solution methodology. Differently from the NEWAVE model, in DECOMP all hydro power plants are modeled individually and other constraints, such as Kirchhoff's Voltage Law in the linear model (DC), are also taken

[2] As of 2016, the NEWAVE model actually comprises 9 equivalent reservoirs divided amongst 4 subsystems.

[3] Only up to two months are used in official studies.

into account. Finally, the last month in DECOMP's planning horizon is coupled with the recourse function evaluated by NEWAVE corresponding to the following month.

Hence, the actual implementation of operation policies in the Brazilian system, which are highly based on outcomes from the short-term planning model (DECOMP), does not follow the same rules as the medium-/long-term planning of the system does. This falls precisely on the definition of time inconsistency defined in [42] and discussed in Chapter 1. The question is whether time inconsistency leads the power system to potentially dangerous states. Water reservoirs situation in Brazil in the year of 2012 reinforce this question. In that year, the Brazilian power system begun the wet season with reservoirs levels reaching a recent historical maximum and ended the same year in a recent historical minimum. Fig 2.9 shows reservoirs levels in percentage of the maximum storage capacity for the SE subsystem. What is intriguing is that no serious drought occurred in 2012. Fig. 2.10 shows for the SE subsystem that inflow realization in percentage of the long-term mean (LTM) in 2012 was higher than 30% of all inflow realizations in the historic.

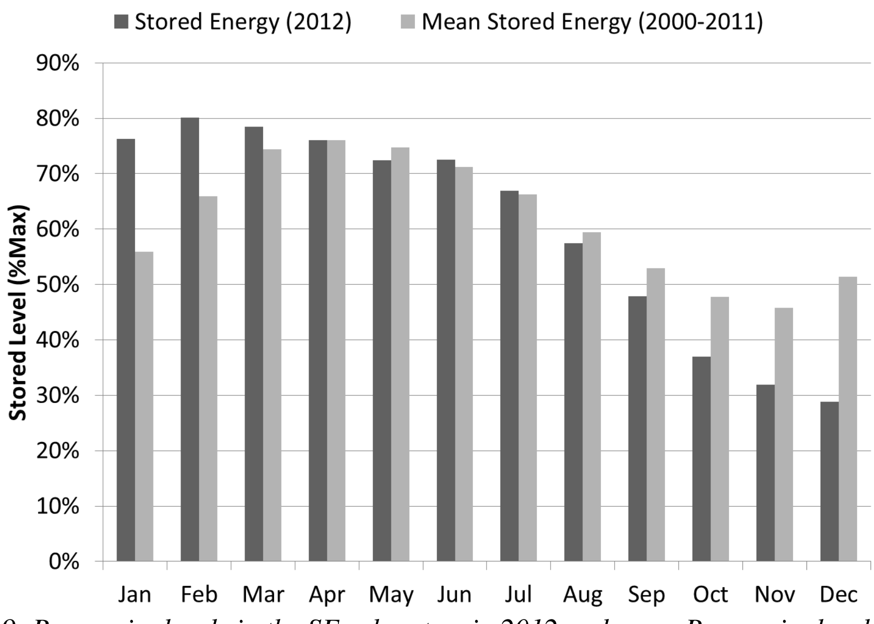

Fig. 2.9: Reservoirs levels in the SE subsystem in 2012 and mean Reservoirs levels between the years of 2000 and 2011. [4]

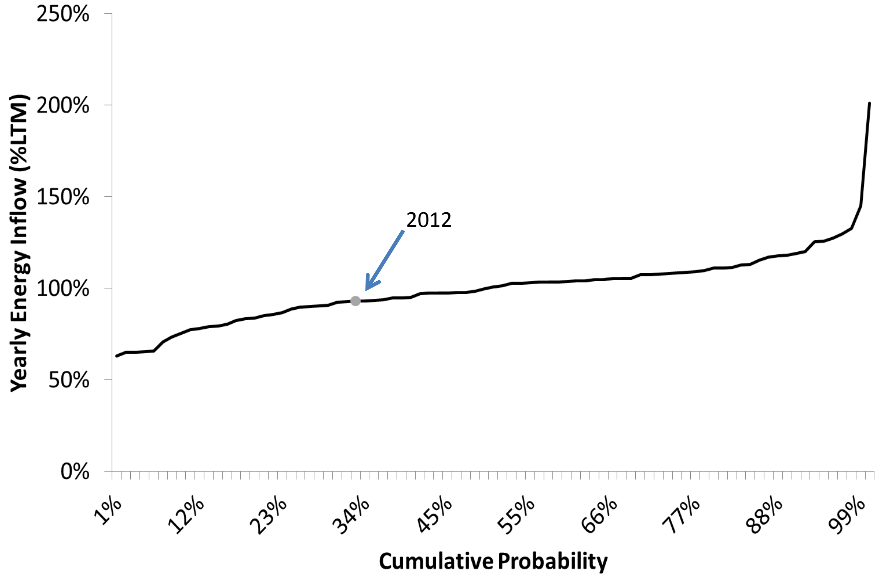

Fig. 2.10: Inflow realization in the SE subsystem [4].

As no security criteria is accounted for in the planning step and in 2012 the $n-3$ security criteria was being implemented, it seems reasonable to further investigate whether the sharp depletion of reservoirs and time inconsistency might indeed be related. Motivated by this, in Chapter 4 a methodology is proposed to investigate whether deviations from what was actually planned to what was implemented might indeed be due to time inconsistency.

3
Stochastic Dual Dynamic Programming

The problem of future planning hydrothermal power systems can become computationally intractable as the number of scenarios and stages grow. A class of sampling-based decomposition algorithms such as SDDP [12] and its variants [13–15] deals with the usual intractability of this type of problems. The attention here is retained to the medium-/long-term power system planning via SDDP algorithm. To begin discussing the SDDP algorithm it is supposed a finite and discrete set Ω_t of scenario inflows. Then, by sampling a scenario $\omega \in \Omega_t$ with probability $p_{t,\omega}$, the core of the models used by the ISO to operate the system can then be described here, in a simplified manner, by problem (3-1)-(3-4) as follows.

$$Q_t(v_{t-1}, \mathrm{w}_{t,\omega}) = \min_{g_t,\ ,v_t,\ y_t,\ f_t} c_t^\top g_t + J \cdot \mathcal{Q}_{t+1}(v_t) \tag{3-1}$$

subject to

$$A_t g_t + B_t y_t + C_t f_t = d_t \tag{3-2}$$

$$H_t y_t = v_{t-1} + \mathrm{w}_{t,\omega} \ : \ (\pi_{t,\omega}) \tag{3-3}$$

$$(v_t,\ y_t,\ g_t, f_t) \ \in \mathcal{X}_t. \tag{3-4}$$

Decision vector y_t encompasses the volume of water discharged (u_t) and spilled (s_t) during period t, and nodal-phase angles (θ_t). That is, $y_t^\top = [u_t^\top \ s_t^\top \ \theta_t^\top]$. Decision vectors g_t, f_t represent thermal generation and power flow in transmission lines respectively. Decision vector v_t represent water stored at the end of period t, whilst $\pi_{t,\omega}$ represent the dual vector associated with constraint (3-3). Constraint (3-2) models the nodal-energy balance, where d_t is the nodal-energy demand vector. Notice that it is considered a single load block. Constraint (3-3) accounts for the water balance equation and plays the role of state-transition function, linking the state of the system between two consecutive periods: $v_{t-1} \mapsto v_t$. In (3-3) $\mathrm{w}_{t,\omega}$ accounts for inflow realization at period t and scenario ω. Set $\mathcal{X}_t$ in constraint (3-4) accounts for bounds and other constraints such as second Kirchhoff's Voltage Law.

The recourse function $\mathcal{Q}_{t+1}(v_t)$ can be defined as the following:

$$\mathcal{Q}_{t+1}(v_t) = \sum_{\omega \in \Omega_{t+1}} p_{t+1,\omega} Q_{t+1}(v_t, \mathrm{w}_{t+1,\omega}). \tag{3-5}$$

The recourse function is a real-valued function that associates to each state of the system at the end of a given stage t (period of time) a measure of the optimal operation cost of the following, $t+1$, until the end of the time horizon. This function provides ISOs with a policy rule comprising a sequence of decisions made under the revelation of states induced by the uncertain parameters (generally, inflows and demand). Finally, J is a discount factor used to compute the present value of the expected future operation cost.

The main idea of the SDDP method is to iteratively construct an outer approximation of the recourse function using Benders cuts, or just *cuts*, to obtain a lower approximation for it. Afterwards, a simulation procedure can be used to evaluate the policy. In this section a brief explanation of the SDDP algorithm functionality is given, for a more detailed explanation and discussions of the SDDP algorithm refer to [34] and [17]. For the sake of simplicity and didactic purposes, in each iteration, m, the algorithm performs a *forward step* consisting of one sampled scenario and a feasible path of states, $\{v_t^{(m)}\}_{t=1}^{T}$, often called *trial points*, is evaluated based on the approximated recourse function. Then, the algorithm performs a *backward step* in which a single cut is found for each stage, $t = T-1, \ldots, 1$, and used to improve the approximation of the recourse function by its inclusion into the set of cuts $\mathcal{K}^{(m)}$.

More specifically, in a given iteration, m, of the method, the $t+1$ recourse function in (3-1) is replaced by an auxiliary decision variable α_{t+1} and the following set of cuts:

$$\alpha_{t+1} \geq \tilde{\mathcal{Q}}_{t+1}^{(k)}(v_t^{(k)}) + \left(\tilde{\pi}_{t+1}^{(k)}\right)^{\top}(v_t - v_t^{(k)});\ \forall k \in \mathcal{K}^{(m)}, \tag{3-6}$$

where, $\tilde{\mathcal{Q}}_{t+1}^{(k)}(v_t^{(k)}) = \sum_{\omega \in \Omega_{t+1}} p_{t+1,\omega} \tilde{Q}_{t+1}^{(k)}(v_t^{(k)}, \mathrm{w}_{t+1,\omega})$ and $\tilde{\pi}_{t+1}^{(k)} = \sum_{\omega \in \Omega_{t+1}} p_{t+1,\omega} \tilde{\pi}_{t+1,\omega}^{(k)}$. Function $\tilde{\mathcal{Q}}_t^{(k)}$ is the resulting approximated function by cuts in (3-6). Note that as $\mathcal{Q}_{T+1} \equiv 0$ then $\tilde{Q}_T^{(k)} = Q_T$ for all k. As a consequence of this change in model (3-1)-(3-4), a (lower) approximation for the recourse function of period t in a given iteration m of the algorithm can be found by the following linear program:

$$\tilde{Q}_t^{(m)}(v_{t-1}, \mathrm{w}_{t,\omega}) = \min_{\substack{g_t,\ v_t,\ y_t,\ f_t,\\ \alpha_{t+1}}} c_t^{\top} g_t + J \cdot \alpha_{t+1} \tag{3-7}$$

subject to

$$A_t g_t + B_t y_t + C_t f_t = d_t \tag{3-8}$$

$$H_t y_t = v_{t-1} + \mathrm{w}_{t,\omega} \ : \ (\tilde{\pi}_{t,\omega}^{(m)}) \tag{3-9}$$

$$(v_t,\ y_t,\ g_t, f_t) \ \in \mathcal{X}_t. \tag{3-10}$$

$$\alpha_{t+1} \geq \tilde{\mathcal{Q}}_{t+1}^{(k)}(v_t^{(k)}) + \left(\tilde{\pi}_{t+1}^{(k)}\right)^{\top} (v_t - v_t^{(k)});\ \forall k \in \mathcal{K}^{(m)}. \tag{3-11}$$

In problem (3-7)-(3-11), the optimal value of α_{t+1} describes the maximum within all cuts used to approximate the recourse function of stage $t+1$. Hence, for $t = 2, \ldots, T$, (3-7)-(3-11) converges to (3-1)-(3-4). The object value of the approximated problem in the first stage is referred to as lower bound $(\underline{z})$ and an estimator for the expected total operation cost is referred to as upper bound $(\overline{z})$.

Finite convergence proof for the class of sampling-based decomposition algorithms appeared for the first time in [13] for the CUPPS algorithm. Then in [72] the authors used the proof for the CUPPS algorithms convergence and gave a general proof under mild regularity conditions for the class of algorithms discussed here. One key issue taken into account to ensure convergence is the independence of scenarios and the need to re-sample scenarios in the forward pass. Then in [73] the authors gave a simpler proof for the sampling-based decomposition algorithms class based on the finiteness of the set of distinct cut coefficients. There are also discussions regarding convergence for models with convex sub-problems [74] and convex stochastic control problems not necessarily linear [75].

However, key points of these proofs such as the need to re-sample scenarios in the forward step could lead the convergence to take unreasonable computational times as the number of scenarios grow. In this sense, one must choose a stopping criteria for the algorithm. It was originally proposed in [12] that the algorithm should stop whenever the lower bound exceeds the inferior quantile of the 95% confidence interval of the upper bound. In [17], however, the author claims that such stopping criteria could be too optimistic. A stopping criteria based on hypothesis test is given in [18]. Three different hypothesis tests to stop the algorithm are presented and all of them present flaws such as premature convergence or on the other extreme, convergence might never be achieved due to over-conservativeness of the test. The authors in [19] use a maximum number of iterations criteria. It gives no convergence guarantee but it is a good approach for comparing results of different experiments. Another proposed approach is stopping the algorithm when the lower bound stabilizes [17]. Although results point out that this approach may give a superior solution quality, there is no guarantee that a given policy is optimal. Finally, [17] suggests stopping the algorithm when the lower bound exceeds a give superior quantile for the upper bound estimate. Even though this seems a better approach when compared to what was originally proposed in [12], computational experiments also show that depending on the choice of parameters, this criterion could also be too conservative and convergence might never be achieved. Thus, literature is yet to present a satisfying stopping criteria for the SDDP method. However, aiming to devise high-quality solutions, and giving up from achieving theoretical convergence [17, 73], in this work the SDDP algorithm is stopped based on a heuristic stopping criterion that checks the stabilization of the upper and lower bound. In this procedure, a large number of iterations (each one comprised by one *forward* followed by one *backward step*) is carried out, e.g., 1000, and after that an *evaluation step* is performed based on a simulation of the system (for a large number of simulated scenarios[1]) in order to assess the average cost obtained by means of current approximations for the recourse functions.

Thereby, the stopping criterion is devised by means of the following steps:

Algorithm 1 Stopping criteria

1: a few additional iterations are carried out, say, 100, in order to enhance recourse functions approximation and a new *evaluation step* is performed by means of newly generated large sample of inflows;

2: a hypothesis test for checking the significance of the difference between the average of two random samples is performed with the current and previous simulated scenarios obtained from the last two *evaluation steps*;

3: the difference between lower bounds obtained for the last two *evaluation steps* is computed;

4: finally, if both the hypothesis test do not reject the null hypothesis (two samples may come from distributions with equal averages) and the lower bound increase lies within a given tolerance, say, 1%, then the algorithm stops;

5: Else, if one of the two conditions are not verified in step 4, then the algorithm continues and we go back to step 1.

Summing it up, the SDDP algorithm discussed in this work can be written as:

[1] It is important to mention that the number of scenarios for the *evaluation step* should be calibrated in order to ensure a maximum estimation error under a given confidence level. For instance, the confidence interval distance from the average estimative (the error) should be limited to, e.g., 5% of the estimated cost in order to avoid premature convergence when increasing the confidence level as argued in [17]

Algorithm 2 SDDP Algorithm

Require: Initial state v_0.

1: Set $m \leftarrow 1$ and $m_e = 1000$.

Forward Step

2: Sample one scenario path.

3: **for** $t \leftarrow 1, \dots, T-1$ **do**

4: Solve (3-7)-(3-11) and store $v_t^{(m)}$.

5: **end for**

Backward Step

6: **for** $t \leftarrow T, \dots, 2$ **do**

7: **for** each $\omega \in \Omega_t$ **do**

8: Solve (3-7)-(3-11) with $\mathrm{w}_{t,\omega}$ and $v_{t-1}^{(m)}$ storing $\tilde{Q}_t^{(m)}(v_{t-1}^{(m)}, \mathrm{w}_{t,\omega})$ and $\tilde{\pi}_{t,\omega}^{(m)}$.

9: **end for**

10: Evaluate the cut as in (3-6) and store them in $\mathcal{K}^{(m)}$.

11: **end for**

12: Solve (3-7)-(3-11) for all $\omega \in \Omega_1$ to evaluate the lower bound as $\underline{z} = \sum_{\omega \in \Omega_1} p_{1,\omega} \tilde{Q}_1^{(m)}(v_0, w_{1,\omega})$

13: **if** $m = m_e$ **then**

14: Run evaluation step according to Algorithm 1 to check convergence.

15: **if** $convergence = true$ **then** stop the algorithm **end if**

16: Set $m_e \leftarrow m_e + 100$

17: **end if**

18: Set $m \rightarrow m + 1$ and go to step 2

3.1 Illustrative Example

In this section a simple example is given in order to illustrate the SDDP method functionality. Suppose a three-bus power system as shown in Fig. 3.1. The system has one hydro generator connected at bus 1, a cheap and an expensive thermal generator connected at buses 2 and 3 respectively. The planning horizon is equal to $T = 3$ with $|\Omega_t| = 2 \, \forall t \in \{1, 2, 3\}$. Energy demand is constant at $100MWh$ and inflow scenarios are as follows: $\mathrm{w}_{1,1} = 80m^3$, $\mathrm{w}_{1,2} = 40m^3$, $\mathrm{w}_{2,1} = 70m^3$, $\mathrm{w}_{2,2} = 35m^3$, $\mathrm{w}_{3,1} = 60m^3$ and $\mathrm{w}_{3,2} = 30m^3$ all with same probability. For didactic purposes, the hydro production coefficient is supposed to be $1MW/m^3$.

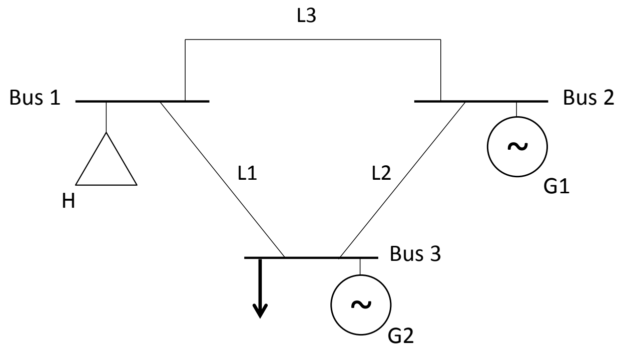

Fig. 3.1: Three Bus System

Table 3.1 shows data for thermal generators, table 3.2 shows data for the hydro generator and finally, table 3.3 shows data for transmission lines.

Tab. 3.1: Thermal Generator Data

Thermal Unit	c R$/MWh	$\overline{G}$ MW	$\underline{G}$ MW
G_1	20	20	0
G_2	100	50	0

Tab. 3.2: Hydro Generator Data (m^3)

Hydro Unit	$\overline{V}$	$\overline{U}$	v_0
H	150	100	50

Tab. 3.3: Transmission Lines Data (MW)

Transmission Line	$\overline{F}$
T_1	100
T_2	70
T_3	30

Applying the SDDP algorithm for the proposed power system we have for any t:

$$\tilde{Q}_t^{(m)}(v_{t-1}^{(m)}, \mathrm{w}_{t,\omega}) = \min_{\substack{\mathbf{g}_t,\, v_t,\, u_t,\\ s_t,\, \mathbf{f}_t,\, \alpha_{t+1}}} \; 20g_{1,t} + 100g_{2,t} + \alpha_{t+1} \tag{3-12}$$

subject to

$$u - f_{1,t} - f_{3,t} = 0 \tag{3-13}$$

$$g_{1,t} - f_{2,t} + f_{3,t} = 0 \tag{3-14}$$

$$g_{2,t} + f_{1,t} + f_{2,t} = 100 \tag{3-15}$$

$$v_t = v_{t-1}^{(m)} + \mathrm{w}_{t,\omega} - u_t - s_t : (\pi_{t,\omega}^{(m)}) \tag{3-16}$$

$$0 \leq g_{1,t} \leq 20 \tag{3-17}$$

$$0 \leq g_{2,t} \leq 50 \tag{3-18}$$

$$0 \leq v_t \leq 150 \tag{3-19}$$

$$-100 \leq f_{1,t} \leq 100 \tag{3-20}$$

$$-70 \leq f_{2,t} \leq 70 \tag{3-21}$$

$$-30 \leq f_{3,t} \leq 30 \tag{3-22}$$

$$\alpha_{t+1} \geq \tilde{\mathcal{Q}}_{t+1}^{(k)}(v_t^{(k)}) + \tilde{\pi}_{t+1}^{(k)}(v_t - v_t^{(k)});\ \forall k \in \mathcal{K}^{(m)}. \tag{3-23}$$

More specifically, in the forward step of the SDDP algorithm, at the first iteration $(m = 1)$ and supposing scenario $\omega = 1$ was sampled we have for $t = 1$:

$$\min_{\substack{\mathbf{g}_1,\, v_1,\, u_1,\\ s_1,\, \mathbf{f}_1,\, \alpha_2}} \; 20g_{1,1} + 100g_{2,1} + \alpha_2 \tag{3-24}$$

subject to

$$u_1 - f_{1,1} - f_{3,1} = 0 \tag{3-25}$$

$$g_{1,1} - f_{2,1} + f_{3,1} = 0 \tag{3-26}$$

$$g_{2,1} + f_{1,1} + f_{2,1} = 100 \tag{3-27}$$

$$v_1 = 50 + 80 - u_1 - s_1 : (\pi_{1,1}^{(1)}) \tag{3-28}$$

$$0 \leq g_{1,1} \leq 20 \tag{3-29}$$

$$0 \leq g_{2,1} \leq 50 \tag{3-30}$$

$$0 \leq v_1 \leq 150 \tag{3-31}$$

$$-100 \leq f_{1,1} \leq 100 \tag{3-32}$$

$$-70 \leq f_{2,1} \leq 70 \tag{3-33}$$

$$-30 \leq f_{3,1} \leq 30 \tag{3-34}$$

$$\alpha_2 \geq 0. \tag{3-35}$$

Solution to problem (3-24)-(3-35) is $u_1 = 100m^3$, $g_{1,1} = g_{2,1} = 0MW$. As a consequence, the volume stored in reservoir at the end of period 1 is $v_1 = 30m^3$. Then, at $t = 2$ suppose scenario $\omega = 1$ is sampled from Ω_2, the inflow is then equal to $\mathrm{w}_{2,1} = 70m^3$ and the following problem is solved:

$$\min_{\substack{\mathbf{g}_2,\, v_2,\, u_2,\\ s_2,\, \mathbf{f}_2,\, \alpha_3}} \; 20g_{1,2} + 100g_{2,2} + \alpha_3 \tag{3-36}$$

subject to

$$u_2 - f_{1,2} - f_{3,2} = 0 \tag{3-37}$$

$$g_{1,2} - f_{2,2} + f_{3,2} = 0 \tag{3-38}$$

$$g_{2,2} + f_{1,2} + f_{2,2} = 100 \tag{3-39}$$

$$v_2 = 30 + 70 - u_2 - s_2 : (\pi_{2,1}^{(1)}) \tag{3-40}$$

$$0 \leq g_{1,2} \leq 20 \tag{3-41}$$

$$0 \leq g_{2,2} \leq 50 \tag{3-42}$$

$$0 \leq v_2 \leq 150 \tag{3-43}$$

$$-100 \leq f_{1,2} \leq 100 \tag{3-44}$$

$$-70 \leq f_{2,2} \leq 70 \tag{3-45}$$

$$-30 \leq f_{3,2} \leq 30 \tag{3-46}$$

$$\alpha_3 \geq 0. \tag{3-47}$$

Again, the total outflow is $u_2 = 100m^3$ and thermal generators are not dispatched. But now the reservoir is totally depleted ($v_2 = 0m^3$).

Then the SDDP algorithm performs the backward step, starting at $t = 3$. The following problem is solved for scenario $\omega = 1$:

$$\tilde{Q}_t^{(3)}(0, 60) = \min_{\substack{\mathbf{g}_3,\, v_3,\, u_3,\\ s_3,\, \mathbf{f}_3}} \; 20g_{1,3} + 100g_{2,3} \tag{3-48}$$

subject to

$$u_3 - f_{1,3} - f_{3,3} = 0 \tag{3-49}$$

$$g_{1,3} - f_{2,3} + f_{3,3} = 0 \tag{3-50}$$

$$g_{2,3} + f_{1,3} + f_{2,3} = 100 \tag{3-51}$$

$$v_3 = 0 + 60 - u_3 - s_3 : (\tilde{\pi}_{3,1}^{(1)}) \tag{3-52}$$

$$0 \leq g_{1,3} \leq 20 \tag{3-53}$$
$$0 \leq g_{2,3} \leq 50 \tag{3-54}$$
$$0 \leq v_3 \leq 150 \tag{3-55}$$
$$-100 \leq f_{1,3} \leq 100 \tag{3-56}$$
$$-70 \leq f_{2,3} \leq 70 \tag{3-57}$$
$$-30 \leq f_{3,3} \leq 30 \tag{3-58}$$
$$\tag{3-59}$$

In this case, optimal solutions are $u_3 = 60m^3$, $g_{1,3} = 20MW$ and $g_{2,3} = 20MW$. Note that the total cost of this operation is R$2400, thus $Q_3^{(1)}(0, 60) = 2400$. Dual variable solution is $\pi_{3,1}^{(1)} = -100$. Then the SDDP algorithm solves for inflow scenario $\omega = 2$ the following problem for $t = 3$:

$$\tilde{Q}_t^{(1)}(0, 30) = \min_{\substack{\mathbf{g}_3,\, v_3,\, u_3,\\ s_3,\, \mathbf{f}_3}} \quad 20g_{1,3} + 100g_{2,3} \tag{3-60}$$

subject to

$$u_3 - f_{1,3} - f_{3,3} = 0 \tag{3-61}$$
$$g_{1,3} - f_{2,3} + f_{3,3} = 0 \tag{3-62}$$
$$g_{2,3} + f_{1,3} + f_{2,3} = 100 \tag{3-63}$$
$$v_3 = 0 + 30 - u_3 - s_3 : (\tilde{\pi}_{3,2}) \tag{3-64}$$
$$0 \leq g_{1,3} \leq 20 \tag{3-65}$$
$$0 \leq g_{2,3} \leq 50 \tag{3-66}$$
$$0 \leq v_3 \leq 150 \tag{3-67}$$
$$-100 \leq f_{1,3} \leq 100 \tag{3-68}$$
$$-70 \leq f_{2,3} \leq 70 \tag{3-69}$$
$$-30 \leq f_{3,3} \leq 30 \tag{3-70}$$
$$\tag{3-71}$$

Optimal solutions are $u_3 = 30m^3$, $g_{1,3} = 20$ and $g_{2,3} = 50$ and a cost of R$5400, that is $\tilde{Q}_3^{(1)}(0, 30) = 5400$. Solution for the dual variable is again $\tilde{\pi}_{3,1}^{(1)} = -100$. Now the algorithm can evaluate an approximation for the recourse function at $t = 2$

given by the following cut:

$$\alpha_3 \geq \frac{2400 + 5400}{2} + \frac{-100 - 100}{2}(v_2 - 0) = 3900 - 100v_2. \tag{3-72}$$

This cut is stored in set $\mathcal{K}^{(m)}$. Then, the backward step continues at $t = 2$ but accounting for the newly added cut. For $\omega = 1$, the following problem is solved:

$$\tilde{Q}_2^{(1)}(30, 70) = \min_{\substack{\mathbf{g}_2,\, v_2,\, u_2, \\ s_2,\, \mathbf{f}_2,\, \alpha_3}} \; 20g_{1,2} + 100g_{2,2} + \alpha_3 \tag{3-73}$$

subject to

$$u_2 - f_{1,2} - f_{3,2} = 0 \tag{3-74}$$

$$g_{1,2} - f_{2,2} + f_{3,2} = 0 \tag{3-75}$$

$$g_{2,2} + f_{1,2} + f_{2,2} = 100 \tag{3-76}$$

$$v_2 = 30 + 70 - u_2 - s_2 : (\tilde{\pi}_{2,1}) \tag{3-77}$$

$$0 \leq g_{1,2} \leq 20 \tag{3-78}$$

$$0 \leq g_{2,2} \leq 50 \tag{3-79}$$

$$0 \leq v_2 \leq 150 \tag{3-80}$$

$$-100 \leq f_{1,2} \leq 100 \tag{3-81}$$

$$-70 \leq f_{2,2} \leq 70 \tag{3-82}$$

$$-30 \leq f_{3,2} \leq 30 \tag{3-83}$$

$$\alpha_3 \geq 3900 - 100v_2. \tag{3-84}$$

With the introduction of the cut (3-84) the optimal solutions are $u_2 = 61m^3$ $g_{1,2} = 20$ and $g_{2,2} = 19$. Note that it is already different from solution of problem (3-48)- (3-58). The total operation cost is R$2300 ($\tilde{Q}_2^{(1)}(30, 70) = 2300$) and the dual variable is $\tilde{\pi}_{2,1}^{(1)} = -100$. The future cost given by α_3 is zero. Then, the algorithm solves for $\omega = 2$ the following problem:

$$\tilde{Q}_2^{(1)}(30, 35) = \min_{\substack{\mathbf{g}_2,\, v_2,\, u_2, \\ s_2,\, \mathbf{f}_2,\, \alpha_3}} \; 20g_{1,2} + 100g_{2,2} + \alpha_3 \tag{3-85}$$

subject to

$$u_2 - f_{1,2} - f_{3,2} = 0 \tag{3-86}$$

$$g_{1,2} - f_{2,2} + f_{3,2} = 0 \tag{3-87}$$

$$g_{2,2} + f_{1,2} + f_{2,2} = 100 \tag{3-88}$$

$$v_2 = 30 + 35 - u_2 - s_2 : (\tilde{\pi}_{2,2}) \tag{3-89}$$

$$0 \leq g_{1,2} \leq 20 \tag{3-90}$$

$$0 \leq g_{2,2} \leq 50 \tag{3-91}$$

$$0 \leq v_2 \leq 150 \tag{3-92}$$

$$-100 \leq f_{1,2} \leq 100 \tag{3-93}$$

$$-70 \leq f_{2,2} \leq 70 \tag{3-94}$$

$$-30 \leq f_{3,2} \leq 30 \tag{3-95}$$

$$\alpha_3 \geq 3900 - 100v_2. \tag{3-96}$$

Optimal solutions are $u_2 = 65m^3$, $g_{1,2} = 20MW$ and $g_{2,2} = 15MW$. The operation cost is R\$5800 ($\tilde{Q}_2^{(1)}(30, 35) = 5800$) with α_3 equals to R\$3900. Dual variable solution is $\tilde{\pi}_{2,1}^{(1)} = -100$. Then an approximation for the recourse function at $t = 2$ can be approximated by the following cut:

$$\alpha_2 \geq \frac{2300 + 5800}{2} + \frac{-100 - 100}{2}(v_1 - 0) = 4050 - 100v1. \tag{3-97}$$

Then, the algorithm evaluates the lower bound. Setting $t = 1$ the algorithm solves for scenario $\omega = 1$ the following problem:

$$\tilde{Q}_1^{(1)}(50, 80) = \min_{\substack{\mathbf{g}_1,\, v_1,\, u_1, \\ s_1,\, \mathbf{f}_1,\, \alpha_2}} 20g_{1,1} + 100g_{2,1} + \alpha_2 \tag{3-98}$$

subject to

$$u_1 - f_{1,1} - f_{3,1} = 0 \tag{3-99}$$

$$g_{1,1} - f_{2,1} + f_{3,1} = 0 \tag{3-100}$$

$$g_{2,1} + f_{1,1} + f_{2,1} = 100 \tag{3-101}$$

$$v_1 = 50 + 80 - u_1 - s_1 \tag{3-102}$$

$$0 \leq g_{1,1} \leq 20 \tag{3-103}$$

$$0 \leq g_{2,1} \leq 50 \tag{3-104}$$

$$0 \leq v_1 \leq 150 \tag{3-105}$$

$$-100 \leq f_{1,1} \leq 100 \tag{3-106}$$

$$-70 \leq f_{2,1} \leq 70 \tag{3-107}$$

$$-30 \leq f_{3,1} \leq 30 \tag{3-108}$$

$$\alpha_2 \geq 4050 - 100v1. \tag{3-109}$$

Optimal solution to this problem is $\tilde{Q}_1^{(1)}(30, 35) = 210$. Then, the algorithm solves also for $t = 1$ and scenario $\omega = 2$ the following problem:

$$\tilde{Q}_1^{(1)}(50, 40) = \min_{\substack{\mathbf{g}_1,\, v_1,\, u_1,\\ s_1,\, \mathbf{f}_1,\, \alpha_2}} \; 20g_{1,1} + 100g_{2,1} + \alpha_2 \tag{3-110}$$

subject to

$$u_1 - f_{1,1} - f_{3,1} = 0 \tag{3-111}$$

$$g_{1,1} - f_{2,1} + f_{3,1} = 0 \tag{3-112}$$

$$g_{2,1} + f_{1,1} + f_{2,1} = 100 \tag{3-113}$$

$$v_1 = 50 + 40 - u_1 - s_1 \tag{3-114}$$

$$0 \leq g_{1,1} \leq 20 \tag{3-115}$$

$$0 \leq g_{2,1} \leq 50 \tag{3-116}$$

$$0 \leq v_1 \leq 150 \tag{3-117}$$

$$-100 \leq f_{1,1} \leq 100 \tag{3-118}$$

$$-70 \leq f_{2,1} \leq 70 \tag{3-119}$$

$$-30 \leq f_{3,1} \leq 30 \tag{3-120}$$

$$\alpha_2 \geq 4050 - 100v1. \tag{3-121}$$

Optimal solution to this problem is $\tilde{Q}_1^{(1)}(50, 80) = 3450$. Hence, the evaluated lower bound by the SDDP method at this iteration is:

$$\underline{z} = \frac{210 + 3450}{2} = 1830. \tag{3-122}$$

Then the algorithm goes back to the forward step and the same procedure described is repeated until convergence is tested.

The SDDP algorithm described in this section will play a major role in this work. In chapter 4 it will be proposed a further extensions of it in order to evaluate the cost and effects of time inconsistency in hydrothermal power systems planning. Then in chapter 5 it will be used together with the Column-Constraint Generation algorithm to tackle the hybrid robust-stochastic model proposed. The same basic procedure described here will still be valid as well as convergence and stopping criteria.

4
Time Inconsistency in Hydrothermal Power Systems Operation

Due to tractability issues associated with the SDDP algorithm convergence, it is usual to run the algorithm for a simplified model of the system. Generally, the simplified model is less restricted than the original one. Thus, the solution of the former is an optimistic view of the system. This automatically gives rise to a sub-optimal recourse function.[1].

It is recognized that, in practice, simplifications are accompanied by some restrictive measures in order to mitigate the optimistic effect caused by simplifications in planning models. Nevertheless, hardly such restrictions are well calibrated and reproduce the correct effects (it is not trivial to find the restrictions that approximates the simplified model to the operative reality)[2].

In the Brazilian electricity sector, the implemented policy is a sort of hybrid decision rule: it is conceived under a rolling-horizon scheme in which the first-stage decisions are made with the detailed model of the system but using a recourse function obtained with a simplified version of it. In such case, the ISO converges the SDDP algorithm running many forward and backward steps using the simplified model for the planning step. However, to obtain the first-stage decision that is actually going to be implemented, the simplified-recourse function is coupled with a problem that considers a more detailed model for the system. In the following period, the aforementioned procedure is repeated using as initial condition the state of the system achieved in the previous step. Therefore, after some iterations of this process, the implemented decisions may deviate from those devised in the first planning step. In this scenario, we can state that the obtained policy is not optimal neither for the simplified model nor for the detailed one.

One natural question to ask is how much these time inconsistent policies might be negatively affecting system operation. That is, how much does a sub-optimal recourse function leads the operation to potentially dangerous sates and consequently higher operation costs. This Chapter proposes a methodology to as-

[1] Note that if the solution of the former was, on the other hand, a pessimistic view of the system, a sub-optimal recourse function would still be obtained. However, in this work the focus is set to the pessimistic case.

[2] It is interesting to comment that the methodology introduced in this Chapter is an analysis tool to verify whether such restrictions are indeed adequate.

sess the states that might be implemented when sub-optimal recourse functions are coupled with the detailed implementation models. Then, following the ideas in [42] a time inconsistency gap measure is proposed.

4.1 Measuring time inconsistency in dynamic models

In this section a framework is devised to evaluate policies that makes use of two different models for the system, one for the planning step and another for implementing decisions. To do that, we assume that the result of the planning step is a sequence of recourse functions, $\{\mathcal{Q}_t^{plan}\}_{t=1}^{T}$, approximated by the solution of the SDDP algorithm applied to problem (3-1)-(3-4), obtained using a certain model for the system, hereinafter called planning model. The planning model is defined by $\mathcal{X}_t^{plan}$ and $\{\mathcal{Q}_t^{plan}\}_{t=1}^{T}$ is obtained by replacing $\mathcal{X}_t$ by $\mathcal{X}_t^{plan}$ in (3-4).

Additionally, it is defined as implemented decisions for period t, under a given scenario ω and planning-recourse function, $\mathcal{Q}_t^{plan}$, the solution of the following problem:

$$\min_{v_t,\, y_t,\, g_t,\, f_t} \; c_t^\top g_t + J \cdot \mathcal{Q}_{t+1}^{plan}(v_t) \tag{4-1}$$

$$\text{subject to: } Ag_t + By_t + Cf_t = d_t \tag{4-2}$$

$$v_t + H_t y_t = v_{t-1} + \mathrm{w}_{t,\omega} \, : \; (\pi_{t,\omega}) \tag{4-3}$$

$$(v_t,\; y_t,\; g_t,\; f_t) \in \mathcal{X}_t^{imp}. \tag{4-4}$$

Note that in (4-1)-(4-4), the first-stage decisions, for period t, belongs to $\mathcal{X}_t^{imp}$, which can be different from $\mathcal{X}_t^{plan}$, the one used in the planning step to obtain $\mathcal{Q}_{t+1}^{plan}$. In this scheme, model (4-1)-(4-4) assumes the existence of a planning step where $\mathcal{Q}_{t+1}^{plan}$ is previously obtained (approximated) by means of the SDDP algorithm.

In this framework, we can build a set of M sampled scenario paths of implemented decisions, for the entire study horizon $(1, ..., T)$, by successively applying (4-1)-(4-4). This set can be used to devise an evaluation metric for such rolling-horizon decision rule (policy). In order to create a coherent path of decisions, we need to concatenate consecutive decisions for each scenario ω in the sample. In this process, we update the initial condition, v_{t-1}, in (4-1)-(4-4), with its previous stage implemented solution for reservoir storages at the end of period $t-1$. Thus, we refer to the set of M sampled paths of implemented decisions following (4-1)-(4-4) as $\mathcal{P}(\{\mathcal{Q}_t^{plan}\}_{t=1}^T, \{\mathcal{X}_t^{imp}\}_{t=1}^T, \{\mathrm{w}_{t,\omega}\}_{t,\omega=1}^{T,M})$. It is important to emphasize that $\mathcal{X}_t^{imp}$ can be either $\mathcal{X}_t^S$, the simplified model for the system, or $\mathcal{X}_t^D$, the detailed one. Similarly, $\mathcal{Q}_{t+1}^{plan}$ can be either $\mathcal{Q}_{t+1}^S$ or $\mathcal{Q}_{t+1}^D$, depending on the model ($\mathcal{X}_t^S$ or $\mathcal{X}_t^D$) used in the planning step. Note that if $\mathcal{X}_t^{plan} = \mathcal{X}_t^{imp}$, then we have a time consistent policy.

The aforementioned process that iteratively builds $\mathcal{P}(\{\mathcal{Q}_t^{plan}\}_{t=1}^T, \{\mathcal{X}_t^{imp}\}_{t=1}^T, \{\mathrm{w}_{t,\omega}\}_{t,\omega=1}^{T,M})$, with implemented solutions $(v_{t,\omega}^*, y_{t,\omega}^*, g_{t,\omega}^*, f_{t,\omega}^*)$ can be summarized as in Algorithm 3.

Algorithm 3 Rolling-horizon policy simulation procedure

1: Sample M inflow paths, $\{\mathrm{w}_{t,\omega}\}_{t,\omega=1}^{T,M}$.
2: Set $t = 1$ and initial conditions to $\{v_{0,\omega}\}_{\omega=1}^M$.
3: $\mathcal{P} \leftarrow \emptyset$.
4: **for** each sampled path $\omega = 1, \ldots, M$ **do**
5:     Converge SDDP for (3-1)-(3-4) with $\mathcal{X}_\tau \leftarrow \mathcal{X}_\tau^{plan}\ \forall \tau \geq t$.
6:     Store the recourse function $\mathcal{Q}_{t+1}^{plan}$.
7:     Solve problem (4-1)-(4-4) for period t using $\mathcal{Q}_{t+1}^{plan}$.
8:     Update $\mathcal{P}$ with $(v_{t,\omega}^*, y_{t,\omega}^*, g_{t,\omega}^*, f_{t,\omega}^*)$
9: **end for**
10: $t \leftarrow t + 1$.
11: **if** $t = T + 1$ **then**
12:     STOP.
13: **else**
14:     Set initial conditions to $\{v_{t-1,\omega}^*\}_{\omega=1}^M$ stored in $\mathcal{P}$.
15:     Go to step 4.
16: **end if**

The described rolling-horizon policy simulation procedure emulates the actual decision process for a large number of scenarios. However, it is strongly dependent on the SDDP computational burden. Therefore, in the next section we provide a fast-algorithm to find $\mathcal{P}$.

4.2 Fast algorithm for obtaining $\mathcal{P}$: modified-SDDP

The algorithm proposed in section 4.1 still relies on a full simulation of the system for each sampled scenario in order to check convergence. Hence, despite of the benefit of inherited cuts, the SDDP method extended to a rolling-horizon scheme still presents higher computational burden in comparison to the standard SDDP procedure. Thus, a fast-approximative procedure is proposed to build $\mathcal{P}(\{\mathcal{Q}_t^{plan}\}_{t=1}^T, \{\mathcal{X}_t^{imp}\}_{t=1}^T, \{\mathrm{w}_{t,\omega}\}_{t,\omega=1}^{T,M})$ based on a simple modification on the standard SDDP implementation presented in Chapter 3. More objectively, it is proposed a modified-SDDP algorithm where in the *backward step*, recourse function cuts are obtained using the planning model, i.e., by means of model (3-7)-(3-11) with $\mathcal{X}_t \leftarrow \mathcal{X}_t^{plan}$ for all t, and the *forward step* is performed using model (4-1)-(4-4). After the modified-SDDP algorithm terminates, a final *simulation step* is performed for the set of sampled inflow paths $\{\mathrm{w}_{t,\omega}\}_{t,\omega=1}^{T,M}$ and the obtained solutions $(v_{t,\omega}^*, y_{t,\omega}^*, g_{t,\omega}^*, f_{t,\omega}^*)$ are stored in $\mathcal{P}(\{\mathcal{Q}_t^{plan}\}_{t=1}^T, \{\mathcal{X}_t^{imp}\}_{t=1}^T, \{\mathrm{w}_{t,\omega}\}_{t,\omega=1}^{T,M})$. This algorithm is hereinafter referred to as $\mathcal{P}(\mathcal{Q}^S, \mathcal{X}^D)$.

It is worth mentioning that, within this framework, the convergence of the modified-SDDP algorithm is challenged because upper and lower bounds are no more comparable. However, according to the stopping criterion devised at the end of Chapter 3, the lower and upper bound stabilization are independently analyzed. Therefore, the proposed modified-SDDP terminates when both the average cost and the lower bound stabilize.

4.3 Measure of gap due to time inconsistency

In this section a methodology is introduced to evaluate the gap due to the time inconsistency generated by the usage of a simplified model, $\mathcal{X}_t^S$, in the planning step and a detailed model, $\mathcal{X}_t^D$, to implement decisions. According to [42], the time inconsistency gap[3] is the difference between the cost-evaluation of two policies, namely the implemented policy, represented by $\mathcal{P}(\{\mathcal{Q}_t^S\}_{t=1}^T, \{\mathcal{X}_t^D\}_{t=1}^T, \{\mathrm{w}_{t,\omega}\}_{t,\omega=1}^{T,M})$ – hereinafter referred to as *inconsistent policy* –, and the planned one, represented by $\mathcal{P}(\{\mathcal{Q}_t^S\}_{t=1}^T, \{\mathcal{X}_t^S\}_{t=1}^T, \{\mathrm{w}_{t,\omega}\}_{t,\omega=1}^{T,M})$ – hereinafter referred to as *planning policy*. Notice that the planning policy is obtained by running the SDDP algorithm with simplified models for both forward and backward steps. This algorithm will be hereinafter referred to as $\mathcal{P}(\mathcal{Q}^S, \mathcal{X}^S)$. Thereby, the inconsistency gap can be written as follows:

$$GAP = \frac{1}{M}\sum_{t=1}^{T}\sum_{\omega=1}^{M} c^\top g_{t,\omega}^{imp} - \frac{1}{M}\sum_{t=1}^{T}\sum_{\omega=1}^{M} c^\top g_{t,\omega}^{plan}, \tag{4-5}$$

[3] Note that the concept of the inconsistent gap if different from the usual definition of the optimality gap.

where $g^{imp}_{t,\omega} \in \mathcal{P}(\{\mathcal{Q}^S_t\}^T_{t=1}, \{\mathcal{X}^D_t\}^T_{t=1}, \{\mathrm{w}_{t,\omega}\}^{T,M}_{t,\omega=1})$ and $g^{plan}_{t,\omega} \in \mathcal{P}(\{\mathcal{Q}^S_t\}^T_{t=1}, \{\mathcal{X}^S_t\}^T_{t=1}, \{\mathrm{w}_{t,\omega}\}^{T,M}_{t,\omega=1})$ Finally, there still exists the probability that the gap discussed here might be induced by a sampling error. In this sense, a t-test is carried to check if the true population mean of the detailed model cost (μ^{imp}) is equal to the true mean of the simplified model cost (μ^{plan}). That is:

$$\begin{cases} H_0 \ : \ \mu^{imp} = \mu^{plan} \\ H_1 \ : \ \mu^{imp} \neq \mu^{plan}. \end{cases} \tag{4-6}$$

Then, the null hypothesis is accepted if zero belongs to the confidence interval for the GAP defined as

$$GAP \pm Z_{\frac{\alpha}{2}} \cdot \sqrt{(\frac{S^2_{plan} + S^2_{imp}}{M})}, \tag{4-7}$$

where S^2_{plan} and S^2_{imp} are the variance estimates for the first and second terms of the sampled cost used in (4-5) and $Z_{\frac{\alpha}{2}}$ is the $\frac{\alpha}{2}$ quantile for the standard normal distribution. By rejecting H_0, we can say that the inconsistency gap is statistically significant.

4.4 Sources of Time Inconsistency in Hydrothermal Scheduling

A number of real-world systems details are simplified in planning models, such as linearized hydro plants production functions, disregard of fuel cost uncertainty, reservoir aggregation, Kirchhoff's voltage law and security criteria. In this work, the effects of neglecting transmission lines constraints and security criteria in the planning step are studied separately.

Kirchhoff's voltage law can be easily incorporated in planning models with nowadays computational power. Hence, a didactic example regarding time inconsistency due to such source is explored in this Chapter. Studying the effects of neglecting security criteria in planning models, on the other hand, require a conceptual development to show how it is possible to take the $n - K$ security criteria into account in hydrothermal planning. Also, differently from Kirchhoff's voltage law it can still be computationally intractable even with nowadays computational power. Hence, new algorithms must be proposed in order to solve the model. These issues are addressed in Chapter 5.

4.5 Time inconsistency due to transmission line modeling simplifications

Early models for planning hydrothermal power systems, e.g. [11], assumed simplifications in transmission lines modeling. By assuming a linearized DC power flow, two components of the power flow should be accounted for, namely first and second Kirchhoffs laws. While the former is almost always present in most studies (accounted for by expression (3-2)), the latter is often neglected [7, 11]. In [76], the practicality of considering such constraints is analyzed in hydrothermal scheduling models and in [77] the relevance of accounting for such constraints in planning applications is discussed and emphasized.

Hence, for this type of inconsistency the simplified model $\mathcal{X}_t^S = \mathcal{X}_t^{box}$ is defined as a box-constrained set of decisions $(v_t,\ y_t,\ g_t,\ f_t)$, accounting for only lower and upper bounds for each operative variable. It can be written as:

$$\mathcal{X}^{box} = \Bigg\{ (v_t,\ y_t,\ g_t,\ f_t) \ \Bigg| \tag{4-8}$$

$$\underline{V} \leq v_t \leq \overline{V} \tag{4-9}$$

$$\underline{U} \leq u_t \leq \overline{U} \tag{4-10}$$

$$\underline{S} \leq s_t \leq \overline{S} \tag{4-11}$$

$$\underline{G} \leq g_t \leq \overline{G} \tag{4-12}$$

$$-\overline{F} \leq f_t \leq \overline{F} \Bigg\}. \tag{4-13}$$

Constants $\overline{V}$ and $\underline{V}$ state upper and lower bounds for reservoir levels, constants $\overline{U}$ and $\underline{U}$ state upper and lower bounds for water discharge levels, constants $\overline{S}$ and $\underline{S}$ state upper and lower bounds for spillage levels, constants $\overline{G}$ and $\underline{G}$ state upper and lower bounds for thermal generation levels and constant $\overline{F}$ state upper bounds for power flow levels in transmission lines.

On the other hand, the detailed model, $\mathcal{X}_t^D = \mathcal{X}_t^{KVL}$, contains also the Kirchhoff's Voltage Law (KVL), which is defined as:

$$\mathcal{X}^{KVL} = \Bigg\{ (v_t,\ y_t,\ g_t,\ f_t) \ \Bigg| \tag{4-14}$$

$$f_t = S\theta_t \tag{4-15}$$

$$-\overline{F} \leq f_t \leq \overline{F} \tag{4-16}$$

$$\underline{V} \leq v_t \leq \overline{V} \tag{4-17}$$

$$\underline{U} \leq u_t \leq \overline{U} \tag{4-18}$$

$$\underline{S} \leq s_t \leq \overline{S} \tag{4-19}$$

$$\left.\underline{G} \leq g_t \leq \overline{G}\right\}, \tag{4-20}$$

where matrix S accounts for the product of susceptance and (transposed) incidence matrices to model the linearized second Kirchhoffs law.

4.6 Didactic example

In this section a simple example is given in order to illustrate the SDDP algorithm functionality. Notice that this case is a mere illustrative example, the main purpose of it is only to highlight the negative effects of time inconsistency. Along these lines, suppose a three-bus power system as shown in Fig. 4.1. To analyze the consequences of time inconsistency, we also compute a policy consistent with the detailed model, $\mathcal{P}(\{\mathcal{Q}_t^D\}_{t=1}^T, \{\mathcal{X}_t^D\}_{t=1}^T, \{\mathrm{w}_{t,\omega}\}_{t,\omega=1}^{T,M})$, hereinafter referred to as *consistent policy*, and compare it with the actual implemented one (as defined in section 4.3). Notice that this policy is evaluated by the SDDP algorithm using detailed models in both forward and backward steps. Hence, this algorithm will be hereinafter referred to as $\mathcal{P}(\mathcal{Q}^D, \mathcal{X}^D)$. Demand is placed at bus 3 and assumed constant, equal to 100MWmonth. The discount rate is set to be 0.5% of the future cost per month for all cases. A fictitious generator to represent load shedding with cost of 1000R$/MWh is added to bus 3. A planning horizon of 60 periods is assumed but in order to avoid the end-horizon effects the last 12 periods are discarded.

Table 4.1 presents data for the thermal generation while tables 4.2 and 4.3 show the hydro plant and transmission lines details respectively.

Tab. 4.1: Thermal Generator Data

Thermal Unit	c R$/MWh	$\overline{G}$ MW
G_1	20	100
G_2	100	50

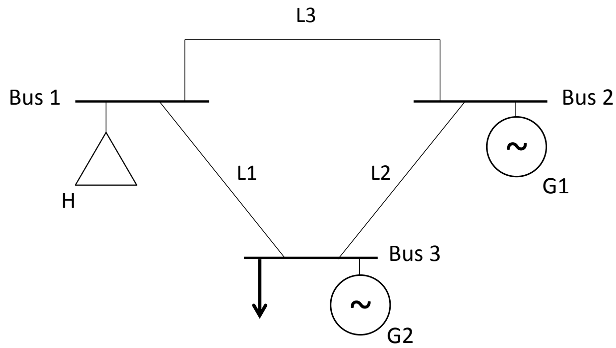

Fig. 4.1: Three bus system for studying the effects of time inconsistency.

Tab. 4.2: Hydro Generator Data (MW)

Hydro Unit	$\overline{V}$	$\overline{U}$	v_0
H	150	80	50

The set of 3 scenarios shown in Fig. 4.2 was used in the studies for each year in the planning horizon. Albeit simplistic, these scenarios have a similar behavior to typical seasonal values of the Southeastern area of the Brazilian power system, which usually faces its dry period from May to October.

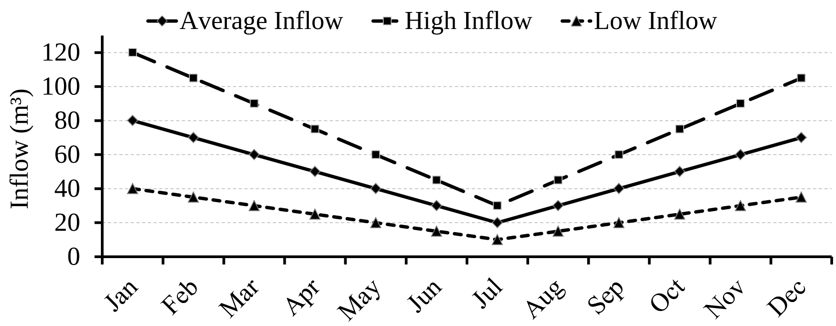

Fig. 4.2: Inflow Scenarios.

SDDP convergence was checked according to the discussions in Chapter 3. After running 1000 iterations, lower bound and upper bound stabilization were checked at every 100 additional iterations. The number simulations used in the evaluation step was 3000.

The evaluated costs and inconsistency GAP for this case is MMR$ 6.67 (17.9% of the expected cost for the planning policy). The 95% confidence interval for the GAP, which values MMR$[6.54, 6.80], does not contain the zero, therefore,

Tab. 4.3: Transmission lines data

Transmission Line	$\overline{F}$ (MW)	x (pu)
L_1	100	1
L_2	65	0.5
L_3	25	1

we can say that the inconsistency GAP obtained is statistically significant.

In Fig. 4.3 the inconsistent policy evaluated by the $\mathcal{P}(\mathcal{Q}^S, \mathcal{X}^D)$ algorithm for reservoir levels is shown. Note that the 99% confidence interval for reservoir levels indicates reservoir full depletion in all periods.

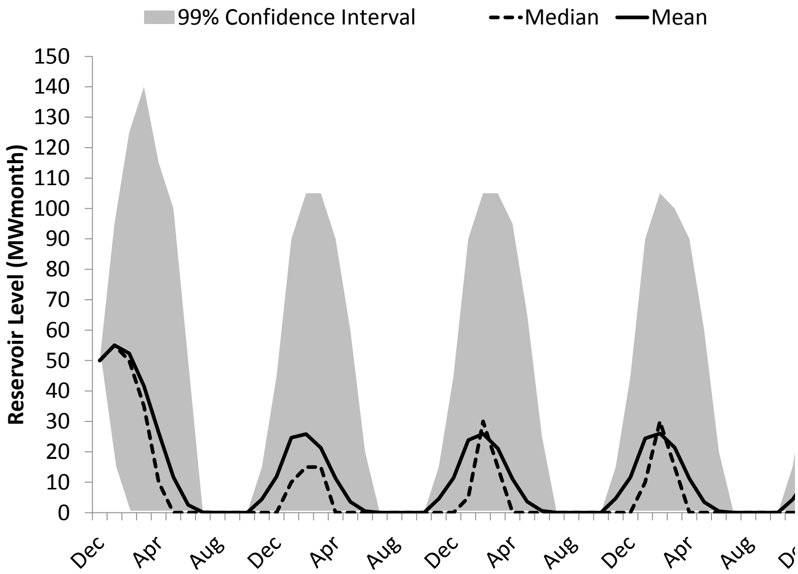

Fig. 4.3: Reservoir levels evaluated by $\mathcal{P}(\mathcal{Q}^S, \mathcal{X}^D)$.

On the other hand, the reservoir level evaluated by the $\mathcal{P}(\mathcal{Q}^D, \mathcal{X}^D)$ algorithm, shown in Fig. 4.4, indicates that in this case there is no full depletion at any given point.

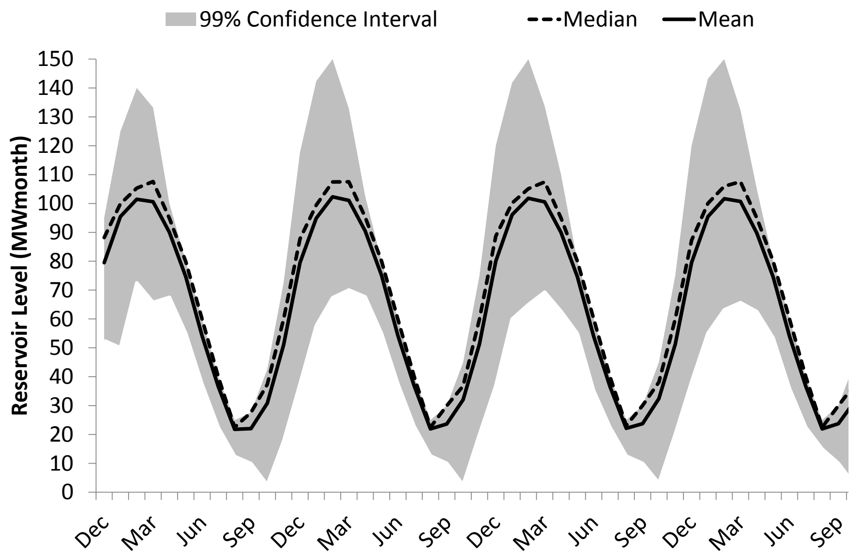

Fig. 4.4: Reservoir levels evaluated by $\mathcal{P}(\mathcal{Q}^D, \mathcal{X}^D)$.

This effect can be better explained by analyzing water discharge and cheap thermal generation behavior. Fig. 4.5 shows that water discharge is well behaved in the consistent policy. Its mean is always between 40 and 60 m^3 with a clear tendency of less water discharge in dry periods.

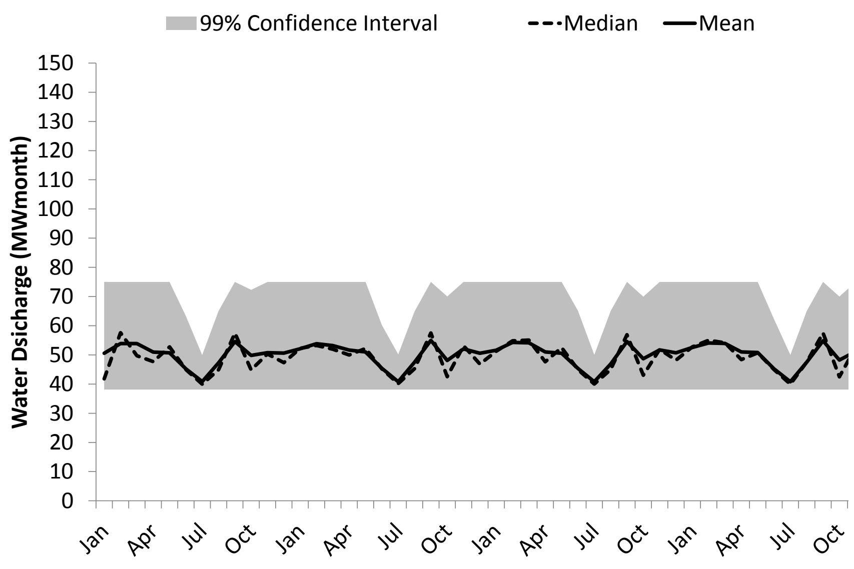

Fig. 4.5: Water discharge evaluated by $\mathcal{P}(\mathcal{Q}^D, \mathcal{X}^D)$.

And Fig. 4.6 shows cheap thermal generation in the consistent policy. Its mean is also well behaved around 40 and 60 MW with a clear tendency of dispatch peaks in dry seasons. The expensive thermal generator is never dispatched in the consistent policy.

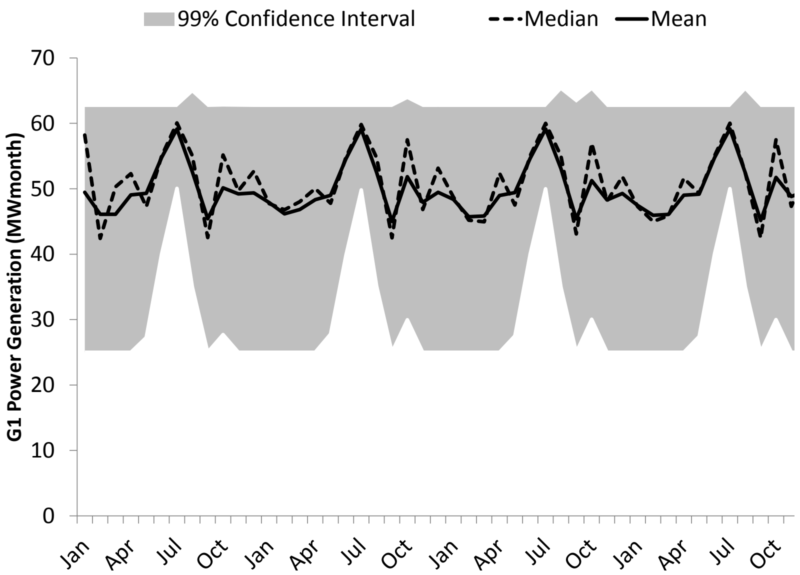

Fig. 4.6: Power generation from G_1 evaluated by $\mathcal{P}(\mathcal{Q}^D, \mathcal{X}^D)$.

The total water discharge in the inconsistent policy is actually similar to the total water discharge in the consistent policy. However, its pattern is different, as Fig. 4.7 indicates. In this case, water discharge is much greater in wet seasons indicating that the evaluated policy values water less than the consistent policy does in these periods. And then, as the dry season approaches, one would expect that water discharge decreases. However, Kirchhoff's Voltage Law (unaccounted for in the planning step) refrains the cheap thermal generator to be dispatched at the desired level, even though its dispatch considerably increases as Fig. 4.8 shows. This leads the hydro unity to be constantly dispatched to the point in which the reservoir is fully depleted and the expensive thermal generator starts being dispatched as Fig. 4.9 depicts.

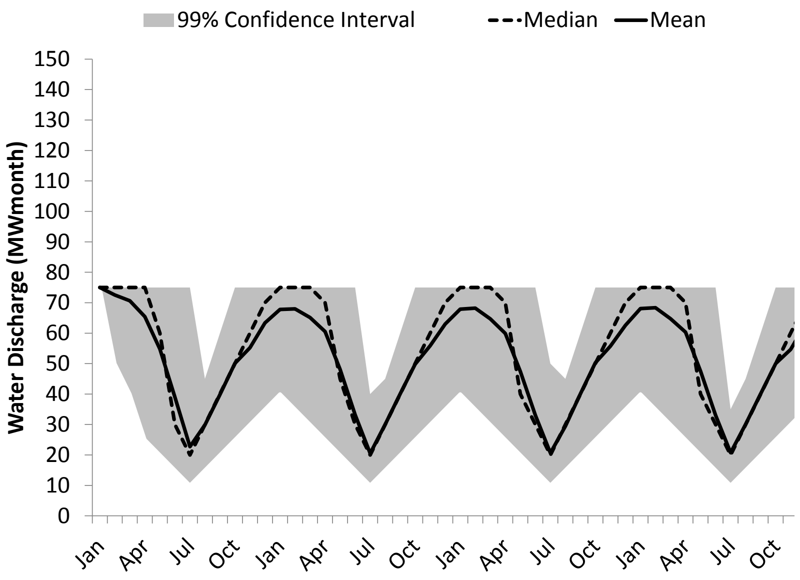

Fig. 4.7: Water discharge evaluated by $\mathcal{P}(\mathcal{Q}^S, \mathcal{X}^D)$.

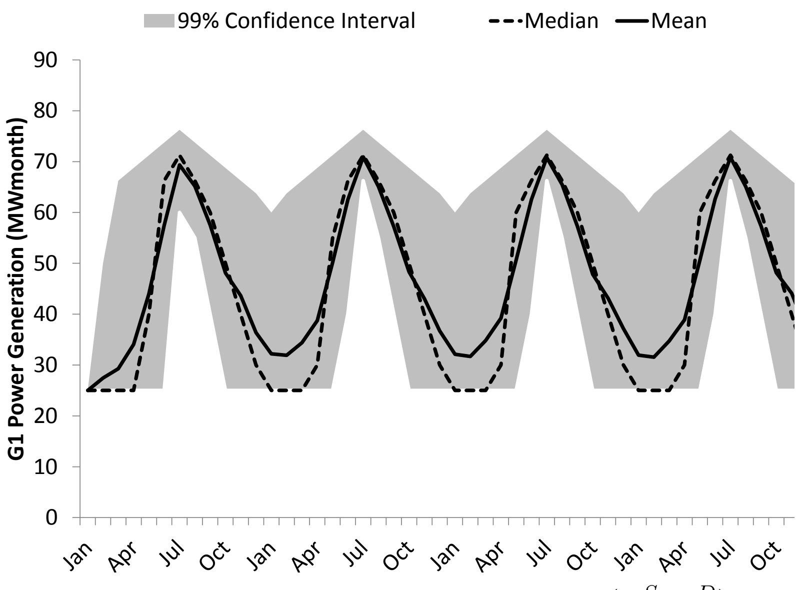

Fig. 4.8: Power generation from G_1 evaluated by $\mathcal{P}(\mathcal{Q}^S, \mathcal{X}^D)$.

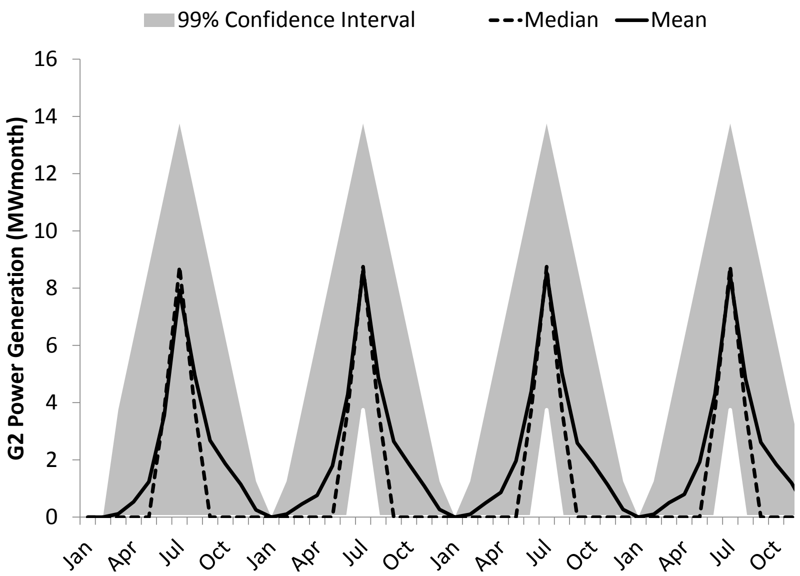

Fig. 4.9: Power generation from G_2 evaluated by $\mathcal{P}(\mathcal{Q}^S, \mathcal{X}^D)$.

Expected spot price in the inconsistent policy is constantly peaking in the dry season, behaving similar to the power generation from the expensive thermal unity as indicated in Fig. 4.10. On the other hand, expected spot prices in the consistent policy are constantly at 20R$/MWh.

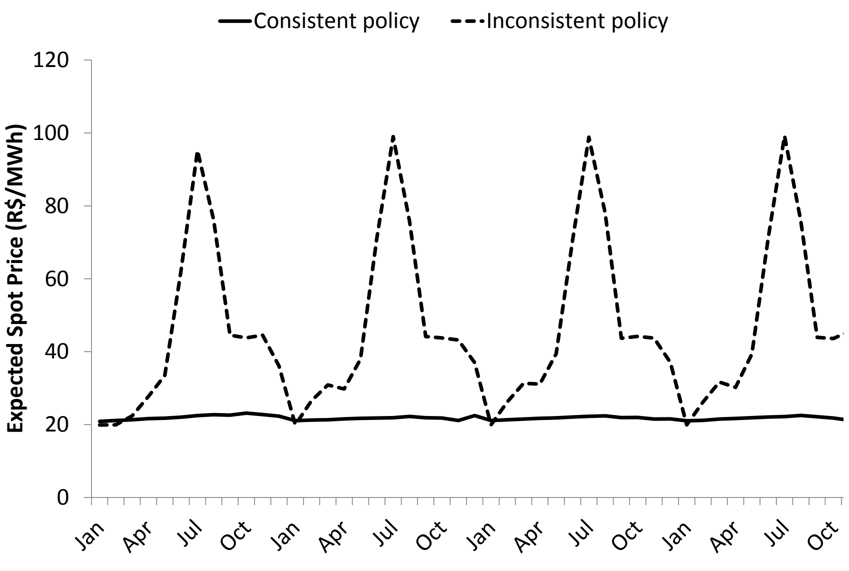

Fig. 4.10: Spot prices evaluated by $\mathcal{P}(\mathcal{Q}^S, \mathcal{X}^D)$ and $\mathcal{P}(\mathcal{Q}^D, \mathcal{X}^D)$.

5
A Hybrid Robust-SDDP Algorithm for Ensuring Reserve Deliverability in Hydrothermal Planning Under an $n - K$ Security Criterion

In Chapter 4, it was discussed that neglecting Kirchhoff's voltage law can lead to time inconsistency effects which might significantly expose the system operation to dangerous states. However, as pointed out in [76], incorporating Kirchhoff's voltage law should not be an issue even in real-world systems with nowadays computational power. Hence, such source of time inconsistency can easily be addressed. Nevertheless, neglecting system operation details such as security criteria might also be a source of time inconsistency, and due to tractability issues its incorporation in planning models is still an open topic.

Recalling from Chapter 1, recent blackouts in the Brazilian power system were attributed precisely to the lack of spinning reserves in the hours that preceded the events. Along these lines, it seems reasonable to investigate new planning models that incorporate security criteria and ensures reserve deployment in the medium-/long-term planning. However, this poses a major challenge as well known security criteria adopted in industry practice, such as $n - K$, makes the size of the model grow exponentially. Hence, it is also necessary to investigate new algorithms that make its consideration tractable.

Indeed, incorporating security criteria is a challenge even for single period problems due to dimensionality issues [40]. However, by means of Adjustable Robust Optimization (ARO) based techniques, this issue has been successfully addressed in [39]. The authors propose a trilevel mixed integer model that can be solved by means of the Column-and-Constraint Generation (CCG) algorithm [78]. In this Chapter, a methodology that incorporates the proposals in [39] into the multistage stochastic hydrothermal framework is introduced. The model is essentially based on the one in [39] and the solution methodology comprises a hybrid Robust-SDDP algorithm. Moreover, it is discussed how to share contingency states identified by the CCG algorithm for all periods and scenarios, resulting in a computationally tractable algorithm that is capable of successfully providing a planning policy in reasonable computational time.

With the proposed algorithm, not only it is possible to conduct planning studies that aim at ensuring reserve deployment but it also allows us to study the effects of time inconsistency due to simplifications of security criteria in planning models for real-world systems. In the next section, sets $\mathcal{X}_t^D$ and $\mathcal{X}_t^S$ for studying time inconsistency due to simplifications in security criteria are described followed by a simple case study, similar to the one in Chapter 4, with didactic purposes. Then, the proposed algorithm is introduced and studies regarding larger size systems are conducted.

5.1 Time inconsistency due to security criteria simplifications

Power systems worldwide operate under standard security criteria, such as $n-1$ and $n-2$ (see [6, 39, 40]). However, this feature is often simplified by generation bounds obtained from off-line contingency analysis. In this work, security is accounted for by ensuring power balance under all post-contingency states within a set of credible contingencies, $\mathcal{C}$, as used in [54]. In this case, the pre-contingency hydrothermal scheduling must allow a feasible operation point under any post-contingency state in $\mathcal{C}$.

For this new application, the detailed model accounts for all the constraints considered in detailed model from section 4.5 and the full set of post-contingency schedules with links between pre- and post-contingency states. Hence, $\mathcal{X}_t^D$ can be defined, compatibly with [39,40,54], as follows:

$$\mathcal{X}_t^D = \left\{ (v_t,\ y_t,\ g_t,\ f_t) \;\middle|\; \exists\, (v_t^c,\ y_t^c,\ g_t^c,\ f_t^c,\ \Delta\boldsymbol{g}_t^{up},\ \Delta\boldsymbol{g}_t^{dn},\ \Delta\boldsymbol{u}_t^{up},\ \Delta\boldsymbol{u}_t^{dn}) \right. \tag{5-1}$$

$$g_t + \Delta g_t^{up} \leq \overline{G} \tag{5-2}$$

$$g_t - \Delta g_t^{dn} \geq \underline{G} \tag{5-3}$$

$$0 \leq \Delta g_t^{up} \leq \overline{\Delta G}^{up} \tag{5-4}$$

$$0 \leq \Delta g_t^{dn} \leq \overline{\Delta G}^{dn} \tag{5-5}$$

$$u_t + \Delta u_t^{up} \leq \overline{U} \tag{5-6}$$

$$u_t - \Delta u_t^{dn} \geq \underline{U} \tag{5-7}$$

$$0 \leq \Delta u_t^{up} \leq \overline{\Delta U}^{up} \tag{5-8}$$

$$0 \leq \Delta u_t^{dn} \leq \overline{\Delta U}^{dn} \tag{5-9}$$

$$v_t^c \geq \gamma \cdot v_t;\ \forall c \in \mathcal{C} \tag{5-10}$$

$$A^c g_t^c + B^c u_t^c + C^c f_t^c + \phi_t^{c+} - \phi_t^{c-} = d_t;\ \forall c \in \mathcal{C} \tag{5-11}$$

$$v_t^c + \beta_t^c \cdot u_t^c + \beta_t^c \cdot s_t^c + M\left(\beta_t^c \cdot u_t^c + \beta_t^c \cdot s_t^c\right) = v_{t-1} + \mathrm{w}_{t,\omega};\ \forall c \in \mathcal{C} \tag{5-12}$$

$$f_t^c = S^c \theta_t^c;\ \forall c \in \mathcal{C} \tag{5-13}$$

$$-Z_L^c \overline{F}_l \leq f_t^c \leq Z_L^c \overline{F}_l;\ \forall c \in \mathcal{C} \tag{5-14}$$

$$Z_T^c(g_t - \Delta g_t^{dn}) \leq g_t^c \leq Z_T^c(g_t + \Delta g_t^{up});\ \forall c \in \mathcal{C} \tag{5-15}$$

$$Z_H^c(u_t - \Delta u_t^{dn}) \leq u_t^c \leq Z_H^c(u_t + \Delta u_t^{up});\ \forall c \in \mathcal{C} \Bigg\}. \tag{5-16}$$

Decision variables Δg_t^{up} and Δg_t^{dn} (with upper bounds equal to $\overline{\Delta G}^{up}$ and $\overline{\Delta G}^{dn}$) correspond, respectively, to up- and down-spinning reserve allocation for thermal generators. Decision variables Δu_t^{up} and Δu_t^{dn} (with upper bounds equal to $\overline{\Delta U}^{up}$ and $\overline{\Delta U}^{dn}$) correspond to up- and down-spinning reserve allocation for hydro generators. Reserves are pre-contingency scheduling variables that allow the system operator to redispatch the system under the event of a contingency (see [54]). Decision vectors with an upper index c accounts for post-contingency decisions. Decision vectors ϕ_t^{c+} and ϕ_t^{c-} correspond to system power imbalance in power flow conservativeness constraints. In this context, for each post-contingency state c, vectors Z_L^c, Z_T^c, Z_H^c represent the availability parameters (each component values 0 if the associated system element is out of service or 1 otherwise) for transmission lines, thermal plants and hydro plants, respectively. Matrix M states relation between upstream and downstream hydro plants in the same river. Constant β_t^c corresponds to the expected duration of each contingency state c.

Note that if t is a given month, then β_t^c can be modeled as a few hours. Hence, instead of modeling every short-term decision period, only a set of representative hours is taken into account. In addition, the number of hours in each contingency state is usually small in comparison to the total number of hours in a month. Then, in case contingency states actually happen, the final reservoir level in the end of t should only deviate from the actually planned one by a user defined fraction, say, γ. This is modeled by means of constraint (5-10). Parameter γ is used to to control the deviation between pre- and post-contingency reservoir levels. Moreover, it does not let the model deplete the reservoir levels in post-contingency states are zero cost.

The relevance of $\widetilde{\beta}_t^c$ parameter notwithstanding, the definition of its value is beyond the scope of this work. Hence, for the sake of simplicity it will be assumed that $\tilde{\beta}_t^c$ is equal to 1 throughout this work. However, there exists a close relation between $\tilde{\beta}_t^c$ and γ. That is, the more a contingency state affects system operation, the less water should remain stored in reservoirs. Thus, it is possible to control how much short-term decisions taken to overcome contingency states affects the long-term operation by means of setting γ to an adequate value. The proposed decision process is illustrated in Fig 5.1.

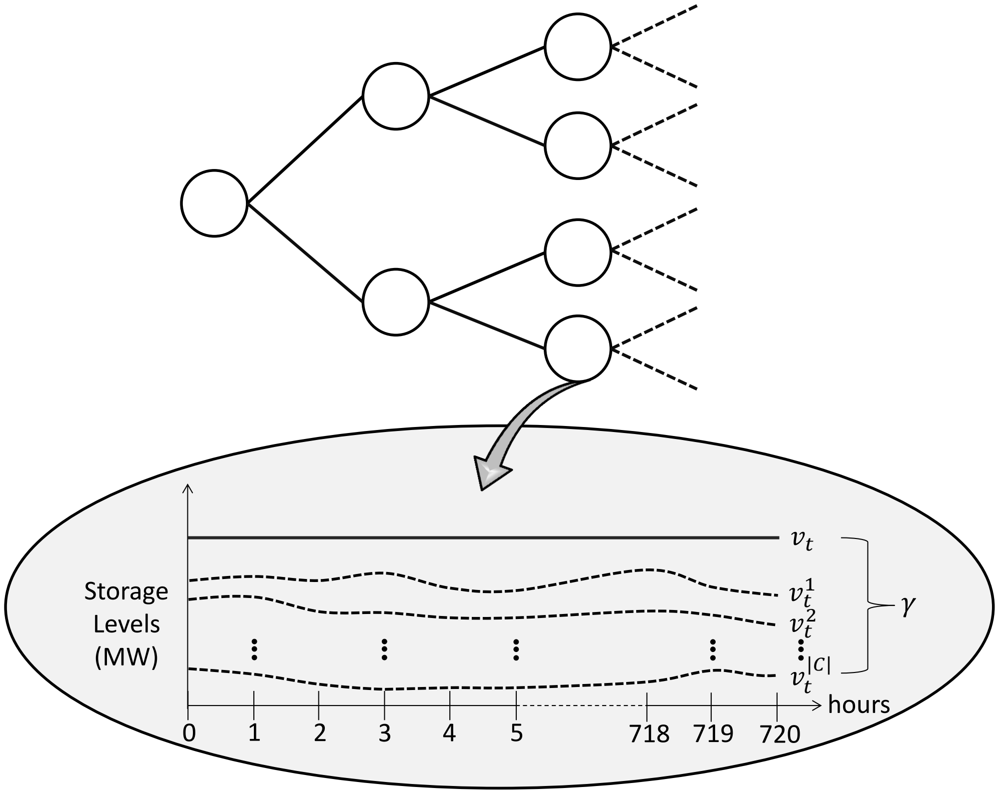

Fig. 5.1: Illustration of the decision process for post-contingency decisions in the long-term planning.

In the proposed model, by imposing that post-contingency storage decisions should be a fraction of pre-contingency storage decisions, time inconsistency could be induced if contingency states actually happen. This is discussed in more depth in Appendix A.

The objective function of the problem must change in order to include the cost of energy reserves and system power imbalance in post-contingency states as follows:

$$Q_t(v_{t-1}, \mathrm{w}_{t,\omega}) =$$

$$\begin{aligned}\min_{\substack{v_t,\, y_t,\, g_t,\, f_t,\, \Delta g^{up},\, \Delta g^{dn},\\ \Delta u^{up},\, \Delta u^{dn}, v_t^c,\, y_t^c,\, g_t^c,\, f_t^c}} \quad & c_t^\top g_t + \sum_{i \in \mathcal{I}^T} (c_{t,i}^{up} \Delta g_{t,i}^{up} + c_{t,i}^{dn} \Delta g_{t,i}^{dn}) + \\ & \sum_{i \in \mathcal{I}^H} (c_{t,i}^{up} \Delta u_{t,i}^{up} + c_{t,i}^{dn} \Delta u_{t,i}^{dn}) + \\ & C^{Imb}\Big(\max_{c \in \mathcal{C}} \{\phi_t^{+c} + \phi_t^{-c}\} \Big) + J \cdot \mathcal{Q}_{t+1}(v_t), \end{aligned} \tag{5-17}$$

where c_t^{up} and c_t^{dn} are, respectively, the cost vectors for up and down-spinning reserves. $C^{Imb}(\cdot)$ is an convex function that models the imbalance cost for post-contingency states which is accounted for by means of the maximum imbalance (worst-case) among all states. The worst-case imbalance metric allows us to make use of the robust optimization to implicitly account for all post-contingency states through a second-level problem [39]. This transformation is further discussed in section 5.2. To implement this function, it is possible to trade $\max_{c \in \mathcal{C}} \{\phi_t^{+c} + \phi_t^{-c}\}$ for decision variable δ_t and the following set of constraints:

$$\delta_t \geq \phi_t^{+c} + \phi_t^{-c};\ \forall c \in \mathcal{C} \tag{5-18}$$

Note that, in formulation (5-1)-(5-16), the state variable v_{t-1} now appears also in the post-contingency constraints. This requires the SDDP method cut presented in Chapter 3 to be modified in order to be correctly applied. Naming $\pi_{t,\omega}^c$ the dual variable associated with post-contingency water balance constraints, the cut at a given iteration m becomes:

$$\alpha_{t+1} \geq \tilde{\mathcal{Q}}_{t+1}^{(k)}(v_t^{(k)}) + (\tilde{\pi}_{t+1}^{(k)} + \sum_{c \in \mathcal{C}} \tilde{\pi}_{t+1}^{c,(k)})^\top (v_t - v_t^{(k)});\ \forall k \in \mathcal{K}^{(m)}, \tag{5-19}$$

where, $\tilde{\pi}_{t+1}^{c,(k)} = \sum_{\omega \in \Omega_{t+1}} p_{t+1,\omega} \pi_{t+1,\omega}^{c,(k)}$.

This planning model is hereinafter referred to as full contingency dependent (FCD) model and is fully shown in (5-20)-(5-44) for explanatory purposes.

$$\begin{aligned} Q_t(v_{t-1}, \mathrm{w}_{t,\omega}) = & \\ \min_{\substack{v_t,\, y_t,\, g_t,\, f_t,\, \Delta g^{up},\, \Delta g^{dn},\\ \Delta u^{up},\, \Delta u^{dn}, v_t^c,\, y_t^c,\, g_t^c,\, f_t^c}} \quad & c_t^\top g_t + \sum_{i \in \mathcal{I}^T} (c_{t,i}^{up} \Delta g_{t,i}^{up} + c_{t,i}^{dn} \Delta g_{t,i}^{dn}) + \\ & \sum_{i \in \mathcal{I}^H} (c_{t,i}^{up} \Delta u_{t,i}^{up} + c_{t,i}^{dn} \Delta u_{t,i}^{dn}) + \\ & C^{Imb}(\delta^{wc}) + J \cdot \mathcal{Q}_{t+1}(v_t) \end{aligned} \tag{5-20}$$

subject to

$$A_t g_t + B_t y_t + C_t f_t = d_t \tag{5-21}$$

$$H_t y_t = v_{t-1} + \mathrm{w}_{t,\omega} \ : \ (\pi_{t,\omega}) \tag{5-22}$$

$$f_t = S\theta_t \tag{5-23}$$

$$-\overline{F} \leq f_t \leq \overline{F} \tag{5-24}$$

$$\underline{V} \leq v_t \leq \overline{V} \tag{5-25}$$

$$\underline{U} \leq u_t \leq \overline{U} \tag{5-26}$$

$$\underline{S} \leq s_t \leq \overline{S} \tag{5-27}$$

$$\underline{G} \leq g_t \leq \overline{G} \tag{5-28}$$

$$g_t + \Delta g_t^{up} \leq \overline{G} \tag{5-29}$$

$$g_t - \Delta g_t^{dn} \geq \underline{G} \tag{5-30}$$

$$0 \leq \Delta g_t^{up} \leq \overline{\Delta G}^{up} \tag{5-31}$$

$$0 \leq \Delta g_t^{dn} \leq \overline{\Delta G}^{dn} \tag{5-32}$$

$$u_t + \Delta u_t^{up} \leq \overline{U} \tag{5-33}$$

$$u_t - \Delta u_t^{dn} \geq \underline{U} \tag{5-34}$$

$$0 \leq \Delta u_t^{up} \leq \overline{\Delta U}^{up} \tag{5-35}$$

$$0 \leq \Delta u_t^{dn} \leq \overline{\Delta U}^{dn} \tag{5-36}$$

$$\delta_t \geq \phi_t^{+c} + \phi_t^{-c}; \ \forall c \in \mathcal{C} \tag{5-37}$$

$$A^c g_t^c + B^c u_t^c + C^c f_t^c + \phi_t^{c+} - \phi_t^{c-} = d_t; \ \forall c \in \mathcal{C} \tag{5-38}$$

$$\begin{aligned} v_t^c + \beta_t^c \cdot u_t^c + \beta_t^c \cdot s_t^c + M\left(\beta_t^c \cdot u_t^c + \beta_t^c \cdot s_t^c\right) \\ = v_{t-1} + \mathrm{w}_{t,\omega} \ : \ (\pi_{t,\omega}^c); \ \forall c \in \mathcal{C} \end{aligned} \tag{5-39}$$

$$f_t^c = S^c \theta_t^c, \ \forall c \in \mathcal{C} \tag{5-40}$$

$$v_t^c \geq \gamma \cdot v_t; \ \forall c \in \mathcal{C} \tag{5-41}$$

$$-Z_L^c \overline{F} \leq f_t^c \leq Z_L^c \overline{F}; \ \forall c \in \mathcal{C} \tag{5-42}$$

$$Z_T^c (g_t - \Delta g_t^{dn}) \leq g_t^c \leq Z_T^c (g_t + \Delta g_t^{up}); \ \forall c \in \mathcal{C} \tag{5-43}$$

$$Z_H^c (u_t - \Delta u_t^{dn}) \leq u_t^c \leq Z_H^c (u_t + \Delta u_t^{up}); \ \forall c \in \mathcal{C} \tag{5-44}$$

And, when applying the SDDP method to the FCD model, problem (5-20)-(5-44) becomes problem

$$
\begin{aligned}
&Q_t(v_{t-1}, \mathrm{w}_{t,\omega}) = \\
&\min_{\substack{v_t,\, y_t,\, g_t,\, f_t,\, \Delta g^{up},\, \Delta g^{dn}, \\ \Delta u^{up},\, \Delta u^{dn}, v_t^c,\, y_t^c,\, g_t^c,\, f_t^c}} \quad c_t^\top g_t + \sum_{i \in \mathcal{I}^T} (c_{t,i}^{up} \Delta g_{t,i}^{up} + c_{t,i}^{dn} \Delta g_{t,i}^{dn}) + \\
&\qquad \sum_{i \in \mathcal{I}^H} (c_{t,i}^{up} \Delta u_{t,i}^{up} + c_{t,i}^{dn} \Delta u_{t,i}^{dn}) + \\
&\qquad C^{Imb}(\delta^{wc}) + J \cdot \alpha_{t+1} && \text{(5-45)} \\
&\qquad \text{subject to} \\
&\qquad \text{constraints (5-21)-(5-44)} && \text{(5-46)} \\
&\qquad \alpha_{t+1} \geq \tilde{\mathcal{Q}}_{t+1}^{(k)}(v_t^{(k)}) + \\
&\qquad\qquad (\tilde{\pi}_{t+1}^{(k)} + \sum_{c \in \mathcal{C}} \tilde{\pi}_{t+1}^{c,(k)})^\top (v_t - v_t^{(k)}); \forall k \in \mathcal{K}^{(m)}. && \text{(5-47)}
\end{aligned}
$$

5.1.1 Didactic example

In this section it is considered the $n-1$ security criterion for transmission lines according to the model described in section 5.1. Thus, generation contingencies are disregarded. Notice that, similarly to the illustrative example from Chapter 4, this case is a mere illustrative example. The main purpose of it is only to highlight the negative effects of time inconsistency.

In this case, the simplified model, $\mathcal{X}_t^S$, meets the detailed model of section 4.5, (4-14)-(4-20). Thus, it accounts for both the first and second Kirchhoffs laws, yet only considering the pre-contingency scheduling. The values of $\overline{\Delta \boldsymbol{U}}^{up}$ and $\overline{\Delta \boldsymbol{U}}^{dn}$ are considered to be equal to $80MW$. And the values of $\overline{\Delta \boldsymbol{G}}^{up}$ and $\overline{\Delta \boldsymbol{G}}^{dn}$ are considered to be 50% of the maximum power generation of each thermal unity. Table 5.1 shows transmission lines data used for this study. Moreover, it is considered $\gamma = 1$ and a fictitious unbounded thermal plant to represent load shedding at a cost of 1000R$/MWh. The cost of power imbalance in post contingency states is also equal to 1000R$/MWh. The remaining values are the same used for the didactic example from section 4.6.

Tab. 5.1: Transmission lines data

Transmission Line	$\overline{F}$ (MW)	x (pu)
L_1	100	1
L_2	70	1
L_3	30	1

The evaluated inconsistency GAP for this case is MMR$ 30.33 (81.5% of the expected cost for the planning policy). In this case, the evaluated GAP 95% confidence interval, which values MMR$[30.17, 30.50], also does not contain the zero, indicating that this inconsistency source also produced a statistically significant GAP.

Fig. 5.2 shows the stored energy in the inconsistent policy evaluated by the $\mathcal{P}(\mathcal{Q}^S, \mathcal{X}^D)$ algorithm. And Fig. 5.3 shows the stored energy in the consistent policy evaluated by the $\mathcal{P}(\mathcal{Q}^D, \mathcal{X}^D)$ algorithm. Notice that reservoir depletion is even more severe in this case, in comparison with results from section 4.6.

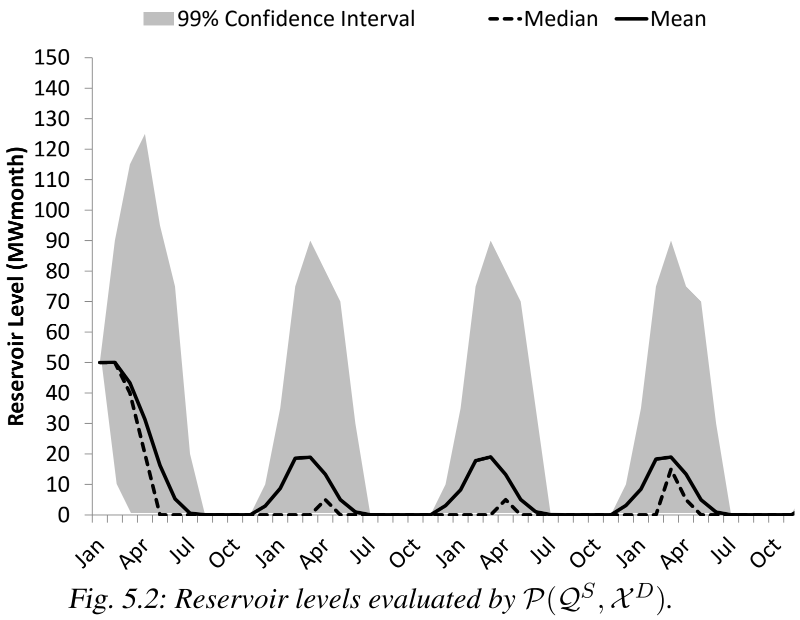

Fig. 5.2: Reservoir levels evaluated by $\mathcal{P}(\mathcal{Q}^S, \mathcal{X}^D)$.

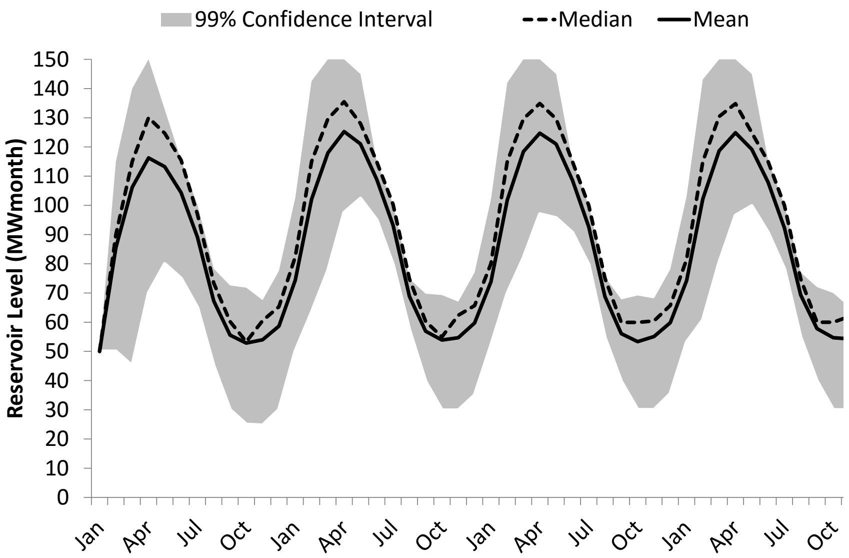

Fig. 5.3: Reservoir levels evaluated by $\mathcal{P}(\mathcal{Q}^D, \mathcal{X}^D)$.

Similar conclusions to the ones drawn in section 4.6 can also be drawn for this case. However, in this case the expensive thermal generation in the consistent policy is constantly at 5MW. But the same thermal unity on the inconsistent policy is constantly peaking in the dry season. The situation in the inconsistent policy is shown in Fig. 5.4.

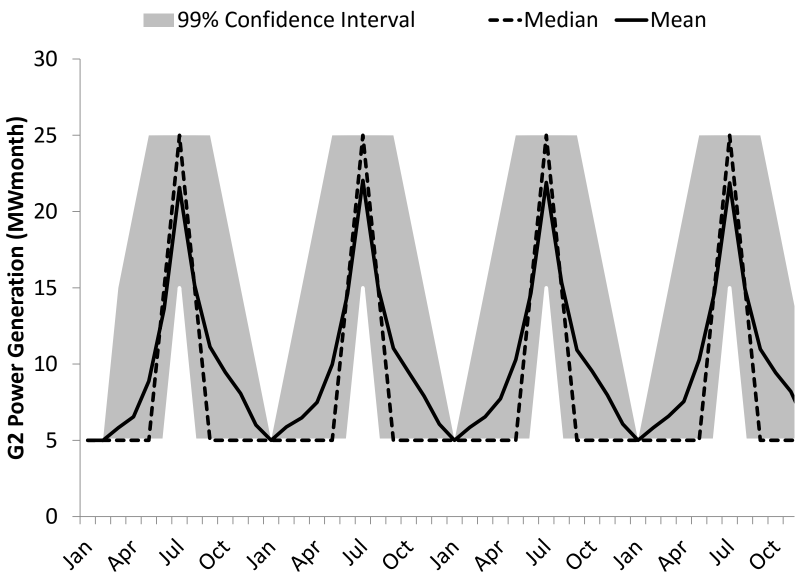

Fig. 5.4: Power generation from G_2 $\mathcal{P}(\mathcal{Q}^S, \mathcal{X}^D)$.

In this inconsistent policy, following the thermal unity behavior, the expected spot price is constantly peaking in the dry seasons as Fig. 5.5 indicates. The expected spot price for the consistent policy, on the other hand, is constantly at 100R$/MWh.

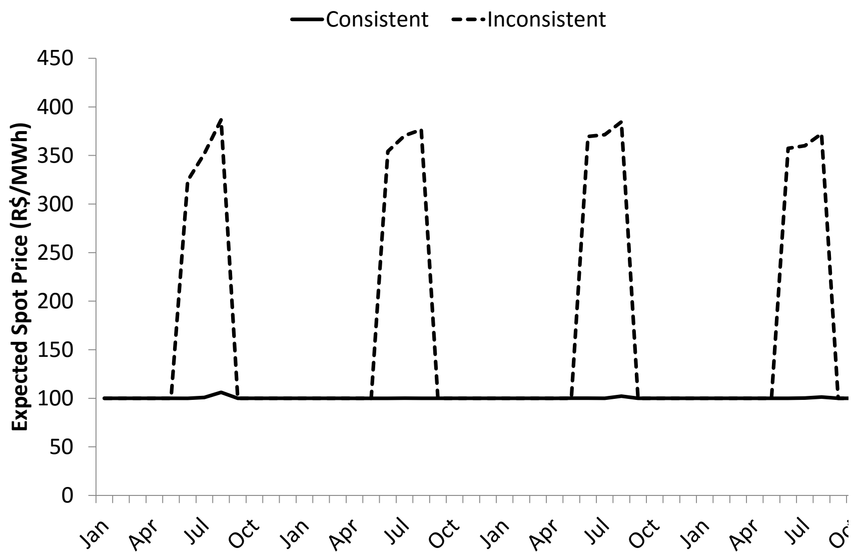

Fig. 5.5: Spot prices evaluated by $\mathcal{P}(\mathcal{Q}^S, \mathcal{X}^D)$ and $\mathcal{P}(\mathcal{Q}^D, \mathcal{X}^D)$.

Finally, there exists a chance of load shedding in the month of July in each year of the planning horizon in the inconsistent policy. Fig. 5.6 depicts the situation. No load shedding occurs in any scenario in the consistent policy.

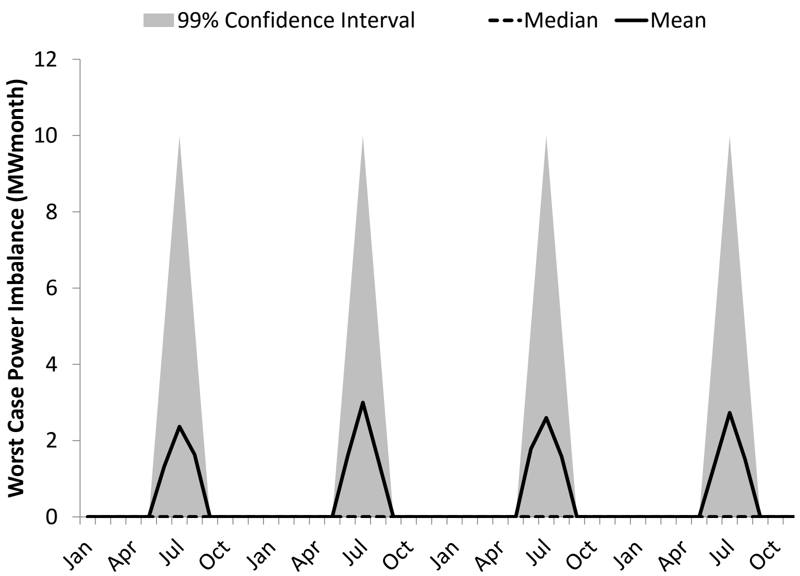

Fig. 5.6: Worst-case system power imbalance evaluated by $\mathcal{P}(\mathcal{Q}^S, \mathcal{X}^D)$.

5.2 The Hybrid SDDP and CCG Solution Methodology

In a SDDP framework, the dispatch problem of each scenario and stage must be solved very quickly in order to ensure reasonable computational times even when applied to medium size problems with few reservoirs. FCD models are generally large-scale optimization problem and can become potentially intractable for $K \geq 2$, specially when applied to real-world systems. Hence, to account for security criteria through model (5-45)-(5-47) in the SDDP scheme this work makes use of the CCG approach according to [39]. In this section it is described the CCG procedure to ensure the security criterion for one given scenario ω and period t, we present the oracle model formulation, and then we show how to expand this procedure to the SDDP framework.

5.2.1 Column-and-Constraint Generation algorithm for a single t and ω

According to [39], for any given trial scheduling of energy and reserves, a search procedure, hereinafter referred to as oracle, can be used to identify the post-contingency state leading to the highest (worst-case) system imbalance. Then, by relaxing post-contingency constraints in model (5-45)-(5-47), an iterative process, namely, CCG, can be built based on the successive incorporation of identified worst-case violated states (post-contingency constraints and variables) to the relaxed version of the problem, hereinafter referred to as master problem. According to [39] and [78], this procedure converges in a finite number of steps to a near-(global) optimal solution of the FCD problem.

The CCG procedure for solving the FCD problem (5-20)-(5-44) is as follows: the master problem starts as a relaxed version of problem (5-20)-(5-44), in which set $\mathcal{C}$ is replaced by subset of contingencies $\mathcal{C}^*_{t,\omega}$ which is initialized as an empty set. Then, for a given solution of the master problem, $X = \begin{bmatrix} g_t & v_t & y_t & \Delta g^{up} & \Delta g^{dn} & \Delta u^{up} & \Delta u^{dn} \end{bmatrix}$, the oracle identifies the worst-case contingency state, i.e., the one leading to the highest system imbalance. This contingency state is then added to set $\mathcal{C}^*_{t,\omega}$, the master problem is updated with the newly added state constraints and variables, and then solved again. This process is repeated until no violation is observed, or until the worst-case imbalance, denoted by $\Phi^{wc}(X)$, identified by the oracle is lower than or equal to a given tolerance level, ϵ, specified by the system operator. It is important to highlight that, in general, the algorithm converges with $|\mathcal{C}^*_{t,\omega}| \ll |\mathcal{C}|$ (see [39, 79] and [64]). Figure 5.7 depicts the CCG algorithm applied to the problem of a given period t and scenario ω of the SDDP procedure.

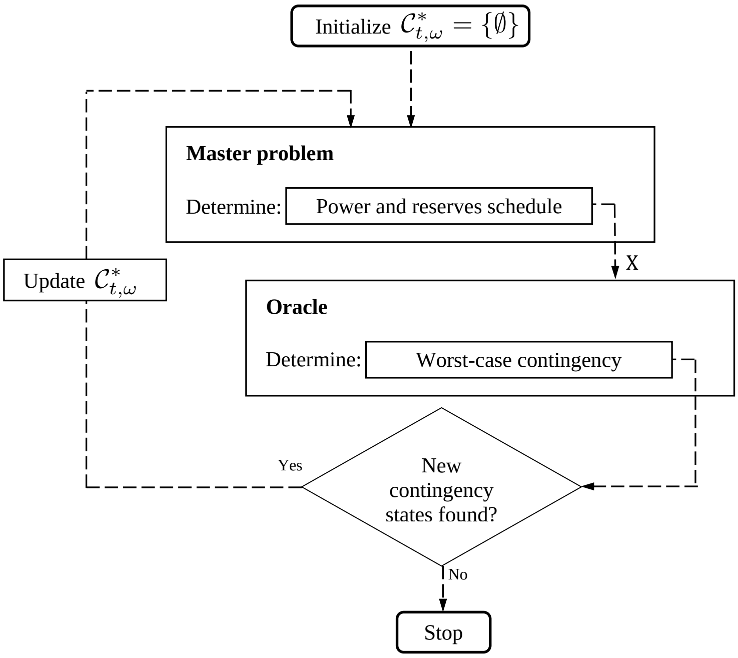

Fig. 5.7: Flowchart of CCG algorithm for single t and single ω.

Different search procedures can be used as oracle, from a simple linear search method, usually referred to as inspection, until more sophisticated methods such as Branch and Cut algorithms. According to [39], the oracle can be formulated as a bilevel mixed integer problem parameterized in the solution given by the master problem, X. In such bilevel formulation, post-contingency states are represented through binary decision vectors whose entries value 0 if the system component associated with such entry (a generation unit or transmission line) is out of service in that state and value 1 otherwise. We use $z^\top = \begin{bmatrix} z_L^\top & z_H^\top & z_T^\top \end{bmatrix}$ to denote such vectors, where $z_L^\top$, $z_H^\top$, and $z_T^\top$ are vectors associated with the availability of transmission lines, hydro power plants, and thermal power plants, respectively. Hence, for a given scheduling, X, the oracle's upper level identifies the worst-case state, defined by the availability vector $z^*(X)$, constrained to a set of linear and integrality constrains that define the security criterion. The aim of the upper level is to maximize the system minimum imbalance given by the lower-level problem. Thus, given the upper-level identified state, the lower level minimizes the system imbalance by redispatching generators within the scheduled reserves allocated in X by the master problem. As a consequence, the oracle model returns the overall system imbalance value, $\Phi^{wc}(X)$, and the availability vector $z^*(X)$ associated with the worst-case post-contingency state. In summary, the CCG algorithm is as follows[1]:

Algorithm 4 CCG algorithm for a given t and inflow scenario ω

```
Initialize C*_{t,ω} = C*_{ini}, convergence ← false, and iter ← 0
while convergence = false do
    Solve problem (5-45)-(5-47) with C ← C*_{t,ω}
    Store the optimal solution X*
    Solve the oracle problem (5-48)-(5-64) for X*
    Store the optimal solution z* and the imbalance Φ^{wc}(X)
    if Φ^{wc}(X) ≤ ε then
        convergence ← true
    else
        iter ← iter + 1
        C*_{t,ω} ← C*_{t,ω} ∪ {iter}
        {Z_L^{iter}, Z_H^{iter}, Z_T^{iter}} ← {D(z*_L), D(z*_H), D(z*_T)}
    end if
end while
```

In Algorithm 4, $\mathcal{C}^*_{ini}$ is an initial set that can be used as the empty set or informed by the user.

[1] In this work we use $\mathbb{D}$ to denote the diagonal operator, which transforms a vector in a diagonal matrix.

5.2.2 Oracle formulation

The oracle formulation provides the system operator with relevant modeling flexibilities, allowing for the consideration of any variant of the $n-K$ security criterion. Depending on the system characteristics, logic constraints involving different components of availability vector can be considered in order to characterize many different aspects. For instance, through well-known linear-binary algebra, dependent outages, different security levels per area of the system, and even disregarding some of the outages, are some of the features that can be accounted for in this framework.

The bilevel formulation for the oracle is as follows:

$$\Phi^{wc}(X) = \max_{z_T, z_H,\, z_L} \left\{ \Phi(X,z) \right| \tag{5-48}$$

subject to:

$$\mathbb{1}^\top z_T + \mathbb{1}^\top z_H + \mathbb{1}^\top z_L \geq (n_T + n_H + n_L) - K \tag{5-49}$$

$$\mathbb{1}^\top z_T \geq n_T - K_T \tag{5-50}$$

$$\mathbb{1}^\top z_H \geq n_H - K_H \tag{5-51}$$

$$\mathbb{1}^\top z_L \geq n_L - K_L \tag{5-52}$$

$$z_T \in \{0,1\}^{n_T} \tag{5-53}$$

$$z_H \in \{0,1\}^{n_H} \tag{5-54}$$

$$z_L \in \{0,1\}^{n_L} \tag{5-55}$$

$$\Phi(X,z) = \min_{\substack{\phi^{+wc},\, \phi^{-wc}, g^{wc} \\ y^{wc},\, f^{wc},\, \theta^{wc},\, v^{wc}}} \left[\mathbb{1}^\top (\phi^{+wc} + \phi^{-wc}) \right| \tag{5-56}$$

subject to:

$$A_t g^{wc} + B_t y^{wc} + C_t f^{wc} + \phi^{+wc} - \phi^{-wc} = d_t \tag{5-57}$$

$$v^{wc} = v_{t-1} - H_t y^{wc} + \mathrm{w}_{t,\omega} \tag{5-58}$$

$$f^{wc} = \mathbb{D}(z_L) S^{wc} \theta^{wc} \tag{5-59}$$

$$v^{wc} \geq \gamma v_t \tag{5-60}$$

$$\mathbb{D}(z_H)(u_t - \Delta u_t^{dn}) \leq u^{wc} \leq \mathbb{D}(z_H)(u_t + \Delta u_t^{up}) \tag{5-61}$$

$$\mathbb{D}(z_T)(g_t - \Delta g_t^{dn}) \leq g^{wc} \leq \mathbb{D}(z_T)(g_t + \Delta g_t^{up}) \tag{5-62}$$

$$f^{wc} \in \mathcal{F}_t,\; y^{wc} \in \mathcal{Y}_t,\; g^{wc} \in \mathcal{G}_t,\; v^{wc} \in \mathcal{V}_t \tag{5-63}$$

$$\phi^{+wc}, \phi^{-wc} \geq 0 \Big] \Big] \Big\}. \tag{5-64}$$

Problem (5-48)-(5-64) comprises two optimization levels: the first level, (5-48)-(5-55), and the second level, (5-56)-(5-64). Note that the upper-level problem is parameterized in X and the lower-level problem is parameterized in both X and z. Expressions (5-49)-(5-52) define the security criterion by means of constraints over availability vectors z. More specifically, constraint (5-50) state that at most K_T thermal units out of a total number of n_T can simultaneously experience an outage. Constraints (5-51) and (5-52) express the same ideas for hydro units and transmission lines respectively. Constraint (5-49) accounts for the joint generation and transmission (GT) $n - K$ security criterion. Constraints (5-53)-(5-55) imposes that variables in z can only take binary values.

The lower-level problem, (5-48)-(5-55), finds an operative point with minimum system imbalance for the identified post-contingency state, z, within scheduled reserves in X. Such mathematical model is equivalent to a phase-one (see [80]) feasibility problem applied to the set of constraints (5-38)-(5-44) for a given post-contingency state c. The system power imbalance is defined as the sum, over all buses, of the absolute value of nodal power balance violations given by artificial variables ϕ^{+wc} and ϕ^{-wc}. Network constraints are considered through (5-57) and (5-59), whereas water-balance constraints are accounted for by (5-58) and (5-60). Constraints (5-61) and (5-62) set the generation limits considering scheduled reserves in X for hydro and thermal generators respectively.

Note that in problem (5-20)-(5-44), constraints (5-38)-(5-44) ensure that for any possible post-contingency state, system power balance is guaranteed. In the ARO-based approach this is equivalent to ensure that the scheduling for energy dispatch and reserves, represented by vector X, is such that $\Phi^{wc}(X) = 0$. If on the other hand, $\Phi^{wc}(X) > 0$, then, it means the criterion is not ensured, because there is at least one state (vector z) within the set uncertainty set, (5-49)-(5-55), for which some amount of energy cannot be served.

One key issue regarding the proposed oracle is that the worst-case imbalance function $\Phi^{wc}(X)$ is the optimal value of a bilevel mixed integer program that cannot be solved by off-the-shelf MILP solvers such as Xpress [81]. This issue is addressed in [39] by applying the following steps:

1. Replace $\Phi(X, z)$ in expression (5-48) by the dual objective function of the lower-level problem (5-56)-(5-64);

2. Replace the lower-level problem by its dual feasibility constraints.
3. Apply linearization techniques to the product of binary and continuous decision variables that arise from the above two steps.

By performing the above steps, the bilevel problem is recast as a single-level MILP problem suitable for commercial solvers. For the complete description of the single-level equivalent MILP formulation of the oracle, we refer to [39].

5.2.3 Master problem formulation

The master problem is used in step 3 of Algorithm 4. It is conceived by a relaxed version of problem (5-20)-(5-44), where $\mathcal{C}$ is replaced by $\mathcal{C}^*_{t,\omega}$. The formulation of the master problem is as follows:

$$\tilde{Q}_t^{(n)}(v_{t-1}, \mathrm{w}_{t,\omega}) =$$

$$\min_{\substack{\phi_t^+, \phi_t^-, \phi_t^{+c}, \phi_t^{-c} \\ v_t,\, g_t,\, y_t, f_t,\, \theta_t, \\ \Delta u^{up},\, \Delta u^{dn}, \\ \Delta g^{up},\, \Delta g^{dn}, \\ g_t^c,\, v_t^c,\, y_t^c,\, f_t^c,\, \theta_t^c, \\ \alpha_{t+1}}} \; c_t^\top g_{t,i} + \sum_{i \in \mathcal{I}^T} (c_i^U \Delta g_{t,i}^{up} + c_i^D \Delta g_{t,i}^{dn}) + \sum_{i \in \mathcal{I}^H} (c_i^U \Delta u_{t,i}^{up} + c_i^D \Delta u_{t,i}^{dn}) + C^{Imb}(\delta^{wc}) + J \cdot \alpha_{t+1} \tag{5-65}$$

subject to

$$\text{Constraints (5-20)-(5-37) with } \mathcal{C} \leftarrow \mathcal{C}^*_{t,\omega} \tag{5-66}$$

$$\alpha_{t+1} \geq \tilde{\mathcal{Q}}_{t+1}^{(k)}(v_t^{(k)}) + \left(\tilde{\pi}_{t+1}^{(k)} + \sum_{c \in \mathcal{C}^*_{t,\omega}} \tilde{\pi}_{t+1}^{c,(k)} \right)^\top (v_t - v_t^{(k)}); \; \forall k \in \mathcal{K}^{(n)} \tag{5-67}$$

It is worth mentioning that if all binding or active states, those identified by the oracle as leading to positive imbalance, are accounted for in $\mathcal{C}^*_{t,\omega}$, the *umbrella set of constraints*, those whose dual variables are nonzero at the optimal solution [39,40], belongs to $\mathcal{C}^*_{t,\omega}$. Thus, because dual variables associated with constraints not considered in $\mathcal{C}^*_{t,\omega}$ value zero, the following equality holds: $\sum_{c \in \mathcal{C}} \tilde{\pi}_{t+1}^{c,(k)} = \sum_{c \in \mathcal{C}^*_{t,\omega}} \tilde{\pi}_{t+1}^{c,(k)}$. As a consequence, the relaxed master problem (5-65)-(5-67) is equivalent to the full contingency dependent problem (5-20)-(5-44), i.e., (5-65)-(5-67) finds a solution in the optimal set of (5-20)-(5-44).

5.2.4 Expanding the CCG algorithm for the SDDP framework

The CCG algorithm described in section 5.2.1, is devoted to ensure the equivalence between the FCD model, (5-20)-(5-44), and the master problem, (5-65)-(5-67). To that end, algorithm 4 must be run for all periods and scenarios in both *forward* and *backward steps* of the SDDP procedure. In this case, the equivalence of the SDDP procedure is ensured because recourse functions approximations are point-wise equivalent. Nevertheless, despite of the reported benefit in terms of computational times provided by the CCG algorithm in comparison to the FCD model, [39], the CCG procedure is still time consuming for practical implementation within the SDDP approach.

In order to devise a tractable implementation for the SDDP procedure using the CCG approach, two important properties should be emphasized. The first relevant property is that the set $\mathcal{C}^*_{t,\omega}$ is not only valid to other periods, t', and scenarios, ω', because it is a subset of $\mathcal{C}$, but it is also very robust in the sense of being likely to contain the *umbrella set of constraints* for the FCD problem of t' and ω'. The second aspect is based on the fact that in the *backward step*, where the recourse functions are approximated from below through Benders cuts, if the CCG algorithm is not converged and the set $\mathcal{C}^*_{t,\omega}$ does not contain all the *umbrella constraints*, the *backward step* is still valid and provides a lower bound for the problem. While the latter aspect is based on the convexity of the recourse functions and relaxation properties, the former is based on the robustness of the *umbrella set* with regard to changes in the right-hand-side of the problem as reported in [79]. The latter aspect is also corroborated in this work by means of numerical experiments.

Therefore, the SDDP applied to the hydrothermal joint scheduling of energy and reserves under a $n - K$ security criterion via CCG can be devised by replacing the FCD problem (5-20)-(5-44) by an iterative process presented in Algorithm 4. Notwithstanding, based on the two properties, this approach can be enhanced by:

1) *Sharing identified contingency sets, $\mathcal{C}^*_{t,\omega}$, through period and scenarios* – This can be done by initializing Algorithm 4 with the current aggregated set of identified contingency states, $\mathcal{C}^*$, that encompasses the union all previous runs (for different periods and scenarios) of the CCG algorithm. In this case, in the first run of the scheduling model, the aggregated set is defined as empty, $\mathcal{C}^* \leftarrow \emptyset$. During the SDDP *forward* and *backward steps*, Algorithm 1 is always initialized with the aggregated set, $\mathcal{C}^*_{ini} \leftarrow \mathcal{C}^*$, which is then updated with any newly identified post-contingency state.

2) *Turning off the CCG if no new violated state is identified* – After an entire SDDP iteration in which no new state is identified as violated, i.e., leading to positive imbalance (infeasible redispatch within scheduled reserves), it means that the aggregated set of contingencies, $\mathcal{C}^*$, was capable to capture the diversity of all critical states needed to ensure security for all periods in a given *forward iteration*. By turning off the CCG algorithm, the oracle is not run and the master problem relies solely on the already identified post-contingency states on $\mathcal{C}^*$, which speeds up the process without compromising the lower bound and the SDDP procedure. Nevertheless, from time to time, say, after 100 *forward and backward* iterations with the CCG turned off, the CCG algorithm is turned on once again until no new state is identified in a complete iteration.

5.3 Model analysis

In this section, we use a simplified Brazilian interconnected power system configuration to test the efficiency of the proposed methodology. Subsystems in the planning model are connected by means of a transmission network comprised of 10 transmission lines that is responsible for exchanging energy amongst the subsystems. In addition, there is a total of 95 thermal generators spread throughout the subsystems. We use the last 25 years of the Brazilian monthly historical data as inflow scenarios, each with equal probability, and the planning horizon is comprised of 84 months (7 years). Moreover, we consider a fictitious unbounded thermal plant to represent energy deficit at a cost of 2,300 R$/MWh at each subsystem, which is also the cost of the penalization for the worst case load shedding. Finally, the fraction of pre-contingency stored energy that should be preserved (γ) is set to be equal to 0.9. The cost of load shedding is not taken into account when presenting operation costs. However, it is used in the SDDP convergence. Remaining data for the system is presented in Appendix B.

We applied the proposed methodology to the following cases: (i) case $n - 0$ in which no security criteria was applied, (ii) case $n_T - 1$ in which the $n - 1$ security criteria is applied to transmission lines solely, (iii) case $n_{GT} - 1$ in which the $n - 1$ security criteria is applied jointly to transmission lines and thermal units simultaneously and (iv) case $n_{GT} - 2$ in which the $n - 2$ security criteria was applied to transmission lines and thermal units simultaneously. For fair comparisons purposes, we test the performance of the proposed method against the SDDP model applied to the FCD model. We also test the performance of the MIP oracle against an oracle that identifies violated states by means of a inspection procedure. In the later, the system power imbalance is evaluated for each contingency state, the worst-case contingency is the one with the largest system power imbalance. To check convergence, we firstly run 1000 SDDP iterations and then we run the evaluation step every 100 iterations. And after turning the CCG algorithm off when no contingencies are identified after an entire SDDP iteration, we turn it on again also every 100 iterations. Convergence tolerance ϵ is set to be equal to 1% of the total demand at each period t. Each case study was implemented in Xpress 7.9 on a Intel(R) Core (R) i7-4790K CPU @ 4.0 GHz with 32GB of RAM. We interrupt the algorithm if the running time is greater than 72 hours.

Since no contingency constraint is taken into account in the hydrothermal planning in Brazil, the ISO sets the maximum capacity of each transmission line to be tighter than they actually are. This gives the ISO space to counter the negative effects of contingency states. Hence, in order to approximate our studies towards the operative reality, we let the maximum power flow capacity in post-contingency states to be 1.2 times bigger than they are in pre-contingency states.

Table 5.2 shows the convergence details for each case. To differentiate between the CCG with the MIP model and the CCG algorithm with an inspection procedure we name then CCG_{MIP} and CCG_{INSP} respectively.

Tab. 5.2: Convergence details

Case	Running time (hours)			$\lvert\mathcal{C}^*\rvert$	$\frac{\lvert\mathcal{C}^*\rvert}{\lvert\mathcal{C}\rvert}$
	FCD	CCG_{MIP}	CCG_{INSP}		
$n-0$	6.7	-	-	-	-
n_T-1	22.9	13.8	12.5	3	30.0%
$n_{GT}-1$	#	19.8	19.8	7	6.67%
$n_{GT}-2$	#	27.0	53.6	11	0.19%

The algorithm did not converge within the time limit of 3 complete days.

In all cases, the SDDP algorithm converged with 1100 iterations. Hence, for the stopping criteria proposed in this work, little sensibility regarding the security criteria adopted and the SDDP algorithm convergence was found. The Full Contingency Dependent (FCD) approach quickly loses its applicability due to its high running time, in comparison to instances where the oracle approach was used. Notice that for cases $n_T - 1$ and $n_{GT} - 1$ the running time for both types of oracles is comparable. However, in case $n_{GT} - 2$ the running time was considerably lower when the MIP oracle was applied. Hence, we notice a clear advantage of using the proposed MIP model as security criteria is set to be tighter. This is of extreme importance, since the $n - 2$ criteria is currently being applied in industry practice.

Table 5.3 shows policy details for each case.

Tab. 5.3: Policy details

Case	Operation cost (10^6R$)			Up-spinning Reserve Scheduling (% of total demand)			Down-spinning Reserve Scheduling (% of total demand)		
	$Q_{2.5\%}$	Expected Value	$Q_{97.5\%}$	$Q_{2.5\%}$	Expected Value	$Q_{97.5\%}$	$Q_{2.5\%}$	Expected Value	$Q_{2.5\%}$
$n - 0$	14,889.60	15,165.83	15,442.06	-	-	-	-	-	-
$n_T - 1$	15,447.24	15,722.47	15,977.69	0.949	0.951	0.953	0.957	0.960	0.963
$n_{GT} - 1$	15,576.18	15,853.69	16,129.89	1.178	1.184	1.190	0.971	0.974	0.977
$n_{GT} - 2$	20,191.23	20,465.32	20,739.41	3.991	4.000	4.009	4.000	4.454	4.467

The expected cost in case $n_T - 1$ is about the same expected operation cost of case $n - 0$. Hence, the $n - 1$ security criteria applied to this system does not significantly increase system operation. Similar conclusions can be made for case $n_{GT} - 1$. In case $n_{GT} - 2$, however, the expected cost is about 29% greater than the operation cost of case $n - 0$. This can be explained by the fact that reserve scheduling significantly increases in this case.

5.3.1 SDDP convergence analysis

Fig. 5.8 shows to lower bound evolution for each case.

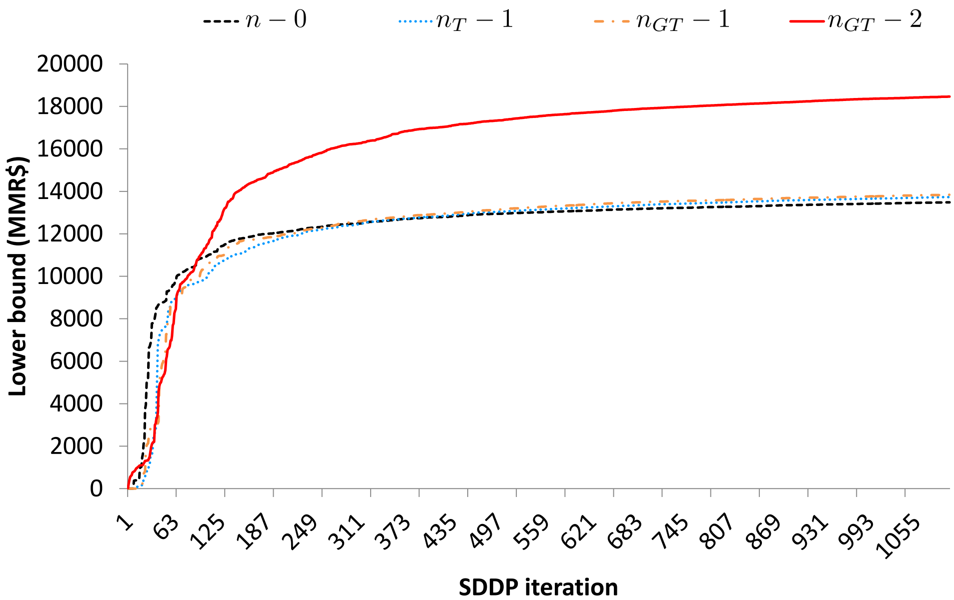

Fig. 5.8: Lower bound evolution.

In all cases, the SDDP algorithm converged with 1100 iterations. Hence, for the stopping criteria proposed in this work, little sensibility regarding the security criteria adopted and SDDP algorithm convergence was found. Cases $n-0$ and n_T-1 converge to similar values indicating that the $n-1$ criteria in this case has little effect on the system's operation. Case $n_{GT}-1$ converged to a slightly higher value than the first two cases. This is congruent with the fact that there is more reserve scheduling for this case, making the operation cost more expensive. Finally, case $n_{GT}-2$ converged to a much greater value than the other three cases. This is also explained by the high amount of reserve scheduling for this case.

5.3.2 Contingencies found by the oracle

Fig. 5.9 shows the number of contingency states identified in each SDDP method iteration by the oracle for all cases.

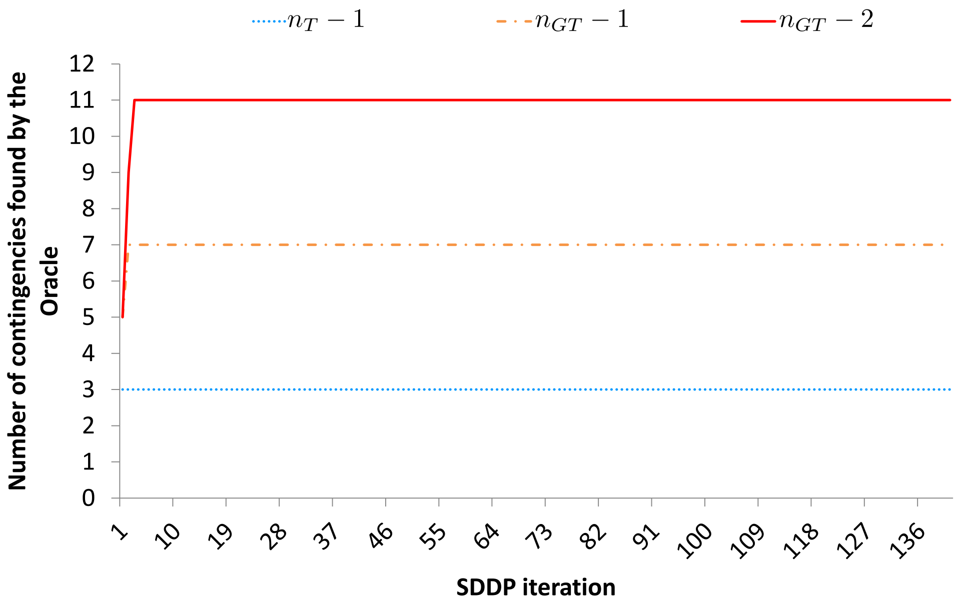

Fig. 5.9: Contingencies found by the oracle.

In case $n_T - 1$, 3 violated contingency states were identified in the very first SDDP iteration and no other contingency states were identified by the oracle in any subsequent iteration of the SDDP method. In case $n_{GT} - 1$ there were 5 violated contingency states identified in the first iteration of the SDDP method and another 2 contingencies were identified in the second SDDP iteration. In case $n_{GT} - 2$, there were 7 violated states identified in the first SDDP iteration, 4 identified in the second SDDP iteration and another 2 were identified in the third SDDP iteration. Notice that in all cases, no contingency states were identified after the first few SDDP iterations. In Appendix C, a summary for the identified contingency states is shown.

5.3.3 Operation cost

Fig. 5.10 shows the operation cost distribution for cases $n_T - 1$, $n_{GT} - 1$ and $n_{GT} - 2$ in percentage of the expected operation cost of case $n - 0$.

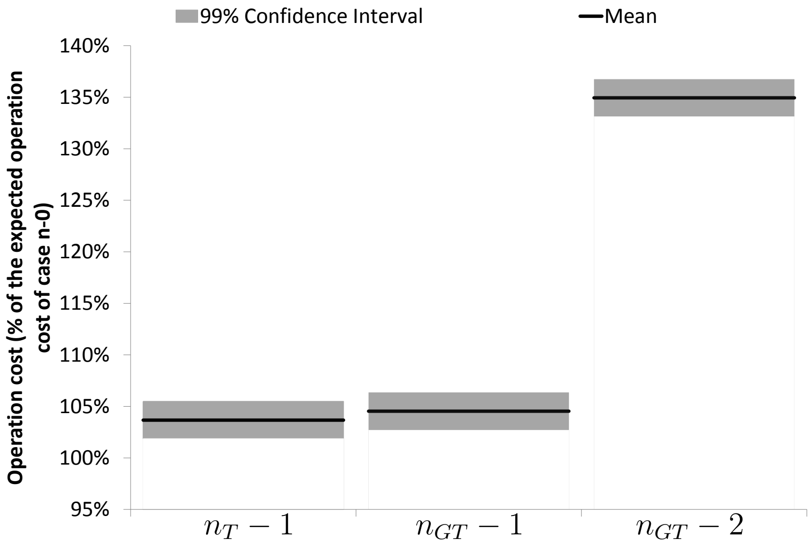

Fig. 5.10: Operation cost.

One important thing that should be mentioned is that one could question the usage of security criteria such as these ones, since they make the operation cost more expensive. However, the considerably low cost of case $n-0$, in comparison to the cost of case $n_{GT}-2$, for example, should not actually take place in reality. This is because the operation policy provided in such case is not robust to contingency states. Then, in case contingency actually happens, the operation cost of the $n-0$ security criteria could be significantly higher than the operation cost of a system operation with an $n-2$ security criteria experiencing the same contingency state.

5.3.4 Reserve scheduling

The total reserve scheduling for years 3 and 4 in case n_T-1 is shown in Fig. 5.11. Displayed values are in terms of % of the total demand in all subsystems. There is a clear tendency of allocating more spinning reserve during the months of Jan-Mai, which is congruent to the fact the energy demand is higher in such months. But reserve allocation dispersion tends to increase during the dry period. Hence, the model leads to an optimal reserve allocation that is state-dependent. Also, most of scheduled reserve comes from hydro power plants. This can be explained by the fact that they have a much bigger installed capacity in the Brazilian system and are also much cheaper than thermal units. Also it is interesting to notice that at some periods, specially when energy demand is low, no spinning reserve is scheduled.

This happens in scenarios of high inflows and low energy demand in which no thermal generator is dispatched.

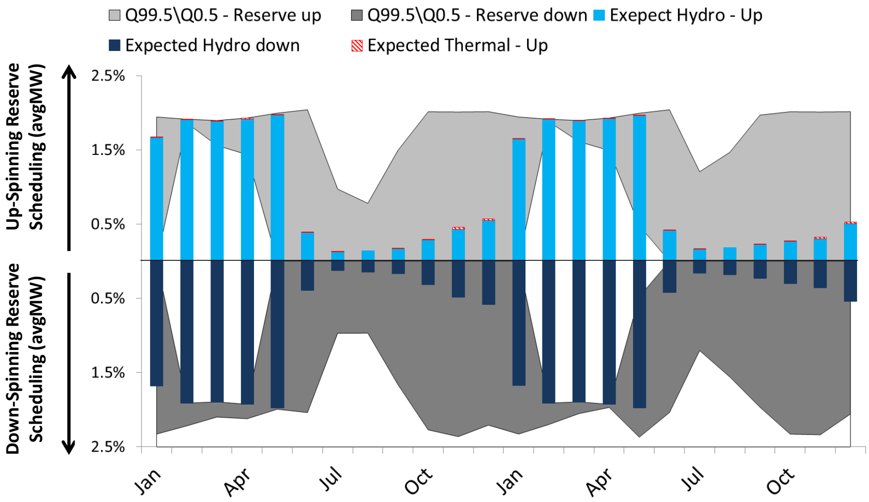

Fig. 5.11: Total reserve scheduling in case $n_T - 1$.

Fig. 5.12 shows up-spinning allocation by subsystem. In this case we see that most up-spinning reserve scheduling comes from the SE subsystem during the wet season. However, in the dry season, most of up-spinning reserve allocation comes from the NE subsystem. One very interesting conclusion from Fig. 5.12 is that the model is capable of providing optimal nodal allocation of reserves at each generator and subsystem to ensure deliverability. This is important since power flow in transmission lines is limited and might become an issue when exchanging energy from one subsystem to another in case of contingency.

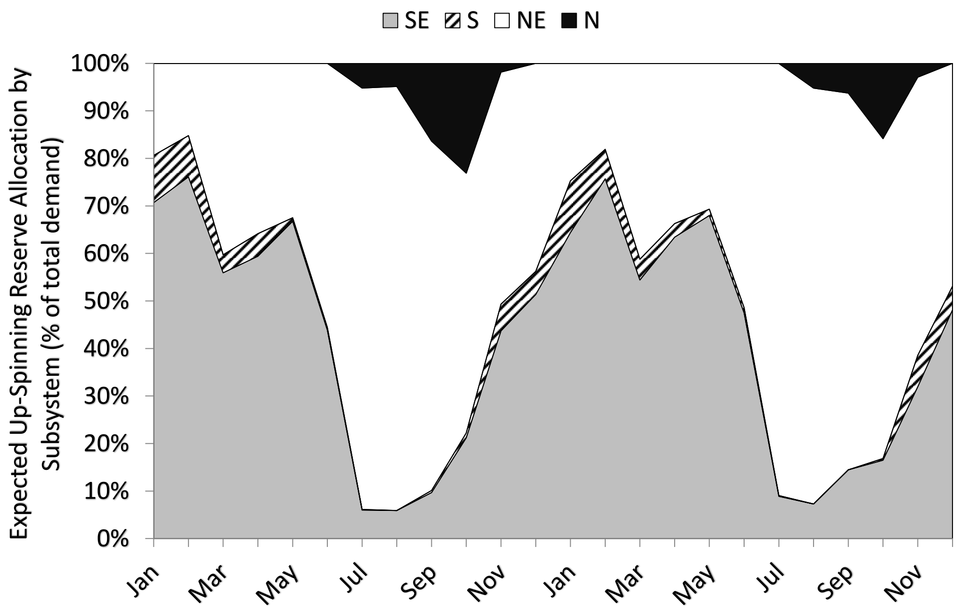

Fig. 5.12: Expected up-spinning reserve scheduling by subsystem in case $n_T - 1$.

Fig. 5.13 shows reserve allocation in case $n_{GT} - 1$. Whilst the expected reserve allocation is almost the same during the wet season and slightly increased in the dry seasons, when compared with case $n_T - 1$, it is noticeable from the quantiles that there is more dispersion in this case, specially during the dry season. Again, most of reserve allocation comes from hydro sources.

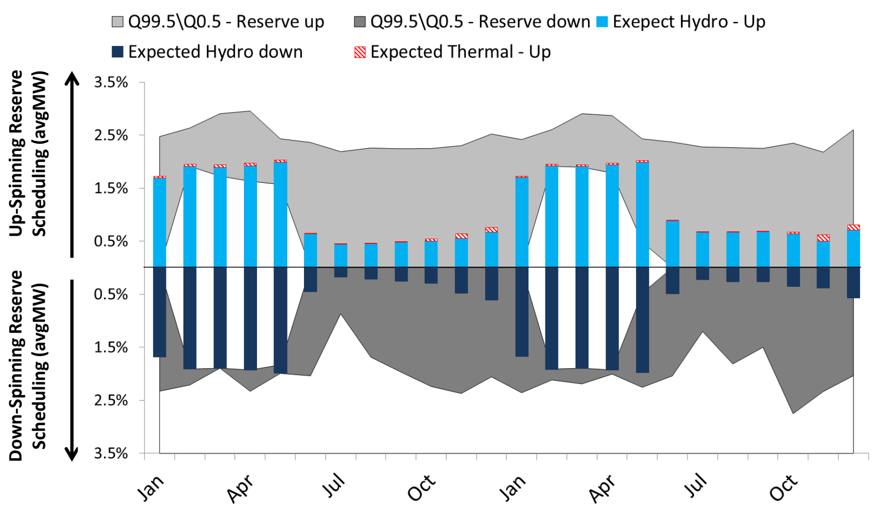

Fig. 5.13: Total reserve scheduling in case $n_{GT} - 1$.

Fig. 5.14 shows up-spinning reserve allocation by subsystem for this case.

Similar to case $n_T - 1$, most of scheduled reserve comes from the SE and NE subsystem. However, in this case reserve allocation in the SE subsystem is greater than it is in the other subsystems in all months.

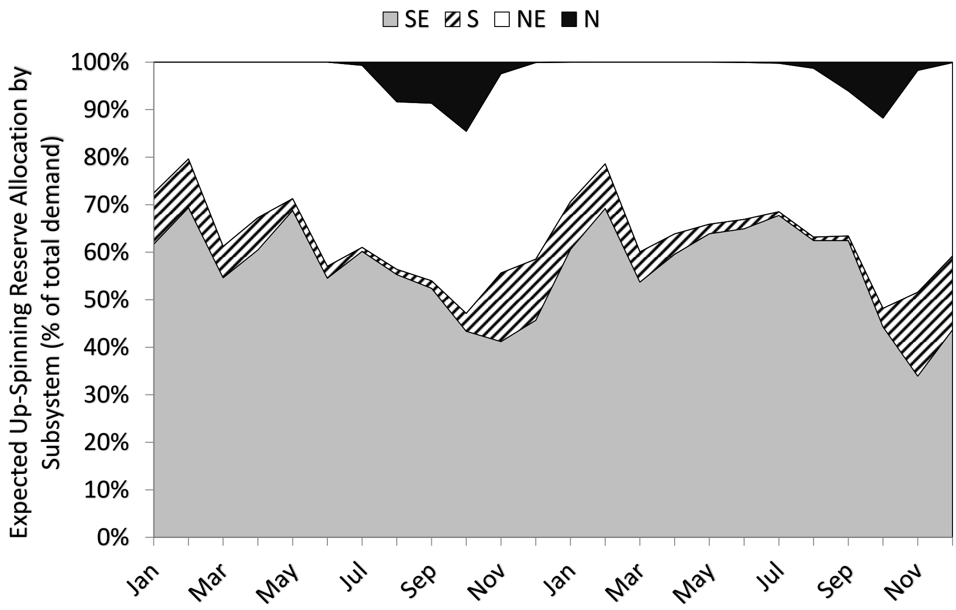

Fig. 5.14: Expected up-spinning reserve scheduling by subsystem in case $n_{GT} - 1$.

Fig. 5.15 shows reserve allocation for case $n_{GT} - 2$. In this case the expected allocation is significantly increased in all months and the dispersion is also greater. Notice that, differently from the two former cases, the quantiles indicate that reserve scheduling might be greater in dry seasons than it is in the wet season.

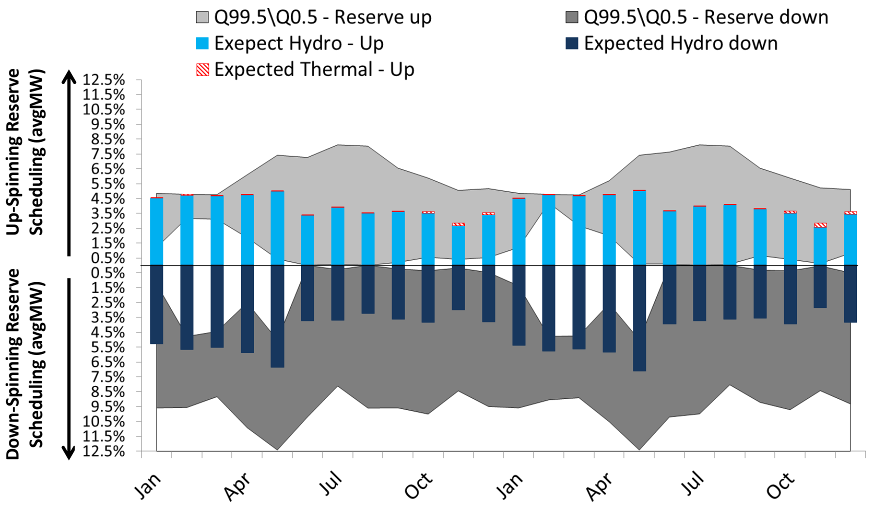

Fig. 5.15: Total reserve scheduling in case $n_{GT} - 2$.

Finally, Fig. 5.16 shows that in this case the total up-spinning reserve is still greater in the SE subsystem than it is in the other ones. Also, reserve scheduling in the NE subsystem is decreased but it increases in the S subsystem.

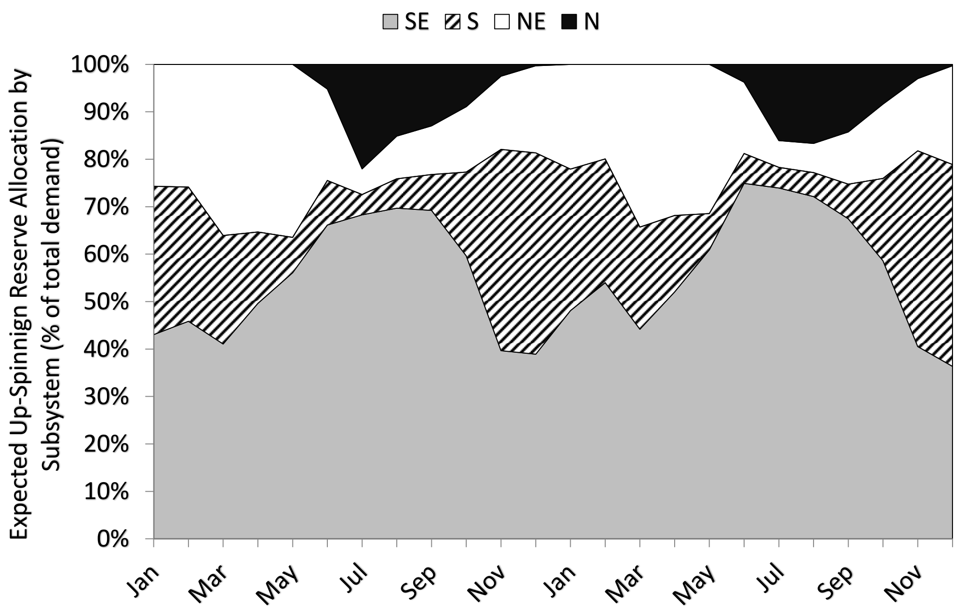

Fig. 5.16: Expected up-spinning reserve scheduling by subsystem in case $n_{GT} - 2$.

5.4 Time inconsistency analysis

In this section the effects of time inconsistency in the Brazilian based system are explored. Costs and gaps are evaluated disregarding load shedding costs in post-contingency states. Since in the Brazilian power systems the planning model does not contain neither contingency constraints and Kirchhoff's voltage law, a new case, named $n-0^*$, was run. Hence, in this case we have $\mathcal{X}_t \leftarrow \mathcal{X}_t^{box}$. Table 5.4 shows the inconsistency gap and operation cost for each case. Notice all gaps do not contain 0. Hence, we claim that they are statistically significant.

Tab. 5.4: Operation cost of time inconsistent policies and inconsistency gap

Case	Operation cost (MMR$)			GAP (MMR$)	GAP - 95% confidence interval (MMR$)	
	$Q_{2.5\%}$	Expected Value	$Q_{97.5\%}$		Lower bound	Upper bound
$n-0^*$	14,535.5	14,806.3	15,077.1	-	-	-
n_T-1	20,021.6	20,339.0	20,656.4	5,532.7	5,115.4	5,949.9
$n_{GT}-1$	20,648.7	20,978.3	21,307.8	6,172.0	5,745.4	6,598.5
$n_{GT}-2$	25,107.1	25,438.3	25,769.5	10,632.0	10,204.2	11,059.8

To further analyze the results, we pick two consecutive typical years in the resulting policies from case $n_{GT}-2$. We choose to show and analyze years 3 and 4 in the planning horizon. Fig. 5.17 shows the expected stored energy in the main reservoirs of the Brazilian system. Notice that in the consistent policy the stored energy in the SE reservoir is actually lower than it is in the inconsistent policy, whilst the opposite happens in the NE subsystem. This is because the inconsistent policy does not acknowledge the value of exchanging the stored energy from the SE to the NE subsystem as the consistent policy does. This materializes from a greater expected power flow from the SE subsystem to the NE subsystem in the consistent policy in contrast to the inconsistent policy. This situation is depicted in Fig. 5.18

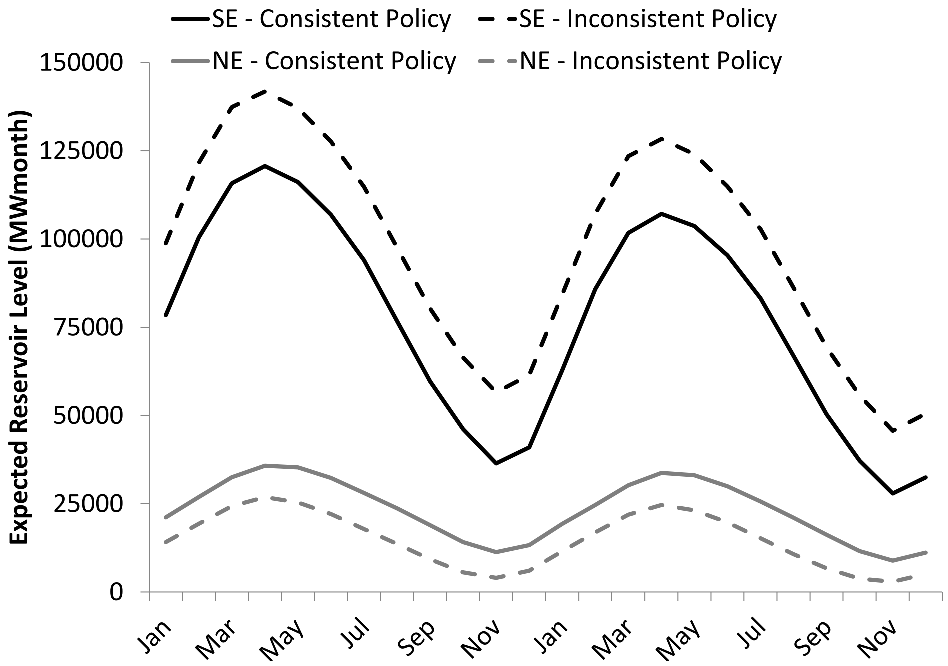

Fig. 5.17: SE and NE subsystems stored energy.

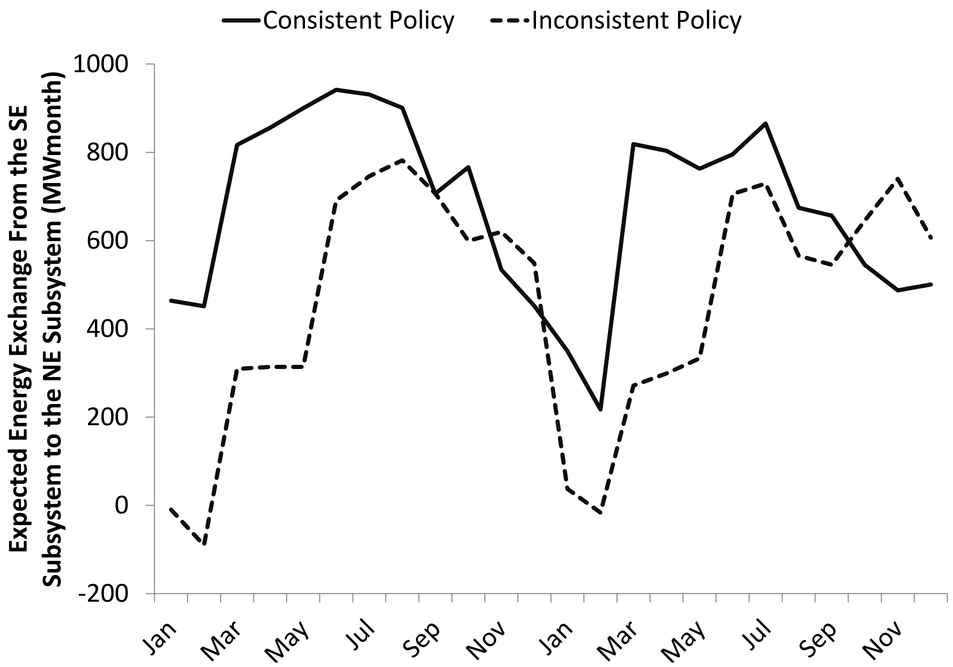

Fig. 5.18: Energy exchange from the SE subsystem to the NE subsystem.

As a direct consequence of less stored energy in the NE subsystem, thermal generation grows and starts to peak in dry seasons. Spot prices also increase in this situation and the price peaks in the inconsistent policy are about 5 times greater than the expected cost in the consistent policy. This is shown in Fig. 5.19.

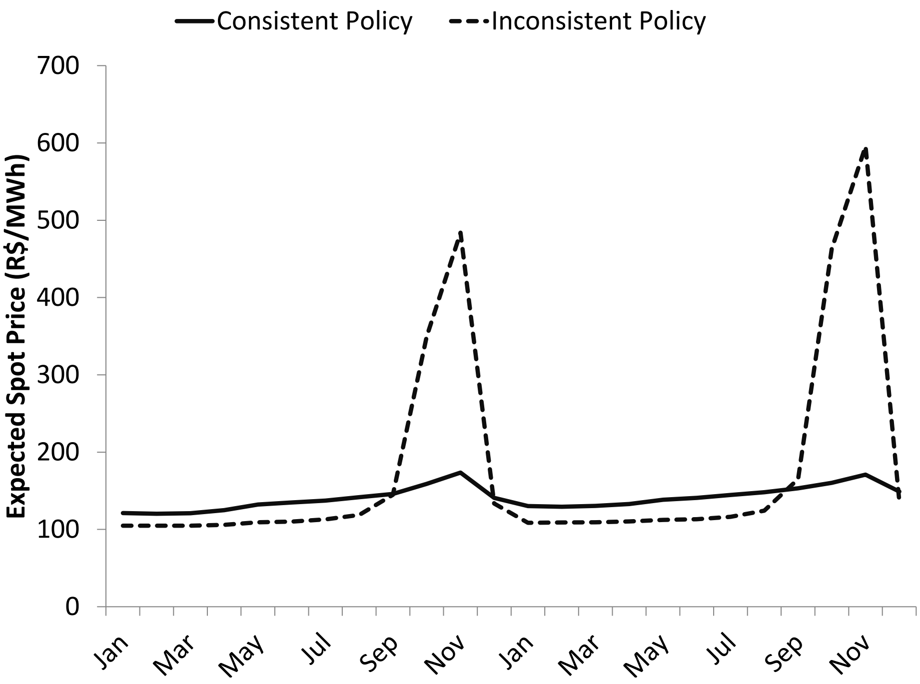

Fig. 5.19: Northeastern spot prices.

Another highly negative aspect of the inconsistency operation is that load-shedding increases significantly in contrast to load-shedding in the consistent policy. This is shown in Fig. 5.20.

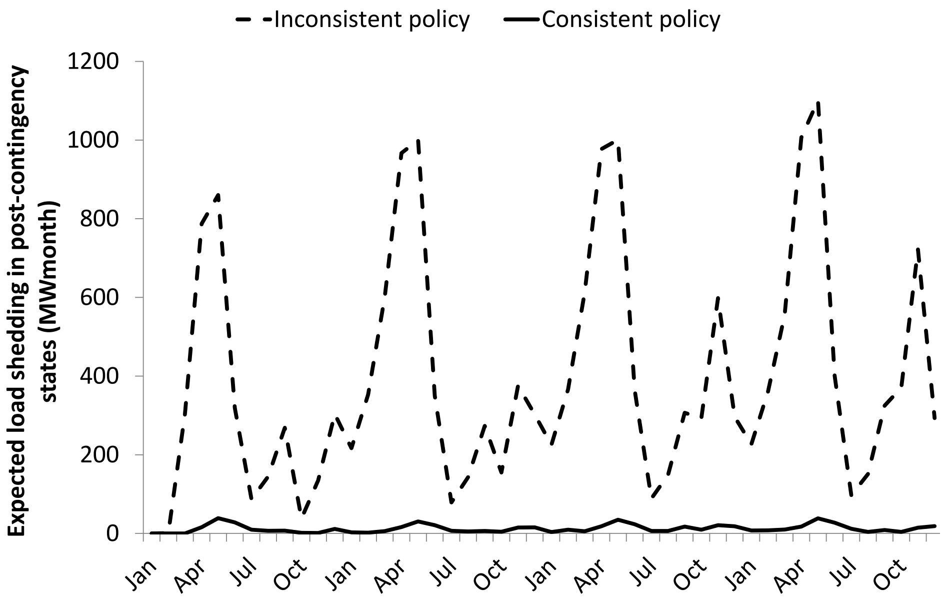

Fig. 5.20: Expected load shedding in post-contingency states.

6
Conclusions

In hydrothermal power systems operation planning, several system details are neglected in the planning model in exchange for computational tractability. However, such system details are taken into account in system implementation models. According to recent literature, when the system is planned differently than it is actually implemented, negative time inconsistency effects might rise.

In the planning model used by the Brazilian energy sector, no security criterion and reserve scheduling are considered. And the Brazilian system experienced a, previously unaccounted for, sharp depletions of its main reservoir precisely on the same year in which tight security criterion was being implemented in the system. In addition, recent blackouts in the Brazilian system were attributed to the lack of spinning reserve in the hours that preceded the events. These facts raise the question of whether time inconsistency is actually responsible for such negative events.

Along these lines, this work introduces the discussion of time inconsistency due to modeling simplifications in hydrothermal power systems operation. A methodology to investigate the costs and consequences of time inconsistency is introduced. The proposed method consists of simulating the system operation coupled with a sub-optimal recourse function. Also, an extension to the sub-optimal gap proposed in [42] is proposed in order to evaluate the cost of time inconsistency. The effects of time inconsistency are investigated for the two following modeling simplifications: Kirchoff's Voltage Law and security criteria. In both case studies, statistical significant gap values are observed. Moreover, results in example systems show that time inconsistency might lead to lower steady state levels for the hydro reservoir while increasing expensive thermal generation. As a consequence, under such inconsistent policies, spot prices are likely to peak exhibiting system vulnerabilities.

Hence, it seems reasonable that new models and solution algorithms should be investigated in order to mitigate the effects of time inconsistency and ensure reserve deployment in hydrothermal power systems. This work proposes then, a new hybrid robust-stochastic algorithm that merges the Column-and-Constraint Generation (CCG) and the SDDP algorithms in order to turn security criteria into a tractable detail to be incorporated in the planning model. This algorithm makes use of the fact that the umbrella set of contingencies is very similar for each period and scenario in the planning horizon and shares active contingency states identified by the CCG algorithm. Hence, The method was tested with a Brazilian based power system planning model for three different security criteria: (i) $n-1$ in transmission lines only, (ii) joint $n-1$ in transmission lines and thermal generation units, and (iii) joint $n-2$ in transmission lines and thermal generation units. Results show that the proposed algorithm is capable of providing a planning policy that takes reserve scheduling and security criteria into account whilst achieving reasonable computational time. Also, the proposed model provides nodal reserve allocation and is state dependent. Moreover, the efficient solution methodology also allows us to investigate the effects of time inconsistency in real-world systems. Results indicate that the tighter the security criterion adopted is, the higher the inconsistent gap will be with respect to the planning performed without security constraints.

Future research derived from this work involves new models and solution methodologies to mitigate the effects of time inconsistency in hydrothermal power systems operation induced from other modeling simplifications such as linear hydro constraints, uncertainty regarding fuel cost, renewable energy uncertainty, and reservoir aggregation.

Bibliography

[1] Operador Nacional do Sistema - ONS, Brasil. http://www.ons.org.br/conheca_sistema/pop_diagrama_esquemat_usinas.aspx.

[2] Global Wind Energy Council - GWEC, "Global Wind Statistics." http://www.gwec.net/wp-content/uploads/vip/GWEC-PRstats-2015_LR_corrected.pdf.

[3] Empresa de Pesquisa Energética - EPE, Brasil, "Plano Decenal de Expansão de Energia Elétrica." http://www.epe.gov.br/PDEE/Relat%C3%B3rio%20Final%20do%20PDE%202024.pdf.

[4] Operador Nacional do Sistema - ONS, Brasil. http://www.ons.org.br/historico/energia_armazenada.aspx.

[5] Agência Nacional de Energia Elétrica - ANEEL, Brasil. http://www.aneel.gov.br/aplicacoes/capacidadebrasil/capacidadebrasil.cfm.

[6] A. J. Wood and B. F. Wollenberg, *Power Generation, Operation, and Control*. 2nd ed. New York, NY, USA: Wiley, 1996.

[7] M. E. P. Maceira, V. S. Duarte, D. Penna, L. A. M. Moraes, and A. C. G. Melo, "Ten years of application of stochastic dual dynamic programming in official and agent studies in brazil-description of the newave program," *16th PSCC, Glasgow, Scotland*, pp. 14–18, 2008.

[8] L. A. Barroso, J. Rosenblatt, A. Guimaraes, B. Bezerra, and M. V. Pereira, "Auctions of contracts and energy call options to ensure supply adequacy in the second stage of the brazilian power sector reform," in *Power Engineering Society General Meeting, 2006. IEEE*, pp. 8–pp, IEEE, 2007.

[9] B. Fanzeres, A. Street, and L. A. Barroso, "Contracting strategies for renewable generators: a hybrid stochastic and robust optimization approach," *IEEE Transactions on Power Systems*, vol. 30, no. 4, pp. 1825–1837, 2015.

[10] M. E. P. Maceira, L. A. Terry, F. S. Costa, J. M. Damázio, and A. C. G. Melo, "Chain of optimization models for setting the energy dispatch and spot price in the brazilian system," in *Proceedings of the Power System Computation Conference-PSCC*, vol. 2, pp. 24–28, 2002.

[11] M. V. F. Pereira and L. M. V. G. Pinto, "Stochastic optimization of a multireservoir hydroelectric system: a decomposition approach," *Water resources research*, vol. 21, no. 6, pp. 779–792, 1985.

[12] M. V. Pereira and L. M. V. G. Pinto, "Multi-stage stochastic optimization applied to energy planning," *Mathematical programming*, vol. 52, no. 1-3, pp. 359–375, 1991.

[13] Z.-L. Chen and W. B. Powell, "Convergent cutting-plane and partial-sampling algorithm for multistage stochastic linear programs with recourse," *Journal of Optimization Theory and Applications*, vol. 102, no. 3, pp. 497–524, 1999.

[14] C. J. Donohue and J. R. Birge, "The abridged nested decomposition method for multistage stochastic linear programs with relatively complete recourse," *Algorithmic Operations Research*, vol. 1, no. 1, 2006.

[15] M. Hindsberger and A. B. Philpott, "Resa: A method for solving multistage stochastic linear programs," *Journal of Applied Operational Research*, vol. 6, no. 1, pp. 2–15, 2014.

[16] "Centro de Pesquisas de Energia Elétrica - CEPEL, Brasil". `http://www.cepel.br/`.

[17] A. Shapiro, "Analysis of stochastic dual dynamic programming method," *European Journal of Operational Research*, vol. 209, no. 1, pp. 63–72, 2011.

[18] T. H. de Mello, V. L. de Matos, and E. C. Finardi, "Sampling strategies and stopping criteria for stochastic dual dynamic programming: a case study in long-term hydrothermal scheduling," *Energy Systems*, vol. 2, no. 1, pp. 1–31, 2011.

[19] M. P. Soares, A. Street, and D. M. Valladao, "On the solution variability reduction of stochastic dual dynamic programming applied to energy planning," in *PES General Meeting— Conference & Exposition, 2014 IEEE*, pp. 1–5, IEEE, 2014.

[20] M. V. F. Pereira, G. C. Oliveira, C. C. G. Costa, and J. Kelman, "Stochastic streamflow models for hydroelectric systems," *Water Resources Research*, vol. 20, no. 3, pp. 379–390, 1984.

[21] D. L. D. D. Jardim, M. E. P. Maceira, and D. M. Falcao, “Stochastic streamflow model for hydroelectric systems using clustering techniques,” in *Power Tech Proceedings, 2001 IEEE Porto*, vol. 3, pp. 6–pp, IEEE, 2001.

[22] D. D. J. Penna, M. E. P. Maceira, and J. M. Damázio, “Selective sampling applied to long-term hydrothermal generation planning,” in *17th PSCC-Power Syst. Comp. Conf*, 2011.

[23] L. A. Barroso, A. Street, S. Granville, and M. V. Pereira, “Offering strategies and simulation of multi-item iterative auctions of energy contracts,” *Power Systems, IEEE Transactions on*, vol. 26, no. 4, pp. 1917–1928, 2011.

[24] A. Eichhorn and W. Römisch, “Polyhedral risk measures in stochastic programming,” *SIAM Journal on Optimization*, vol. 16, no. 1, pp. 69–95, 2005.

[25] V. Guigues and W. Römisch, “Sampling-based decomposition methods for multistage stochastic programs based on extended polyhedral risk measures,” *SIAM Journal on Optimization*, vol. 22, no. 2, pp. 286–312, 2012.

[26] R. Rockafellar and S. Uryasev, “Optimization of conditional value-at-risk,” *Journal of risk*, vol. 2, pp. 21–42, 2000.

[27] A. Street, “On the conditional value-at-risk probability-dependent utility function,” *Theory and Decision*, vol. 68, no. 1-2, pp. 49–68, 2010.

[28] A. Street, L. A. Barroso, R. Chabar, A. T. S. Mendes, and M. V. Pereira, “Pricing flexible natural gas supply contracts under uncertainty in hydrothermal markets,” *Power Systems, IEEE Transactions on*, vol. 23, no. 3, pp. 1009–1017, 2008.

[29] J. L. Higle and S. W. Wallace, “Managing risk in the new power business: a sequel,” *Computer Applications in Power, IEEE*, vol. 15, no. 2, pp. 12–19, 2002.

[30] M. Carrión, A. J. Conejo, and J. M. Arroyo, “Forward contracting and selling price determination for a retailer,” *Power Systems, IEEE Transactions on*, vol. 22, no. 4, pp. 2105–2114, 2007.

[31] S.-E. Fleten, S. W. Wallace, and W. T. Ziemba, “Portfolio management in a deregulated hydropower based electricity market,” in *Hydropower*, vol. 97, pp. 197–204, of, 1997.

[32] S. Bruno, S. Ahmed, A. Shapiro, and A. Street, “Risk neutral and risk averse approaches to multistage renewable investment planning under uncertainty,” *European Journal of Operational Research*, 2015.

[33] L. Freire, A. Street, D. A. Lima, and L. A. Barroso, “A hybrid milp and benders decomposition approach to find the nucleolus quota allocation for a renewable energy portfolio,” *IEEE Transactions on Power Systems*, vol. 30, no. 6, pp. 3265–3275, 2015.

[34] A. Shapiro, W. Tekaya, and J. P. da Costa M. P. Soares, “Risk neutral and risk averse stochastic dual dynamic programming method,” *European journal of operational research*, vol. 224, no. 2, pp. 375–391, 2013.

[35] A. B. Philpott and V. L. de Matos, “Dynamic sampling algorithms for multi-stage stochastic programs with risk aversion,” *European Journal of Operational Research*, vol. 218, no. 2, pp. 470–483, 2012.

[36] L. G. B. Marzano, *Portfolio optimization of energy contracts in hydrothermal systems under a centralized dispatch*. PhD thesis, Pontifical Catholic University of Rio de Janeiro, 2004.

[37] M. E. P. Maceira, L. G. B. Marzano, D. D. J. Penna, A. L. Diniz, and T. Justino, “Application of cvar risk aversion approach in the expansion and operation planning and for setting the spot price in the brazilian hydrothermal interconnected system,” *International Journal of Electrical Power & Energy Systems*, vol. 72, pp. 126–135, 2015.

[38] L. S. A. Martins, A. T. Azevedo, and S. Soares, “Nonlinear medium-term hydro-thermal scheduling with transmission constraints,” *Power Systems, IEEE Transactions on*, vol. 29, no. 4, pp. 1623–1633, 2014.

[39] A. Street, A. Moreira, and J. M. Arroyo, “Energy and reserve scheduling under a joint generation and transmission security criterion: an adjustable robust optimization approach,” *Power Systems, IEEE Transactions on*, vol. 29, no. 1, pp. 3–14, 2014.

[40] A. Street, F. Oliveira, and J. M. Arroyo, “Contingency-constrained unit commitment with security criterion: A robust optimization approach,” *Power Systems, IEEE Transactions on*, vol. 26, no. 3, pp. 1581–1590, 2011.

[41] A. Moreira., A. Street, and J. M. Arroyo, “Energy and reserve scheduling under correlated nodal demand uncertainty: An adjustable robust optimization approach,” *International Journal of Electrical Power & Energy Systems*, vol. 72, pp. 91–98, 2015.

[42] B. Rudloff, A. Street, and D. M. Valladão, “Time consistency and risk averse dynamic decision models: Definition, interpretation and practical consequences,” *European Journal of Operational Research*, vol. 234, no. 3, pp. 743–750, 2014.

[43] A. Shapiro, “On a time consistency concept in risk averse multistage stochastic programming,” *Operations Research Letters*, vol. 37, no. 3, pp. 143–147, 2009.

[44] T. Asamov and A. Ruszczyński, “Time-consistent approximations of risk-averse multistage stochastic optimization problems,” *Mathematical Programming*, pp. 1–35, 2014.

[45] T. H. de Mello and B. K. Pagnoncelli, “Risk aversion in multistage stochastic programming: A modeling and algorithmic perspective,” *European Journal of Operational Research*, vol. 249, no. 1, pp. 188–199, 2016.

[46] M. J. Machina, “Dynamic consistency and non-expected utility models of choice under uncertainty,” *Journal of Economic Literature*, pp. 1622–1668, 1989.

[47] Operador Nacional do Sistema - ONS, Brasil, “Inflow energy data from the brazilian hydro system.” `http://www.ons.org.br/operacao/enas_subsistemas.aspx`.

[48] “Ata da 81ª Reunião CMSE, `http://www.mme.gov.br/documents/10584/1139121/CMSE_-_Ata_da_81x_Reunixo_Plenxria_x26-04-2010x.pdf`,” 26th April 2010.

[49] Operador Nacional do Sistema - ONS, Brasil, “Nota Complementar à Imprensa - 04/02/2015.” `http://www.ons.org.br/download/sala_imprensa/notacomplementaraimprensa--04022014.pdf`.

[50] Operador Nacional do Sistema - ONS, Brasil, "Nota à imprensa (19/01/2015)." http://www.ons.org.br/download/sala_imprensa/notaaimprensa_19012015.pdf.

[51] G. Teles, "Document Reveals That Instability Begun 3 Hours Before the Blackout," *O Globo*, Jan, 2015.

[52] A. Salomão, "Power System Functions With Reserve Levels Bellow the Recommended," *O Globo*, Fev, 2014.

[53] J. Wang, N. E. Redondo, and F. D. Galiana, "Demand-side reserve offers in joint energy/reserve electricity markets," *Power Systems, IEEE Transactions on*, vol. 18, no. 4, pp. 1300–1306, 2003.

[54] J. M. Arroyo and F. D. Galiana, "Energy and reserve pricing in security and network-constrained electricity markets," *Power Systems, IEEE Transactions on*, vol. 20, no. 2, pp. 634–643, 2005.

[55] F. D. Galiana, F. Bouffard, J. M. Arroyo, and J. F. Restrepo, "Scheduling and pricing of coupled energy and primary, secondary, and tertiary reserves," *Proceedings of the IEEE*, vol. 93, no. 11, pp. 1970–1983, 2005.

[56] J. Wang, M. Shahidehpour, and Z. Li, "Contingency-constrained reserve requirements in joint energy and ancillary services auction," *Power Systems, IEEE Transactions on*, vol. 24, no. 3, pp. 1457–1468, 2009.

[57] K. W. Hedman, R. P. O'Neill, E. B. Fisher, and S. S. Oren, "Optimal transmission switching with contingency analysis," *Power Systems, IEEE Transactions on*, vol. 24, no. 3, pp. 1577–1586, 2009.

[58] K. W. Hedman, M. C. Ferris, R. P. O'Neill, E. B. Fisher, and S. S. Oren, "Co-optimization of generation unit commitment and transmission switching with n-1 reliability," *Power Systems, IEEE Transactions on*, vol. 25, no. 2, pp. 1052–1063, 2010.

[59] A. Street, F. Oliveira, and J. M. Arroyo, "Energy and reserve scheduling under an nk security criterion via robust optimization," in *Proc. 17th Power Systems Computation Conference (PSCC11)*, 2011.

[60] Q. Wang, J. P. Watson, and Y. Guan, "Two-stage robust optimization for n-k contingency-constrained unit commitment," *IEEE Transactions on Power Systems*, vol. 28, pp. 2366–2375, Aug 2013.

[61] D. Bertsimas and M. Sim, "The price of robustness," *Operations research*, vol. 52, no. 1, pp. 35–53, 2004.

[62] A. Ben-Tal, A. Goryashko, E. Guslitzer, and A. Nemirovski, "Adjustable robust solutions of uncertain linear programs," *Mathematical Programming*, vol. 99, no. 2, pp. 351–376, 2004.

[63] B. Zeng and L. Zhao, "Solving two-stage robust optimization problems using a column-and-constraint generation method," *Operations Research Letters*, vol. 41, no. 5, pp. 457 – 461, 2013.

[64] A. J. Ardakani and F. Bouffard, "Identification of umbrella constraints in dc-based security-constrained optimal power flow," *Power Systems, IEEE Transactions on*, vol. 28, no. 4, pp. 3924–3934, 2013.

[65] "Ministério de Minas e Energia - MME, Brasil." `http://www.mme.org.br/`.

[66] N. V. Arvanitidits and J. Rosing, "Composite representation of a multireservoir hydroelectric power system," *Power Apparatus and Systems, IEEE Transactions on*, no. 2, pp. 319–326, 1970.

[67] N. V. Arvanitidis, , and J. Rosing, "Optimal operation of multireservoir systems using a composite representation," *Power Apparatus and Systems, IEEE Transactions on*, no. 2, pp. 327–335, 1970.

[68] L. A. Terry, M. E. P. Maceira, C. V. Mercio, and V. S. Duarte, "Equivalent reservoir model for hydraulic coupled systems," *IX SEPOPE -Symposium of Simposium of Specialists in Electric Operational and Expansion Planning*, 2004.

[69] A. Street, D. A. Lima, A. Veiga, B. Fânzeres, L. Freire, and B. Amaral, "Fostering wind power penetration into the brazilian forward-contract market," in *Power and Energy Society General Meeting, 2012 IEEE*, pp. 1–8, IEEE, 2012.

[70] A. M. Silva, W. S. Sales, L. A. F. Manso, and R. Billinton, "Long-term probabilistic evaluation of operating reserve requirements with renewable sources," *Power Systems, IEEE Transactions on*, vol. 25, no. 1, pp. 106–116, 2010.

[71] J. R. Birge, "Decomposition and partitioning methods for multistage stochastic linear programs," *Operations Research*, vol. 33, no. 5, pp. 989–1007, 1985.

[72] K. Linowsky and A. B. Philpott, "On the convergence of sampling-based decomposition algorithms for multistage stochastic programs," *Journal of optimization theory and applications*, vol. 125, no. 2, pp. 349–366, 2005.

[73] A. B. Philpott and Z. Guan, "On the convergence of stochastic dual dynamic programming and related methods," *Operations Research Letters*, vol. 36, no. 4, pp. 450–455, 2008.

[74] P. Girardeau, V. Leclere, and A. B. Philpott, "On the convergence of decomposition methods for multistage stochastic convex programs," *Mathematics of Operations Research*, vol. 40, no. 1, pp. 130–145, 2014.

[75] K. Barty, "A note on the convergence of the sddp algorithm," *optimization-online.org*, 2012.

[76] S. Granville, G. C. Oliveira, L. M. Thomé, N. Campodónico, M. L. Latorre, M. V. F. Pereira, MVF, and L. A. Barroso, "Stochastic optimization of transmission constrained and large scale hydrothermal systems in a competitive framework," in *Power Engineering Society General Meeting, 2003, IEEE*, vol. 2, IEEE, 2003.

[77] A. Liu, B. F. Hobbs, J. Ho, J. McCalley, V. Krishnan, M. Shahidehpour, and Q. Zheng, "Co-optimization of transmission and other supply resources," *Prepared for the Eastern Interconnection States Planning Council, NARUC*, 2013.

[78] B. Zeng and L. Zhao, "Solving two-stage robust optimization problems using a column-and-constraint generation method," *Operations Research Letters*, vol. 41, no. 5, pp. 457–461, 2013.

[79] F. Bouffard, F. D. Galiana, and J. M. Arroyo, "Umbrella contingencies in security-constrained optimal power flow," in *15th Power Systems Computation Conference, PSCC*, vol. 5, 2005.

[80] D. Bertsimas and J. N. Tsitsiklis, *Introduction to linear optimization*, vol. 6. Athena Scientific Belmont, MA, 1997.

[81] Xpress Optimization Suite. http://www.fico.com/.

Appendices

Appendix A
Discussions on Time Inconsistent Models For Hydrothermal Power Systems Operation

Models discussed in Chapter 5 accounts for the $n - K$ security criterion in order to mitigate the effects of time inconsistency in hydrothermal power systems operation. However, in order to be time consistent, solution for the model should account for water spillage in pre-contingency states. This is because constraint (5-10) impose that water left in reservoir in post-contingency states should be a fraction of water left in reservoirs in pre-contingency states. Hence, pre-contingency solution should account for high levels of spillage if the value of γ is set too high, say, equal to 1.

For instance, suppose a reservoir has 100MW available by means of initial stored energy and water inflow. Without taking contingency states into account at first, the water balance equation could be written as:

$$v_t = 100 - u_t - s_t. \tag{A-1}$$

Suppose the optimal solution is $u_t = 1$ and $s_t = 1$, which leads to $v_t = 99$. Then, if post-contingency decisions is taken into account, the problem becomes:

$$v_t = 100 - u_t - s_t \tag{A-2}$$

$$v_t^c \geq \gamma v_t;\ \forall c \in \mathcal{C} \tag{A-3}$$

$$v_t^c = 100 - u_t^c - s_t^c;\ \forall c \in \mathcal{C}. \tag{A-4}$$

Suppose that at a given contingent state c the optimal solution is $u_t^c = 2$ and $s_t^c = 0$, which leads to $v_t^c = 98$. Note that, if $\gamma = 1$, then s_t must be equal to 1 so that $v_t = 98$. Hence, there is waste of cheap resources, which is a highly undesirable situation.

To overcome this issue, what should be done is allow final reservoir levels at post-contingency states (v_t^c) to be, say, at least 90% of pre-contingency levels. Note that this can be done by setting $\gamma = 0.9$ in constraint (5-10). Hence, spillage in pre-contingency states would not happen if hydro reserves were scheduled to be up to 10% of the final pre-contingency reservoir levels. However, this introduces a potential source of time inconsistency as some contingencies might lead the implemented policy to deviate from the planned one.

As an alternative, one could think of discounting up-spinning hydro reserve in equation (5-22) as follows:

$$H_t y_t = v_{t-1} + \mathrm{w}_{t,\omega} - \Delta u_t^{up}, \tag{A-5}$$

and eliminating (5-41). In this way, when contingency states happen, it would be possible to discharge all reserve and sustain post-contingency reservoir levels equal to the pre-contingency ones. Nevertheless, yet another source of time inconsistency in pre-contingency states arises from this formulation. This happens because if no contingency states occur, the final planned reservoir level should be shorter than the effectively implemented one, which would then be used in the following period as the initial storage to contemplate the reserve level fictitiously accounted for but not used.

Along these lines, there exists a trade-off between the adoption of one formulation or the other. If, by the one hand, the former is adopted, time inconsistency occurs when a contingency state happens. Even though unlikely, contingency states are harmful for the system and less water then planned should remain in reservoirs. On the other hand, in the later formulation time inconsistency arises in pre-contingency states which are the most likely states. However, in this source of time inconsistency, there will be more water than previously accounted for. In this case, even though implemented states should be less harmful, there would still be deviation from the planned ones and possible negative effects, such as market distortions, should still occur. In this sense, the later model is more risk-averse than the former.

Appendix B
Data For Case Studies From Chapter 5

Tab. B.1: Reserve cost for hydro plants for case studies from Chapter 5

Hydro plant	c^{up}	c^{dn}
SE	5	2
S	5.5	2.5
NE	6	3
NE	6.5	3.5

Tab. B.2: Transmission line data for case studies from Chapter 5

Transmission line	From	To	$\overline{F}$ (MW)	x (pu)
1	SE	S	3850	1
2	SE	S	3850	1
3	SE	NE	500	1
4	SE	NE	500	1
5	SE	Imperatriz	2000	1
6	SE	Imperatriz	2000	1
7	NE	Imperatriz	1980	1
8	NE	Imperatriz	1980	1
9	N	Imperatriz	1574	1
10	N	Imperatriz	1574	1

Tab. B.3: SE subsystem inflow data for case studies from Chapter 5 (MWmonth)

	Jan	Feb	Mar	Apr	Mai	Jun	Jul	Aug	Sep	Oct	Nov	Dec
1989	57492	60841	53980	36202	28100	23593	21316	25463	26246	20358	27336	62655
1990	79711	41397	43143	34741	29663	23024	24399	22020	25830	26548	24366	25119
1991	47675	64956	67589	68237	39812	29407	24668	19672	17125	26392	22818	35153
1992	59939	85850	55549	50229	49954	34213	26046	22294	27881	33842	45942	53800
1993	47618	68043	55607	46683	32297	31268	23083	20688	23187	29337	21151	35122
1994	64242	51156	60587	43217	31965	28561	24260	18859	15101	15980	23728	36155
1995	52033	83089	51899	46963	34553	24851	23659	16810	15453	25645	25113	33841
1996	54705	40757	53675	36294	26398	20891	18138	15966	21040	21942	36214	45654
1997	91733	72623	57340	44941	32515	39236	28081	21218	20253	24862	33307	50420
1998	42917	53523	55192	45015	34691	26449	20732	22483	23157	33401	28656	39389
1999	58172	50152	58904	33859	25772	24001	22141	15666	16599	13760	19991	30979
2000	55086	67193	61750	37938	24808	21243	19637	18794	29810	18570	29025	44900
2001	40408	40077	37906	28635	22673	20285	17172	14625	15492	21866	25856	40097
2002	63205	70382	48800	31251	28539	20773	18110	16350	17336	13128	22553	34851
2003	59676	61144	48336	42433	26791	22631	19317	15453	14901	15661	21409	33553
2004	46920	70979	62252	48041	37449	33344	27521	19268	15114	21647	25949	40178

2005	66456	58500	56761	37543	31017	27843	21228	16947	19565	23056	28733	56438
2006	46497	48707	58816	50040	29101	23156	20355	17288	18415	25962	28972	56495
2007	94605	90929	51458	35442	29123	24070	23365	18878	13222	13424	23682	29875
2008	37972	63252	63738	52206	36211	28072	21178	22681	16272	20869	26112	38238
2009	54583	65848	47528	48871	31401	25564	27969	24338	31695	36870	37511	61945
2010	70653	59278	53828	45650	29402	23375	20568	15930	13799	21837	29116	44302
2011	76036	49825	85999	54975	33691	27975	24232	23952	16530	24899	27107	44359
2012	73094	49275	36886	32008	29755	38166	26257	17135	14598	14999	23056	27619
2013	46596	56166	48967	51081	29018	38001	30589	18994	16897	23751	22610	39726

Tab. B.4: S subsystem inflow data for case studies from Chapter 5 (MWmonth)

	Jan	Feb	Mar	Apr	Mai	Jun	Jul	Aug	Sep	Oct	Nov	Dec
1989	10015	14803	7614	7628	12712	3661	8645	10981	29655	12087	5343	3299
1990	17794	10643	6737	12555	13063	31507	14909	14605	20464	24132	17537	7448
1991	3562	3757	2684	2986	2480	10326	7652	7733	2870	8446	7725	9281
1992	5877	7272	8378	7363	25120	29089	21343	17347	12963	7858	8587	5302
1993	5828	9531	8802	5977	12571	11666	19584	6257	12121	22723	6600	11064
1994	4574	13808	7749	6964	11646	16075	19577	7237	4647	11031	12958	7349
1995	25351	13093	7411	4321	2541	5224	12140	6013	7468	15085	5876	4270
1996	12526	17123	13359	11481	3187	7951	14943	10566	13445	18316	11402	8896
1997	10510	22849	9004	3008	3283	10093	12053	18320	8024	36592	34385	13231
1998	15722	24215	19229	31326	22116	8683	14049	25154	26920	25902	7383	5788
1999	5629	8580	5935	8828	4682	10099	20342	4960	5523	13595	5410	4061
2000	5182	7117	8154	4443	4890	5547	11771	6587	26617	24910	8000	6365
2001	13144	20969	11073	9057	12036	11179	14288	8026	9590	26456	7693	8538
2002	7376	6043	4699	4170	9309	11276	7234	12131	15002	19032	17410	16827
2003	7858	9222	8343	4096	4283	7693	7293	3224	2795	5779	7433	17167
2004	8992	4548	3299	3955	8788	8269	12697	4569	8550	14378	12819	5909
2005	5569	2942	2573	6292	14535	17194	9609	7846	27044	29785	12724	4256
2006	4540	3963	3840	2906	1583	2328	3152	5180	5402	5093	7176	7422
2007	6974	7358	9612	8571	19665	7757	12541	6603	8851	10132	14213	7649
2008	7451	5085	4359	5922	9796	9816	6697	9304	8232	22119	19426	4999
2009	5695	5014	4486	1862	2632	3873	12625	18792	30253	25244	14547	12101
2010	16384	15184	9942	20292	23843	10941	11674	9290	7004	6927	5666	16675
2011	12389	21137	12896	11436	6362	8429	22914	31180	25780	11655	7324	3937
2012	6990	5649	4078	4044	5820	14990	10151	8130	4967	7659	4927	4661
2013	9078	7007	12929	7776	5029	18794	16478	18308	17427	13700	6656	6572

Tab. B.5: NE subsystem inflow data for case studies from Chapter 5 (MWmonth)

	Jan	Feb	Mar	Apr	Mai	Jun	Jul	Aug	Sep	Oct	Nov	Dec
1989	11194	7856	9535	6027	4212	3290	3238	3019	2826	3093	5352	20447
1990	28067	12446	9684	6659	4265	3403	3495	3215	3238	3547	4457	5189
1991	10432	15733	14340	15656	7794	4836	3861	3524	3295	4174	6198	9605
1992	15181	29912	39282	13269	8672	5730	4635	4245	4262	5672	12706	16230
1993	18067	13811	12534	7948	5716	4339	3792	3630	3240	3813	4036	5835
1994	15087	14584	14948	15324	6896	4954	4220	3449	3420	2703	3052	9121
1995	8982	8889	9310	8447	5581	4258	3322	2936	2344	2781	5084	9730
1996	13799	7081	6496	5738	4020	3152	2644	2095	2045	2459	5112	10188
1997	17760	14926	13824	13654	7953	5300	4077	3663	3217	3328	3883	9219
1998	10338	9769	9557	4850	3614	2868	2501	2301	2052	2097	5878	9932
1999	9340	5689	11711	7668	3950	2799	2391	2090	2334	1879	4862	10070
2000	13150	15038	13523	11028	5502	3711	2929	3008	2787	2469	5287	11423
2001	10238	5363	5356	4030	2645	2559	2075	1921	2030	2296	3600	6474
2002	16842	14630	10691	6948	3360	2724	2585	2029	1587	2075	2836	5529
2003	12293	13174	8020	7901	4152	3010	2651	2270	2074	1535	2502	4629
2004	9668	14911	20199	15971	8521	4519	3916	3040	2722	2714	3205	5416
2005	11856	14971	14587	12431	6714	4434	3577	2978	2907	2742	4068	13051
2006	12971	6986	10624	13384	7086	3954	3254	3038	2918	3942	8542	12094
2007	16881	21394	20535	7788	4641	3867	3039	2978	2228	1802	1900	4729
2008	5821	11438	13473	14218	5905	3386	2790	2513	2005	2192	2703	7218
2009	15968	14559	10547	13049	7836	4595	3704	2925	3006	4097	7848	7808
2010	10283	5667	7878	8454	3868	3094	2481	2098	2025	2473	5202	9241
2011	13165	9317	11530	15223	5897	3691	3157	2434	2184	2749	3931	10550

2012	17120	15437	6448	6344	3729	3623	2745	2258	1965	1673	4413	6730
2013	5012	10506	5344	8115	4437	3354	2553	2264	1848	2017	2618	8942

Tab. B.6: N subsystem inflow data for case studies from Chapter 5 (MWmonth)

	Jan	Feb	Mar	Apr	Mai	Jun	Jul	Aug	Sep	Oct	Nov	Dec
1989	9808	10907	14621	17367	13720	6584	4048	2782	2244	2268	4263	13410
1990	22546	14871	18346	14919	8981	4955	3370	2374	2179	2162	2534	3597
1991	8178	11572	13864	18152	13983	7127	3739	2847	2159	2031	2611	4414
1992	7127	21863	15542	15272	9164	4335	2704	2105	1922	2006	3427	8441
1993	10440	11640	13440	12204	8087	3912	2625	2016	1791	1980	2462	4193
1994	10877	14433	20206	18383	10824	5792	3686	2563	2002	1959	2178	5125
1995	9672	14325	15022	17687	15898	8831	4259	2771	1977	1868	3051	6619
1996	10525	9711	12615	14031	10365	5578	3767	2659	1883	2097	3219	4277
1997	9975	13368	19266	24233	17185	7286	4232	2854	2201	2089	2413	4220
1998	6762	8943	12022	8542	5294	3107	2373	1506	1369	1375	2533	5106
1999	8095	7999	12717	10661	8754	4451	2792	2035	1654	1728	3054	7427
2000	14472	16263	20872	18425	13266	5624	3837	2679	2152	2105	3400	8148
2001	9383	10190	13200	14094	7790	4733	3112	2165	1651	1906	2999	6595
2002	18488	17699	14872	14881	8180	4416	2541	1727	1400	1476	2128	3064
2003	6957	10976	14414	16306	9789	4758	2839	1997	1469	1376	2413	3438
2004	8130	22285	23999	21828	12559	5272	3256	2358	1742	1713	2353	3805
2005	6497	12755	18797	16329	11812	5066	3008	1888	1394	1386	1893	6223
2006	10399	10605	13439	20756	17282	7176	3684	2308	1747	2041	3836	4715
2007	6271	14947	17012	13827	8026	4071	2649	1848	1392	1321	1522	3171
2008	5113	10648	15443	18073	13295	5880	3265	2174	1589	1475	1981	5876
2009	8053	11544	14076	16603	19464	9348	4234	2462	1896	2205	4132	6396
2010	11880	12044	12351	15956	7848	4026	2714	2101	1515	1574	2681	5073
2011	10339	14545	20164	19933	14357	5964	3633	2377	1661	2058	3880	7133
2012	13914	16688	16056	11412	6489	3829	2650	1696	1394	1353	2463	5029
2013	7028	12718	12770	15087	10869	4916	3036	2086	1607	1626	2670	5773

Tab. B.7: Thermal generators data for case studies from Chapter 5

Thermal Unit	Subsystem	c (R$/MWh)	$\overline{G}$ (MW)	$\overline{\Delta G}^{up}$ (MW)	$\overline{\Delta G}^{dn}$ (MW)	c^{up} (R$/MWh)	c^{dn} (R$/MWh)
1	SE	145.2	657.5	328.8	131.5	131.5	72.6
2	SE	139.6	1351.2	675.6	270.2	270.2	69.8
3	SE	937.2	37.2	18.6	7.4	7.4	468.6
4	SE	208.9	251.4	125.7	50.3	50.3	104.4
5	SE	222.5	251.5	125.7	50.3	50.3	111.2
6	SE	151.6	29.6	14.8	5.9	5.9	75.8
7	SE	106.2	529	264.5	105.8	105.8	53.1
8	SE	584.6	44	22	8.8	8.8	292.3
9	SE	100.4	255	127.5	51.0	51.0	50.2
10	SE	120.8	235.9	117.9	47.2	47.2	60.4
11	SE	166.8	386.3	193.2	77.3	77.3	83.4
12	SE	251	387.9	193.9	77.6	77.6	125.5
13	SE	635	147	73.5	29.4	29.4	317.5
14	SE	190.9	226.3	113.2	45.3	45.3	95.4
15	SE	646.5	131.6	65.8	26.3	26.3	323.3
16	SE	153.4	87.3	43.7	17.5	17.5	76.7
17	SE	141	205.1	102.6	41.0	41.0	70.5
18	SE	294.5	924.3	462.1	184.8	184.8	147.2
19	SE	254.6	923.6	461.8	184.7	184.7	127.3
20	SE	158.9	400.4	200.2	80.1	80.1	79.5
21	SE	180	101.1	50.5	20.2	20.2	90.0
22	SE	103.2	200.3	100.1	40.1	40.1	51.6
23	SE	155.3	169.7	84.8	33.9	33.9	77.6
24	SE	183	387.9	193.9	77.6	77.6	91.5
25	SE	164	30.3	15.1	6.1	6.1	82.0
26	SE	470.5	200.9	100.4	40.2	40.2	235.2
27	SE	183.7	273.5	136.8	54.7	54.7	91.8
28	SE	525.2	30.2	15.1	6.0	6.0	262.6
29	SE	311.5	441.9	220.9	88.4	88.4	155.8
30	SE	214.5	565.1	282.6	113.0	113.0	107.3

31	SE	108.7	259.6	129.8	51.9	51.9	54.3
32	SE	141.5	258.8	129.4	51.8	51.8	70.7
33	SE	293.2	258.8	129.4	51.8	51.8	146.6
34	SE	611.6	65.7	32.8	13.1	13.1	305.8
35	SE	487.9	340.1	170	68.0	68.0	244.0
36	SE	130.8	1059.9	530	212.0	212.0	65.4
37	SE	215.7	1058.5	529.3	211.7	211.7	107.9
38	SE	1049.1	10.3	5.2	2.1	2.1	524.5
39	SE	101	198.1	99.1	39.6	39.6	50.5
40	SE	463.7	176.2	88.1	35.2	35.2	231.9
41	SE	198	207.1	103.6	41.4	41.4	99.0
42	SE	845	55.8	27.9	11.2	11.2	422.5
43	S	565.3	66.6	33.3	13.3	13.3	282.6
44	S	219.9	486.6	243.3	97.3	97.3	110.0
45	S	220.8	486.9	243.4	97.4	97.4	110.4
46	S	173.9	351.9	176	70.4	70.4	87.0
47	S	542.4	161.3	80.6	32.3	32.3	271.2
48	S	164.5	72.5	36.3	14.5	14.5	82.2
49	S	192.7	5.3	2.7	1.1	1.1	96.3
50	S	343.5	21.3	10.6	4.3	4.3	171.8
51	S	201.6	100.9	50.5	20.2	20.2	100.8
52	S	158.6	133.1	66.6	26.6	26.6	79.3
53	S	149.5	263.1	131.5	52.6	52.6	74.8
54	S	125.1	364.1	182	72.8	72.8	62.5
55	S	781.4	24	12	4.8	4.8	390.7
56	S	117	127.9	64	25.6	25.6	58.5
57	S	115.9	321.3	160.6	64.2	64.2	58.0
58	S	248.9	21.6	10.8	4.3	4.3	124.5
59	S	142.1	640.1	320.1	128.0	128.0	71.1
60	NE	537	13.6	6.8	2.7	2.7	268.5
61	NE	532.1	12.3	6.2	2.5	2.5	266.1
62	NE	647.2	34	17	6.8	6.8	323.6
63	NE	536.8	11.4	5.7	2.3	2.3	268.4
64	NE	836.1	348.5	174.3	69.7	69.7	418.1
65	NE	710	152.6	76.3	30.5	30.5	355.0
66	NE	709.8	151.7	75.8	30.3	30.3	354.9
67	NE	464.7	169.4	84.7	33.9	33.9	232.4
68	NE	580.7	13.6	6.8	2.7	2.7	290.3
69	NE	581.4	15.5	7.8	3.1	3.1	290.7
70	NE	188.4	220.4	110.2	44.1	44.1	94.2
71	NE	494.1	221.4	110.7	44.3	44.3	247.1
72	NE	536.1	14.1	7	2.8	2.8	268.1
73	NE	540.9	15.7	7.9	3.1	3.1	270.4
74	NE	189.4	138.9	69.5	27.8	27.8	94.7
75	NE	208.4	347.2	173.6	69.4	69.4	104.2
76	NE	463	150.7	75.4	30.1	30.1	231.5
77	NE	468.8	150.7	75.4	30.1	30.1	234.4
78	NE	535.3	16.7	8.3	3.3	3.3	267.6
79	NE	537.1	15.8	7.9	3.2	3.2	268.6
80	NE	449.7	169.3	84.7	33.9	33.9	224.9
81	NE	560.4	14.3	7.2	2.9	2.9	280.2
82	NE	565.8	14.9	7.4	3.0	3.0	282.9
83	NE	928.4	103	51.5	20.6	20.6	464.2
84	NE	779.8	136.4	68.2	27.3	27.3	389.9
85	NE	840.7	54.8	27.4	11.0	11.0	420.4
86	NE	836.7	66.7	33.4	13.3	13.3	418.4
87	NE	204.8	186.5	93.3	37.3	37.3	102.4
88	NE	458.9	51	25.5	10.2	10.2	229.5
89	NE	927.5	157.3	78.7	31.5	31.5	463.8
90	NE	460.9	171.5	85.7	34.3	34.3	230.5
91	NE	465.9	172.9	86.5	34.6	34.6	233.0
92	NE	190.2	533.1	266.5	106.6	106.6	95.1
93	NE	289.2	324.4	162.2	64.9	64.9	144.6
94	N	465.5	166.3	83.1	33.2	33.2	232.7
95	N	470.1	166.4	83.2	33.3	33.3	235.0

Tab. B.8: Demand data for case studies from Chapter 5 (MWmonth)

Period (month)	SE	S	NE	N

1	40117	11127	9248	4344
2	41110	11383	9020	4365
3	41221	11473	9257	4502
4	40360	11114	9302	4539
5	38621	10446	9049	4600
6	38079	10387	8701	4578
7	38223	10291	8680	4553
8	38652	10128	8492	4602
9	39095	10102	8677	4620
10	39004	10151	8839	4583
11	38809	10431	8862	4574
12	38770	10469	8781	4517
13	40117	11127	9248	4344
14	41110	11383	9020	4365
15	41221	11473	9257	4502
16	40360	11114	9302	4539
17	38621	10446	9049	4600
18	38079	10387	8701	4578
19	38223	10291	8680	4553
20	38652	10128	8492	4602
21	39095	10102	8677	4620
22	39004	10151	8839	4583
23	38809	10431	8862	4574
24	38770	10469	8781	4517
25	40117	11127	9248	4344
26	41110	11383	9020	4365
27	41221	11473	9257	4502
28	40360	11114	9302	4539
29	38621	10446	9049	4600
30	38079	10387	8701	4578
31	38223	10291	8680	4553
32	38652	10128	8492	4602
33	39095	10102	8677	4620
34	39004	10151	8839	4583
35	38809	10431	8862	4574

36	38770	10469	8781	4517
37	40117	11127	9248	4344
38	41110	11383	9020	4365
39	41221	11473	9257	4502
40	40360	11114	9302	4539
41	38621	10446	9049	4600
42	38079	10387	8701	4578
43	38223	10291	8680	4553
44	38652	10128	8492	4602
45	39095	10102	8677	4620
46	39004	10151	8839	4583
47	38809	10431	8862	4574
48	38770	10469	8781	4517
49	40117	11127	9248	4344
50	41110	11383	9020	4365
51	41221	11473	9257	4502
52	40360	11114	9302	4539
53	38621	10446	9049	4600
54	38079	10387	8701	4578
55	38223	10291	8680	4553
56	38652	10128	8492	4602
57	39095	10102	8677	4620
58	39004	10151	8839	4583
59	38809	10431	8862	4574
60	38770	10469	8781	4517
61	40117	11127	9248	4344
62	41110	11383	9020	4365
63	41221	11473	9257	4502
64	40360	11114	9302	4539
65	38621	10446	9049	4600
66	38079	10387	8701	4578
67	38223	10291	8680	4553
68	38652	10128	8492	4602
69	39095	10102	8677	4620
70	39004	10151	8839	4583

71	38809	10431	8862	4574
72	38770	10469	8781	4517
73	40117	11127	9248	4344
74	41110	11383	9020	4365
75	41221	11473	9257	4502
76	40360	11114	9302	4539
77	38621	10446	9049	4600
78	38079	10387	8701	4578
79	38223	10291	8680	4553
80	38652	10128	8492	4602
81	39095	10102	8677	4620
82	39004	10151	8839	4583
83	38809	10431	8862	4574
84	38770	10469	8781	4517

Appendix C
Summary of Contingency States Identified by the Oracle

Tab. C.1: Contingency states identified by the solution oracle for case $n_T - 1$

Contingency state	Transmission line	Thermal generator
1	$\{9\}$	-
2	$\{1\}$	-
3	$\{3\}$	-

Tab. C.2: Contingency states identified by the solution oracle for case $n_{GT} - 1$

Contingency state	Transmission line	Thermal generator
1	$\{9\}$	-
2	$\{1\}$	-
3	$\{3\}$	-
4	-	$\{6\}$
5	-	$\{40\}$
6	-	$\{63\}$
7	-	$\{65\}$

Tab. C.3: Contingency states identified by the solution oracle for case $n_{GT} - 2$

Contingency state	Transmission line	Thermal generator
1	$\{1, 2\}$	-
2	$\{9, 10\}$	-
3	$\{3\}$	$\{92\}$
4	$\{5, 6\}$	-
5	-	$\{2, 36\}$
6	-	$\{1, 59\}$
7	-	$\{36, 59\}$
8	-	$\{2, 59\}$
9	-	$\{19, 37\}$
10	$\{3\}$	$\{41\}$
11	-	$\{5, 40\}$